AFFIDAVIT

I declare that I have authored this thesis independently, that I have not used other than the declared sources/resources, and that I have explicitly indicated all material which has been quoted either literally or by content from the sources used. The text document uploaded to TUGRAZonline is identical to the present master‘s thesis dissertation.

Date

Signature

Abstract

Transcription factors (TFs) play an important role in transcriptional regulation of gene expression. Multiple factors such as chaperones, secretory vesicle components and vesicle fusion machinery are known to influence the secretion level of recombinant proteins *in Pichia pastoris*. The role of diverse factors in protein secretion in *Pichia* is often deduced in analogy to other eukaryotic hosts preferentially *Saccharomyces cerevisiae*. However, transcriptional regulation of these factors in *Pichia pastoris* is still a field for discovery and development. Engineering on the transcriptional level may provide new insights in protein secretion and enhance the secretion level of recombinant proteins in *P. pastoris*. In this study, *Pichia* strains co-expressing one of eight target TFs were tested for improved secretion of the HyHEL-Fab model protein by ELISA. Two TFs were identified by pool-screenings to raise the yield of the model protein by 89 % and 46 % on average, respectively. Single clones constitutively expressing either of the two TFs and showing yield improvement between 70 – 126 % were selected for bioreactor cultivations.

Kurzfassung

Transkriptionsfaktoren (TF) spielen eine wichtige Rolle bei der transkriptionellen Regulation der Genexpression. Es ist bekannt, dass viele Faktoren wie Chaperone, Komponenten von sekretorischen Vesikeln und die Maschinerie für die Vesikelfusion Einfluss auf das Sekretionslevel von rekombinanten Proteinen in *Pichia pastoris* haben. Für die Rolle dieser Faktoren bei der Proteinsekretion in *Pichia* wird oft die Analogie zu anderen eukaryotischen Wirtssystemen, vorzugsweise *Saccharomyces cerevisiae* herangezogen. Trotzdem, beziehungsweise gerade deshalb ist die Regulation auf Transkript-Ebene in *Pichia pastoris* noch weites Forschungsgebiet. Veränderungen auf transkriptioneller Ebene könnten neue Einblicke in den Ablauf der Proteinsekretion in *P. pastoris* geben, und mögliche Ansatzpunkte für die Erhöhung der Proteinsekretionsrate beziehungsweise -ausbeute liefern. In dieser Studie wurden *Pichia* Stämme, die einen von acht ausgesuchten TF co-exprimieren mittels ELISA auf die verbesserte Sekretion des HyHEL-Fab Modellproteins getestet. Dadurch wurden mit Hilfe eines Pool-Screenings 2 TF identifiziert, die die finalen HyHEL-Titer um 89 % und 46 % steigerten. Einzelklone, die jeweils einen der beiden TF co-exprimieren wurden auf Grund ihrer um 70 – 126 % gesteigerten Produktausbeuten für die Bioreaktorkultivierung ausgewählt.

Acknowledgments:

I would especially like to thank my mother Maria, my father Johann and my sister Eva-Maria for their love, understanding and entire support during my study and my previous life. I would also like to thank Mrs. Dipl. Ing. Viktorija Vidimce-Risteski for her patience and effort while supervising my laboratory work. I would like to express my profound gratitude to Prof. Dipl. Ing. Dr. techn. Harald Pichler, Ms. Dipl. Ing. Dr. techn Claudia Ruth and again Mrs. Dipl. Ing. Viktorija Vidimce-Risteski. Thank you for your great support in the theoretical background of my project and while emerging my master's thesis. I am also thankful to my colleagues in the third floor for their help dealing with the daily problems of laboratory work. I am very grateful to my closest friends Gernot, Iris and Gerlinde for staying at my side in good and especially in bad times.

Content

1. Introduction

1.1. *Pichia pastoris*: Host for Heterologous Protein Expression

Methylotrophic yeasts utilizing methanol as sole carbon source for energy and carbon supply were described over 40 years ago by Koichi Ogata[1]. *Pichia pastoris* was of great importance for the production of single cell protein (SCP) as high protein animal feed until the oil shock 1973. In the next decade, Salk Institute Biotechnology/Industrial Associates, Inc. (SIBIA, La Jolla, CA) developed methods for the genetic manipulation of *P. pastoris* on behalf of Philips Petroleum. Researchers developed vectors and strains based on the alcohol oxidase 1 gene and promoter (P_{AOX1}). High levels of heterologously expressed protein under control of the alcohol oxidase 1 promoter and the availability of cultivation methods for SCP production led to the commercialization of the *P. pastoris* expression system. Philips Petroleum sold the patent position to Research Corporation Technologies (Tuscon, AZ) and licensed Invitrogen for selling system components. The major advantages of *P. pastoris* as host for heterologous protein production are easy genetic manipulation, the ability to express high levels of protein intracellularly and extracellularly, and the ability to carry out glycosylation, disulfide-bond formation and proteolytic processing[2]. Hence, several proteins could be expressed functionally *in P. pastoris* in contrast to bacteria, *Saccharomyces cerevisiae* or Baculovirus, where a functional production failed[3]. Also the preferences for respiratory growth without production of ethanol or acetic acid are benefits of *P. pastoris*.

1.1.1. Methanol Metabolism in *P. pastoris*

Yeast such as *Candida*, *Hansenula*, *Pichia* and *Torulopsis* are known for growth on methanol[4]. The key enzyme of methanol oxidation, the alcohol oxidase (AOX), was already discovered before, also in organisms, which are not capable of growth on methanol. Methanol oxidation takes place in a special single membrane organelle named peroxisome. The alcohol oxidase catalyses the first step of methanol oxidation in the presence of oxygen as electron acceptor[1]. Methanol is oxidized to formaldehyde creating hydrogen peroxide. The enzyme catalase disposes harmful hydrogen peroxide by splitting it into water and oxygen. A part of the generated formaldehyde leaves the peroxisome and is oxidized by formaldehyde dehydrogenase and formate dehydrogenase to formate and carbon dioxide. These reactions generate nicotinamide adenine dinucleotide (NADH), which serves as energy source for growing cells. Dihydroxyacetone synthase (DHAS) assimilates the remaining formaldehyde by condensation with xylose 5-phosphate inside the peroxisome. The reaction products, glyceraldehyde 3-phosphate and dihydroxyacetone leave the peroxisome entering a cytoplasmic pathway for the regeneration of xylose 5-phosphate, producing one net molecule of glyceraldehyde 3-phosphate per 3 MeOH molecules (Figure 1). Methanol utilization pathway (Mut) genes are induced by methanol. Assimilatory genes, responsible for the building of cell constituents are repressed by glucose, in contrast dissimilatory genes for the production of energy are not[5, 6]. Proliferation of peroxisomes is supported by growth

on methanol while the number of peroxisomes in cells with repressed methanol utilization is strongly reduced[7]. The localization of alcohol oxidase and catalase to the peroxisomes is crucial. The compartmentalization enables the correct partitioning of formaldehyde over the dissimilatory and assimilatory pathway. Additionally it allows the disposal of hydrogen peroxide without the need of energy consuming processes in the cytoplasm. Oxygen peroxide metabolism in the cytoplasm by cytochrome c peroxidase or non-enzymatic oxidation of glutathione would negatively influence the energy balance compared to the disposal in peroxisomes by catalase.

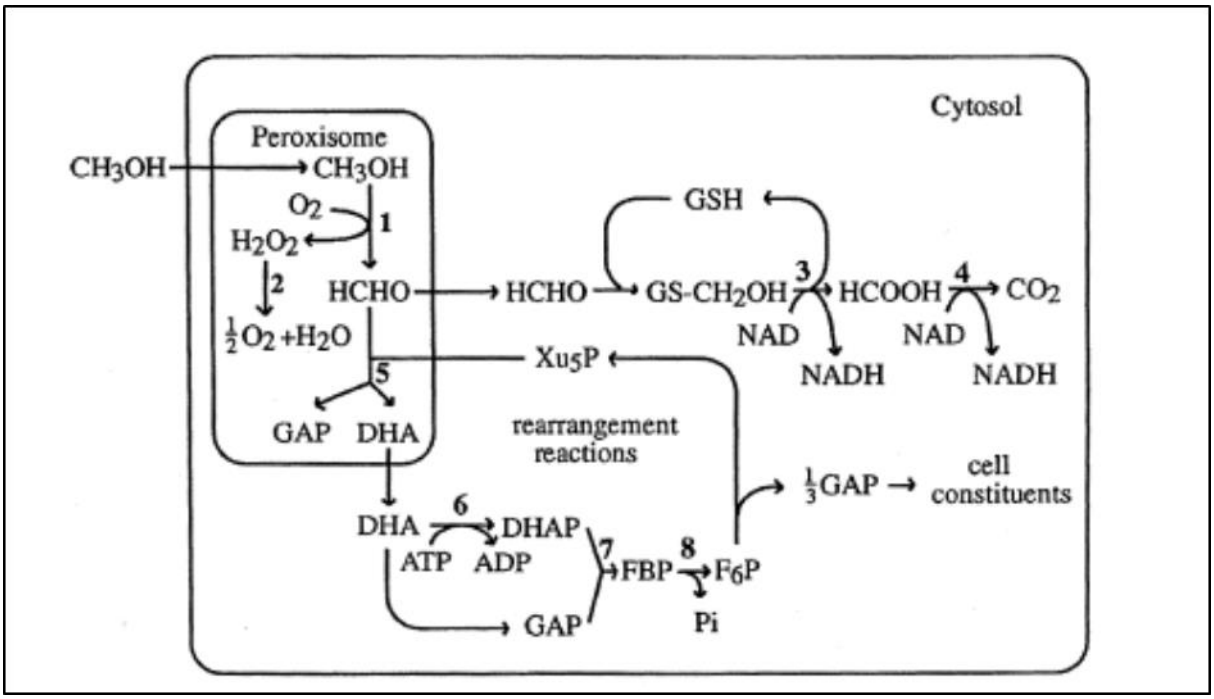

Figure 1: Methanol utilization pathway in *P. pastoris*. *Peroxisomal enzymes*: 1, alcohol oxidase; 2, catalase; 5, dihydroxyacetone synthase. *Cytosolic enzymes*: 3, formaldehyde dehydrogenase; 4, formate dehydrogenase; 6, dihydroxyacetone kinase; 7, fructose 1,6-bisphosphate aldolase; 8, fructose 1,6-bisphosphatase[1].

1.1.2. Promoters for Protein Expression in *P. pastoris*

Recombinant proteins in *P. pastoris* are usually expressed under control of the strong inducible *AOX1* or constitutive *GAP* (glyceraldehyd-3-phosphate dehydrogenase) promoters. Among the inducible promoters, the *AOX1* promoter is most commonly used. Alternative inducible promoters like P_{FLD1}, P_{PEX8} and P_{YPT1} or P_{AOX1} variants are also available[8, 1]. Constitutive promoters were disregarded for a long time due to the hypothesis that constitutive production of foreign proteins may harm the host organism[9, 10]. However, recent observations do not support the assumption of cytotoxicity hypothesis and also show good results for the production of heterologous proteins, e.g. for the production of exo-levanase (LsdB) or β-lactamase under the control of the *GAP* promoter (P_{GAP}).

1.1.2.1. P_{AOX1} (*AOX1* promoter)

Ellis *et al.* (1985) identified a 1 kb large region upstream the translation initiation codon (AUG), which acts as regulatory (promoter) region of the *AOX1* gene[11]. The transcription initiation site was located at position -114. The functionality of the *AOX1* promoter was

tested using sub-fragments of the identified regulatory element for expressing β-lactamase (LacZ)[12]. The second alcohol oxidase gene, *AOX2,* shares 92 % and 97 % homology to *AOX1* at the nucleotide and amino acid sequence level, respectively. 5' and 3' untranslated regions (UTR) of the two genes show low homology and also the strength of P_{AOX2} is low. A 243 bp region (-415 to -172 upstream of ATG) of P_{AOX1} was identified to be crucial for the induction with methanol[6]. This region is bound by the methanol expression regulator 1 (Mxr1p), a homolog of the *S. cerevisiae* transcription factor Adr1p. Deletion of ~152 bp within these 243 bp resulted in a reduction of the promoter activity to ~20 % under inducing conditions. Other regulatory elements have been described, but molecular regulation mechanisms are still not fully disclosed[8]. P_{AOX1} is repressed when *P. pastoris* is grown on glucose, glycerol or ethanol. Under de-repression conditions *AOX1* mRNA levels reached 1-4 % of the induced level[12, 13, 14]. Full induction is only given for growth on methanol. For this reason alternative carbon sources were studied for their non-repressing character and also applied in co-feed studies[14]. Alanine, sorbitol, mannitol and trehalose were identified as non-repressing as shown for the expression of β-galactosidase.

1.1.2.2. P_{GAP} (*GAP* promoter)

In large scale operations the use of high amounts of flammable methanol as inducing agent for P_{AOX1} can be an issue[10]. In 1997, the isolation of the *P. pastoris GAP* gene and its promoter was reported. The *GAP* promoter is constitutively active when cells are grown on glucose, glycerol or methanol. The transcription level of glycerol-grown cells was two-thirds and one-third for cells grown on methanol compared to glucose as carbon source. Expression studies with β-lactamase as a reporter also revealed constitutive expression. However, β-lactamase levels were significantly higher for glucose grown cells compared to methanol grown cells. β-lactamase levels of cells grown on glycerol equalled the level of cells grown on methanol under P_{AOX1} control. For fine-tuned gene expression, researchers generated a P_{GAP} library with promoter activities ranging from 0.6 % up to 19.6 fold of the wild-type promoter[15]. P_{GAP} was also used for the constitutive co-expression of transcription factors (TFs) to enhance the expression of target genes, most of them controlled by P_{AOX1}[13]. The transcriptional activator 'positive regulator of methanol' (PRM1) was co-expressed and increased phytase expression on glucose up to 3-fold compared to a not co-expressing strain. The co-expression of the 'methanol expression regulator 1' (MXR1) resulted in a 7.6-fold increase of phytase activity under control of P_{AOX1}. Unfortunately, both studies lack the comparison to a methanol induced expression of phytase under control of P_{AOX1} or under comparable biomass production.

1.1.3. Recombination in *P. pastoris*

A stable integration of an expression cassette harbouring the gene of interest and a selection marker into the *P. pastoris* genome is beneficial avoiding potential plasmid instability issues. Commonly, expression cassettes are integrated into the genome of *P. pastoris* via homologous recombination (HR) creating stable expression strains without the need of permanent antibiotic addition as it would be for plasmid based systems[16]. A process termed non-homologous end joining (NHEJ) is a mechanism usually involved in repairing double

stand breaks (DSBs), which causes random integration of linearized plasmids into the genome.

1.1.3.1. Homologous Recombination

Linearization of *P. pastoris* vectors within sequences shared by the host genome targets the integration of the vectors to that genomic locus[1]. HR between genomic and artificially introduced DNA results in either single or double crossover-type integration. Commonly used homologous regions are the *AOX1* promoter, the *AOX1* transcription termination region (TT), or a region further downstream (3' *AOX1)*[17]. Single crossover between the *AOX1* loci and the *AOX1* regions on the vectors leads to orientation dependent insertion of one or more copies of the vector up- or downstream the *AOX1* gene. Gene insertion occurs at a high frequency. One to ten percent are multiple insertion events according to Invitrogen's *Pichia* expression kit and its corresponding available vector systems pHIL-D2, pPIC3.5, pHIL-S1 and pPIC9. Strains harbouring multiple copies of an expression cassette have been shown to produce more heterologous protein than single copy strains. For example, Hepatitis B surface antigen (HBsAG) protein yield was directly correlated to the copy number of up to eight direct repeats of the HBsAG expression cassette in *P. pastoris*[18, 1]. Multicopy strains can be identified/generated in different ways. One method uses vectors with the bacterial *Tn903kan*^{r} genes, which gives resistance to the eukaryotic antibiotic geneticin (G418). The vector copy number integrated into the host genome can roughly be related to increasing antibiotic concentration and can reach up to 30 copies. A second approach is the use of the bacterial *Streptoalloteichus hindustanus* bleomycin gene *(Sh ble)*, which confers resistance to the antibiotic zeocin (zeo). Transformants can directly be screened on plates with zeocin and multicopy strains can be enriched by increasing the concentration of the drug. A vector construct with multiple head-to-tail copies of the expression cassette can also be used to generate multicopy strains. Gene replacement at the *AOX1* locus occurs at a frequency of 10-20 %[1]. *AOX1* is deleted due to a double crossover event between the *AOX1* promoter and 3'*AOX1* region of vectors and the genomic DNA (gDNA)[17]. Hence, the growth on methanol depends on *AOX2,* resulting in the phenotype Mut^{S} (methanol utilization slow).

1.1.3.2. NHEJ

NHEJ is a mechanism to repair DSBs and involves the Ku proteins[19]. The Ku complex binds DNA ends, stem loops or bubble structures with strong affinity and is made of two heterodimeric subunits. In *S. cerevisiae*, these subunits are termed Yku70 and Yku80 with a size of ~70 kDa each. In yeast NHEJ requires DNA ligase IV encoded by the *DNL4* gene[20]. Both proteins play an important role in NHEJ and are responsible for the genetic rearrangement of DSBs lacking homology. Nevertheless, annealed ends of DSBs show short common sequences with micro-homology. The term micro-homology describes 1-10 bp long sequences complementary or equal to each other. Integration of DNA fragments with flanking homologous sequences is done by NHEJ and HR in parallel[16]. Because NHEJ is more likely than HR, deletion of the *KU70* homologue of *P. pastoris* (and therefore NHEJ) could significantly increase the efficiency of HR and would lower random integration of vector expression cassettes into the *P. pastoris* genome.

1.1.4. Secretory Pathway in *P. pastoris*

Recombinant proteins can either be produced intracellularly or extracellularly in *P. pastoris*[1]. A big advantage of this organism is the relatively low amount of secreted endogenous proteins. Thus, heterologously secreted proteins make up the majority of the proteins in the extracellular space (i.e. are relatively pure), circumventing costly purification of the protein of interest. Secretion is more powerful for proteins, which are secreted in their natural hosts too, than for naturally intracellular proteins. The secretion pathway offers several advantages like proteolytic modifications, glycosylation or disulfide bond formation which can be important for the correct maturation of a recombinant protein[21]. For these reasons, *P. pastoris* can be used to produce a large variety of functional eukaryotic proteins including human and plant derived ones.

Secretion of newly synthesized proteins involves the intracellular protein trafficking pathway[22]. Proteins are translocated co- or post-translationally into the endoplasmic reticulum (ER) lumen to provide proper folding. After folding, proteins are predominantly transported to the Golgi apparatus by membrane enclosed vesicles. This process of ER-to-Golgi trafficking is part of the so called vesicle or membrane trafficking, which also consists of intra-Golgi and post-Golgi trafficking. The way of newly synthesized protein in the ER is directed to and into defined vesicle populations, which target them to definite compartments or the extracellular space. The whole mechanism of directing proteins to their individual destinations is termed protein targeting or protein sorting. Targeting of a heterologous protein to the secretory pathway requires the attachment of a secretion signal sequence at the protein's N-terminus[1]. The secretion signal can be the native secretion signal of the heterologous protein or a commonly used leader such as *S. cerevisiae* α-factor prepro peptide (α-MF) or the *P. pastoris* acid phosphatase (*PHO1*) signal.

1.1.4.1. *S. cerevisiae* α-Factor Prepro Peptide (α-MF)

The *S. cerevisiae* α-MF signal peptide has successfully been used for the secretion of various recombinant proteins in *P. pastoris* and was first described in 1982[1, 23]. The sequence is made of a 19 amino acid (aa) pre-sequence, which is followed by a 64 aa pro-sequence. A spacer region between the pro-sequence and the α-factor or fusion protein is made of two Glu-Ala repeats. Three sites for N-linked glycosylation exist in the pro-region with a moderate importance for proper processing, transport and secretion[24]. The processing of the prepro signal peptide starts with the removal of the cleavable signal sequence from the precursor protein by SP (signal peptidase) in the ER[25, 1]. Afterwards, the pro-sequence is cleaved between Lys-Arg and $(Glu\text{-}Ala)_2$ by Kex2p[26]. Kex2p is a membrane-bound endopeptidase located in the Golgi. Cleavage by Kex2p produces a fusion protein with Glu-Ala repeats at the proteins N-terminal side. It has been shown that these Glu-Ala repeats are not required for correct processing of hEGF (human epidermic growth factor) fusions, which might be different for other proteins of interest[27]. Glu-Ala repeats are immediately processed by a membrane bound heat-stable dipeptyl aminopeptidase (Ste13p), whose transcription is pheromone induced[28, 29]. Sometimes, unprocessed Glu-Ala repeats remain fused to the secreted protein of interest[27]. Cellular levels of Ste13p have been shown

insufficient to deal with the large amounts of recombinant protein produced under a strong promoter. This might also apply to native α-factor in order to prevent intracellular accumulation of active protein, as the Glu-Ala repeats strongly reduce the biological activity of the α-factor.

1.1.5. The Unfolded Protein Response (UPR)

A lot of recombinant proteins are efficiently secreted at acceptable levels while others are not[22]. As protein secretion involves not only protein synthesis, sole optimization of transcription and translation is sometimes insufficient. Successful secretion of heterologous proteins depends on many processes such as co- or post-translational translocation of emerging proteins, correct folding (ER), post-translational glycosylation in the ER and the Golgi apparatus, intracellular protein trafficking/sorting, proteolytic degradation and stress response upon misfolded proteins. All of these events are potential engineering points to improve the secretion of heterologous proteins.

The UPR is a point for secretion improvement as demonstrated by Guerfal *et al.* (2010)[30]. Linear polypeptide chains enter the ER and are folded to their final shape by a set of ER-resident enzymes and chaperones. The ER possesses a sensitive recognition system for unfolded proteins. Unfolded proteins can have two different fates, folding or degradation, after identification by the surveillance system termed UPR. The UPR steadily coordinates the activity of folding and degradation pathways for unfolded proteins. The levels of unfolded proteins can increase for various reasons including reduced protein glycosylation due to starvation or treatment with tunicamycin, high rates of misfolded proteins or unassembled subunits, a change in redox conditions caused by e.g. reducing agents like dithiothreitol (DTT) or genetic means, or a change in luminal ion content because of ionophores or heavy metals. Secretion stress in yeasts is mainly related to limitations in membrane translocation, signal sequence processing and folding within the ER[31]. The cell can handle ER-stress caused by misfolded proteins in three different ways[32]. The reduction of proteins entering the ER is one way to overcome this stress situation. The reduced protein load is achieved by down regulation of protein synthesis and translocation into the ER, which is a rather rapid process. A more long-term adaption to ER-stress is an increase of the protein folding machinery capacities within the ER, which involves the activation of UPR target genes. If homeostasis cannot be restored mechanisms which ultimately result in autophagy and cell death are initiated. For the underlying pathways three distinct ER-stress transducers have been identified. The transducers are transmembrane proteins responsible for sensing the protein folding status of the ER lumen across the ER membrane into the cytosol.

1.1.5.1. *IRE1*

Signals from inside of the ER interact with cytoplasmic effector proteins, which influence the transcriptional or translational apparatus. Ire1p has a protein kinase domain at its cytoplasmic part functioning as signal transducer [33]. An ER resident HSP70 family chaperone named Kar2p/BiP is involved in the UPR activation by Ire1p[34]. Upon ER-stress Ire1p-bound Kar2p is released. There is new evidence that Ire1p is activated by direct binding of unfolded

proteins, leading to a conformational change and oligomerization of Ire1p[35, 32]. Kinase domains of Ire1p come close for trans-autophosphorylation at the plane of the membrane due to oligomerization. Activation of Ire1p by auto-phosphorylation causes activation of its unconventional effector function, which is a ribonucleolytic one. Ire1p promotes the cleavage of the mRNA coding for the transcription factor Hac1p in yeast. Cleavage of *HAC1* mRNA releases one intron and fragments are re-ligated by tRNA ligase (Trl1). The transcription factor encoded by the spliced mRNA of *HAC1* is an activator of UPR target genes. Dephosphorylation of Ire1p plays an important role in its inactivation in order to attenuate UPR when ER folding capacity has successfully been recovered[36]. Protein phosphatase 1-like gene (*PPM1l*) encodes for the ER-membrane located protein phosphatase (PP2Ce) and seems to be involved in the dephosphorylation of Ire1p[37].

1.1.5.2. Linkage between UPR and ER-Associated Degradation (ERAD)

The ERAD pathway removes unwanted proteins from the ER[38]. Proteins, which cannot be refolded, although ER folding capacity has been boosted by induction of UPR pathway, are degraded. ERAD is responsible for the translocation of such proteins back to the cytosol, where degradation is performed by the proteasome. Sec61p with its associated subunits, the conducting channel also used for delivering new synthesized proteins into the ER lumen, serves as retro-translocation or dislocationpore of the mis- or unfolded proteins. Several ERAD target genes like *DER1*, *HRD1*/*DER3*, *HRD3* and *UBC7* are affected by an up-regulated UPR[39]. Thus, UPR is directly involved in enhancing the capacity of ERAD. These overlapping pathways are also essential for eliminating misfolded proteins under non-stressful conditions.

1.2. Identification and Use of Secretion Enhancing Factors

The use of transcription factors to engineer the secretion capacity is rather novel[40], mostly due to the fact that the whole *P. pastoris* genome sequence has only been available since a few years[41, 42]. The transcription factor Hac1p of *S. cerevisiae* was used to increase the secretion of native invertase and two heterologous proteins, *Bacillus amyloliquefaciens* α-amylase and *Trichoderma reesei* endoglucanase EGI, in *S. cerevisiae*[43]. The constitutive overexpression of *HAC1*, which functions as a regulatory element involved in activation of UPR target genes, increased the secretion of α-amylase by 70 % and invertase two-fold, while EGI secretion was not influenced. Expression of *T. reesei hac1* also showed positive results in *S. cerevisiae* for α-amylase and invertase. Both, *ScHAC1* and *Trhac1* overexpression led to higher Kar2p levels. *S. cerevisiae* Hac1p was also shown to improve the secretion of heterodimeric Fab fragments in *P. pastoris* when constitutively overexpressed[44]. Another study showed the successful co-expression of the endogenous *Aspergillus niger var. awamori HAC1* to boost the secretion of *Trametes versicolor* laccase and bovine prepro-chymosin. Guerfal *et al.* investigated the co-expression of native *P. pastoris HAC1* and its effect on the secretion efficiency of mIL-10 or *Trypanosoma cruzi* trans-sialidase (TS). Co-expression of *HAC1* under control of the inducible *AOX1* promoter showed an up to 2.2-fold increase for mIL-10. Kar2p was also up-regulated in these strains. Also the secretion of TS

was improved up to 2.1-fold compared to a reference strain. A lot of effort was spent on the identification of new target genes to improve the secretion efficiency of *P. pastoris* strains for the production of heterologous proteins in recent years[40]. In 2007, Gasser *et al.* identified 524 genes by microarray analysis, which are remarkably regulated in strains overexpressing human trypsinogen compared to non-expressing strains[45]. Thirteen genes were classified as potentially helpful to improve the secretion capacity and stress management of the cell, including known secretion helpers such as *PDI1, ERO1, SSO2, KAR2/BiP* and *HAC1.* Secretion helper factors homologs from *S. cerevisiae* were co-expressed in *Pichia* strains producing a human antibody fab fragment. The helper factors, *BMH2*, *BFR2*, *C0G6*, *C0Y1*, *CUP5*, *IMH 1*, *KIN2*, *SEC31*, *SSA4* and *SSE1* were shown to increase the specific production rates and the volumetric productivity of the Fab2F5 up to 2.5-fold in fed-batch cultivations[46]. Graf *et al.* developed full genome DNA-microarrays for *P. pastoris* and analysed the UPR[47]. Approximately 4,000 genes and 11,000 open reading frames (ORF) identified by gene finding and annotation were tested in this study and the effect of DTT treatment and *HAC1* overexpression. Similarities, but also differences were found between the baker's yeast and *P. pastoris*. UPR induction with DTT revealed 45 of 93 genes to be regulated as in *S. cerevisiae*. Interestingly, Hac1 overexpression resulted in the activation of many translation relevant genes in *P. pastoris*. Genes involved in ribosome biogenesis, RNA metabolism and translation, a circumstance, which had not been observed in yeasts or filamentous fungi so far, emphasizing the importance of organism-specific microarray analysis. Another method to screen for secretion enhancing factors was described by Stadlmayr *et al.* (2009)[48]. Fluorescence activated cell sorting (FACS) was used to identify cells with increased secretion capacity of a surface displayed model protein. *P. pastoris* cDNA libraries were established under different growth conditions to cover a broad variety of transcription levels. Putative enhancer genes were then tested for improving the secretion of a Fab fragment of a monoclonal antibody against human immunodeficiency virus type 1, finally revealing the genes PIPA05837, PIPA03435, and PIPA02482 as enhancing factors. Homology analysis (*S. cerevisiae)* revealed PIPA05837 as *P. pastoris* RPL33A. PIPA03435 is annotated as the *P. pastoris* homolog of NRG1 and PIPA02482 showed weak homology on protein level to *S. cerevisiae APE2*. DNA microarrays were used in parallel to follow the trends of gene enrichment during consecutive FACS. Analysis revealed quite striking outcomes showing vesicle-mediated transport not limiting for the secretion process of Fab2F5. On the other hand, membrane- and cell wall organization were found to strongly influence secretion. Also genes related to stress response and response to chemical stimuli influenced Fab2F5 expression in a positive way, among them proteins for processing, folding and refolding as described in earlier studies.

1.3. ChIP-seq as Tool for TF-Binding Sites (TFBS) Identification

The genome-wide localization of binding sites for DNA binding proteins such as transcription factors (TFs), the core transcriptional machinery and histones are an emerging topic in the understanding of gene regulatory networks in the living organism[49]. The interplay between chromatin states, which influences the access of DNA binding proteins to the DNA, and

recruitment of effector protein complexes for transcription is a dynamic process. Cis-regulatory elements like promoters and enhancers, which are located in some distance to the transcription initiation site, are common targets for transcription factors[50]. Repressive factors, which bind repressing sequences and/or silencers far away from the transcription start site can also effect gene regulation. To elucidate the mechanisms of these complicated processes powerful technologies for the identification of DNA-protein interactions like ChIP-Chip (chromatin immunoprecipitation with microarray technology) and ChIP-seq (chromatin immunoprecipitation followed by sequencing) are used. Both technologies start with chromatin immunoprecipitation (ChIP) to fix DNA-binding proteins to their target sequences[51, 49]. DNA-associated proteins are cross-linked in vivo to their specific genomic regions by treatment with formaldehyde. Cells are lysed and the chromatin is sheared by sonication to gain DNA fragments of approximately 200 - 600 bp. Another method includes the use of an exonuclease to digest non-bound DNA, raising the resolution of binding site detection and eliminating DNA contaminations[52]. The obtained material is then immunoprecipitated with an antibody against the protein of interest. This could be an antibody against a certain epitope in case of an epitope-tagged DNA-binding protein. Purified DNA is then sequenced by next generation sequencing technologies such as Illumina Genome Analyzer, Applied Biosystems' SOLiD or the Hilicos platform for single molecule sequencing without the need of amplifying the obtained fragments. Several factors can limit the quality of the ChIP-seq. A highly specific and sensitive antibody is required to enrich the protein of interest. Also the quantity and quality of the sample DNA affects ChIP-seq results. An advantage of ChIP-Seq is that a lower amount of DNA is required (10 – 50 ng of) in comparison to ChIP-chip. To overcome limitations such as DNA breakage during sonication, where regions of open chromatin are preferentially represented in the sonicated sample, and platform specific biases, the use of control data sets is essential[53, 54]. Also the binding of transcription-related proteins to highly transcribed genomic loci can influence the results, regardless of the protein analysed. Gene function and established roles of the protein do not always align and can lead to false positives. Two possible sets of control DNA samples are in use: (1) Input DNA, which has been cross-linked and fragmented under the same conditions as the immunoprecipitated sample (but not immunoprecipitated) or (2) a "mock" ChIP. In a "mock" ChIP sample a control antibody that reacts with an irrelevant, non-nuclear antigen is used. A commonly used control antibody is Immununglobulin G (IgG). Common alignment software provided by the Sequencer-manufacturer can be used for sequence analysis, e.g. Eland (Illumnia), Mapping and Assembly with Qualities (MAQ) or Bowtie[49].

Additional information for epitope tagged factors[53]:

ENCODE (ENCyclopedia Of DNA Elements) provides guidelines for comparable results of tagged and endogenous transcription factor using the ChIP-seq technology. It is helpful to use similar amounts of tagged protein to the endogenous one, which can be achieved by the use of low copy vectors and expression driven by the natural promoter. Endogenous protein levels are sometimes not sufficient for ChIP and the use of a stronger promoter to elevate

target protein expression level is useful. The recommended control for epitope-tagged experiments is immunoprecipitation using the same antibody, however with a strain producing untagged protein.

1.4. Aim of the Study

In this study we evaluated different TFs as putative secretion helpers. The antibody (Fab) secreting strain P_{AOX} HyHEL-Fab-#8 was used as background strain. TFs were co-expressed under control of the constitutive $P_{GAP.}$ Different amounts of DNA were used for transformation and the impact on the Fab secretion level was studied. Promising TFs should then be further analysed by a ChIP-Seq procedure to identify TFBS and regulated genes in the *P. pastoris* CBS7435 genome.

1.4.1. TFs as Secretion Enhancing Factors: Identification, Selection and Ranking

In this study, TFs were screened for their potential as secretion helpers. On the one hand, TFs were identified by *in silico* promoter studies. Promoters of genes coding for known secretion enhancing factors, like Kar2p or Hac1p, were examined for TFBS with the software tool MatInspector. The TF Upc2p was found to putatively regulate BiP (TFBS -866 upstream of ATG) and, therefore, was used as a target gene (*UPC2*) in this study. On the other hand, microarray experiments were used to find TF candidates. Transcriptomes of *P. pastoris* strains expressing five different model proteins, including different Fab fragments and enzymes, were isolated from chemostat cultivations, reverse transcribed into cDNA and hybridized on a *P. pastoris* DNA-chip. Results were compared to a WT strain (no model protein overexpressed). Following TFs were found significantly regulated in at least two model protein secreting strains and evaluated in this study as secretion helper: *GAT1, GAT2, CAT8, YRM1* and a not yet annotated TF (PAS_chr4_0425).

The expression of enzymes and transporters necessary for the uptake and utilization of poor nitrogen sources is coordinated by four GATA type TFs, which are encoded by the genes *GAT1, GLN3, DAL80* and *GZF3* in *S. cerevisiae* [55]. Gln3p and Gat1p are activators of nitrogen-regulated genes, whereas Dal80p and Gzf3p act as their antagonists. Gat1p and Gln3p activate genes, whose expression is dependent on the nitrogen source[56]. 91 genes are directly activated by these two TFs, however several other genes are also influenced by the growth on poor nitrogen sources and are temporarily up-regulated (stress-responsive genes) or down-regulated (genes encoding ribosomal proteins and translational factors). Expression of *GAT1* is nitrogen catabolite repression (NCR) sensitive and also involves Gln3p and Dal80p[57]. Gat1p is able to bind DNA with its GATA-type zinc finger motif, similar to Gln3p and Dal80p. Under nitrogen excess, Gat1p and Gln3p are located in the cytoplasm in a phosphorylated state upon Tor-kinase action and, therefore, interact with Ure2p[56, 58]. Under nitrogen limitation Sit4 dephosphorylates Gat1p and Gln3p, releasing them from Ure2p inhibition and triggering translocation into the nucleus, where they can function as NCR gene activators[59].

Currently, not much is known about regulation and function of *S. cerevisiae* Gat2p[60]. *ScGAT2* is homologous to Brg1/Gat2 from *Candida albicans.* In *C. albicans*, Gat2 is involved in biofilm formation, filamentous growth and virulence[61]. Gat2p also contains a zinc-finger DNA binding motif, similar to Gln3p and Gat1p.

The shift from one to another carbon source is called a diauxic shift[62]. A change from glucose to a non-fermentable carbon source leads to vast re-programming of the cells expression patterns, affecting genes of gluconeogenesis, the glyoxylate cycle and also the tricarboxylic acid cycle. The *CAT8* gene encodes a zinc cluster protein involved in the derepression of gluconeogenic enzymes[63]. *CAT8* is repressed by Mig1, which itself is inactivated through phosphorylation by Snf1p kinase[62]. Once activated, Cat8 acts as transcriptional activator by binding promoters of genes containing the carbon source-responsive element (CSRE). The transcriptional regulator Sip4p is also involved in the activation of genes harbouring the CSRE consensus sequence.

S. cerevisiae pleiotropic drug resistance (PDR) is analogous to mammalian multiple drug resistance (MDR), which mediates its resistance through the regulation of membrane transporters or transcriptional regulators[64]. Yrm1p (yeast reveromycin resistance modulator) is a paralog of Yrr1p, sharing 41 % homology on protein level[65]. The DNA binding region of Yrm1p belongs to the C6 zinc cluster family. Yrm1p acts as a transcriptional activator but only interacts with Yrr1p target genes in the absence of Yrr1p (i.e. *yrr1* defective strains). Yrm1p and Yrr1p regulate a set of target genes which is similar, but not identical. Yrm1p up-regulates twenty-three genes, of which fourteen are also direct Yrr1p targets. Yrr1p is mainly involved in providing resistance to the mutagen 4-nitroquinoline N-oxide (4-NQO)[66], acting on the *SNQ2* gene, which codes for multidrug resistance ATP binding cassette superfamily protein and is responsible for 4-NQO export.

The fifth TF studied in this thesis, is a not yet annotated hypothetical protein with a specialized type of zinc finger motif, the RING finger domain (really interesting new gene)[67]. The zinc finger consists of forty to sixty residues, binds atoms of zinc and probably mediates protein-protein interactions. The RING finger domain was found in many unrelated proteins involved in e.g. viral replication, signal transduction and development. Two variants of this special type of Zn-finger exist, C3HC4-type and C3H2C3-type, which differ in their cysteine/histidine pattern. C3H2C3-type is also known as "RING-H2 finger". A subset of RINGs is associated with B-Boxes.

Upc2p and its paralog Ecm22p are sterol regulatory element (SRE) binding proteins (SREBPs) in *S. cerevisiae*[68]. A 7-bp SRE bound by the TFs was identified on *ERG2* and *ERG3* promoters and other genes involved in the sterol biosynthesis. Upc2p and Ecm22p are members of the fungal-specific Zn[2]-Cys[6] binuclear cluster family. *ERG2* and *ERG3* are part of the ergosterol biosynthetic pathway and are activated upon sterol depletion by Upc2p[69]. The transcriptional activation domain of Upc2p is on the carboxy-terminal region.

2. Materials and Methods

2.1.Materials

Table 1: Bacteria and *Pichia* strains

Strain ID	**Description**	**Genotype**	**strain collection number CC (IMBT or acib)**
***E. coli* TOP10F'**	cloning strain	F'{lacIqTn10(TetR)} mcrA Δ(mrr-hsdRMS-mcrBC) ϕ80lacZΔM15 ΔlacX74 recA1 araD139 Δ(ara-leu)7697 galU galK rpsL endA1 nupG	-
***P. pastoris* CBS 7435**	wild type (WT)	-	BT 3445
P_{AOX} HyHEL-Fab-#8 parent strain	parent strain, Mut^S	BT 3445 *aox1*::FRT $AOX1_{TT}$-HyHEL P_{AOX} HyHEL-Fab	acib #323

Table 2: *P. pastoris* strains created by transformation P_{AOX} HyHEL-Fab-#8 parent strain (#323) with linearized plasmid

Strain ID	**Description**	**Characteristics**
P_{AOX} HyHEL-Fab-#8 TF1	P_{AOX} HyHEL-Fab-#8 P_{GAP}_PAS_chr4_0626	Fab secreting and PAS_chr4_0626 co-expressing
P_{AOX} HyHEL-Fab-#8 TF2	P_{AOX} HyHEL-Fab-#8 P_{GAP}_PAS_chr4_0271	Fab secreting and PAS_chr4_0271 co-expressing
P_{AOX} HyHEL-Fab-#8 TF3	P_{AOX} HyHEL-Fab-#8 P_{GAP}_PAS_chr4_0540	Fab secreting and PAS_chr4_0540 co-expressing
P_{AOX} HyHEL-Fab-#8 TF4	P_{AOX} HyHEL-Fab-#8 P_{GAP}_PAS_chr4_0324	Fab secreting and PAS_chr4_0324 co-expressing

P_{AOX} HyHEL-Fab-#8 TF5	P_{AOX} HyHEL-Fab-#8 P_{GAP}_PAS_chr4_0425	Fab secreting and PAS_chr4_0425 co-expressing
P_{AOX} HyHEL-Fab-#8 TF6	P_{AOX} HyHEL-Fab-#8 P_{GAP}_PAS_chr2-1_0114	Fab secreting and PAS_chr2-1_0114 co-expressing
P_{AOX} HyHEL-Fab-#8 TF2ni	P_{AOX} HyHEL-Fab-#8 P_{GAP}_PAS_chr4_0271_no-intron	Fab secreting and PAS_chr4_0271_no-intron co-expressing
P_{AOX} HyHEL-Fab-#8 TF5sv	P_{AOX} HyHEL-Fab-#8 P_{GAP}_PAS_chr4_0425_short-version	Fab secreting and PAS_chr4_0425_short-version co-expressing
P_{AOX} HyHEL-Fab-#8 EVC	P_{AOX} HyHEL-Fab-#8 empty vector control	-
P_{AOX} HyHEL-Fab-#8 EVC #1	standardized benchmark EVC of VTU GmbH	-

Table 3: Backbone Plasmids.

Plasmid ID	**Characteristics**	**Source**	**IMBT straincollection number**
pPUZZLE_KanR_P_{GAP}	Empty vector	acib	6780
pUC19	F´ *tra*D36 *pro*AB+ *lac*Iq *lac*ZΔM15 Δ(*pro-lac*AB) *sup*E *hsd*R17 *rec*A1 *gyr*A96 thi *end*A1 *rel*A1 λ-	Thermo Scientific – Austria GmbH, Vienna, Austria	-

Table 4: Plasmids[1]

Plasmid ID	Characteristics	IMBT straincollection number
pPUZZLE_KanR_P_{GAP}_PAS_chr4_0626	PAS_chr4_0626	6897
pPUZZLE_KanR_P_{GAP}_PAS_chr4_0271	PAS_chr4_0271	6890
pPUZZLE_KanR_P_{GAP}_PAS_chr4_0540	PAS_chr4_0540	6891
pPUZZLE_KanR_P_{GAP}_PAS_chr4_0324	PAS_chr4_0324	6892
pPUZZLE_KanR_P_{GAP}_PAS_chr4_0425	PAS_chr4_0425	6893
pPUZZLE_KanR_P_{GAP}_PAS_chr2-1_0114	PAS_chr2-1_0114	6894
pPUZZLE_KanR_P_{GAP}_PAS_chr4_0271_no-intron	PAS_chr4_0271_no-intron	6895
pPUZZLE_KanR_P_{GAP}_PAS_chr4_0425_short-version	PAS_chr4_0425_short-version	6896
pPUZZLE_KanR_P_{GAP}_EVC	multiple cloning site deleted	5333

Table 5: Fast Digest restriction enzymes used for control (*Asc*I, *Hind*III and *Bam*HI) and preparative digestions (*Asc*I). Data taken from restriction enzyme manual (Thermo Scientific)

Restriction enzyme	Characteristics	Cutting region	Source
***Asc*I**	1 FDU/µL	5'...G G↓C G C G C C...3' 3'...C C G C G C↑G G...5'	Thermo Scientific – Austria GmbH, Vienna, Austria
***Hind*III**	1 FDU/µL	5'...A↓A G C T T...3' 3'...T T C G A↑A...5'	Thermo Scientific – Austria GmbH, Vienna, Austria
***Bam*HI**	1 FDU/µL	5'...G↓G A T C C...3' 3'...C C T A G↑G...5'	Thermo Scientific – Austria GmbH, Vienna, Austria

Table 6: Additionally used enzymes

Enzyme	Characteristics	Source
Phusion® high-fidelity DNA polymerase	2 U/µL	Thermo Scientific – Austria GmbH, Vienna, Austria or New England Biolabs, Ipswich, USA
RNase A	10 mg/mL	Thermo Scientific – Austria GmbH, Vienna, Austria
T4 DNA ligase	5 U/µL	Thermo Scientific – Austria GmbH, Vienna, Austria
T5 exonuclease	10 U/µL	Biozym BioTech Trading GmbH, Vienna, Austria
Taq DNA ligase	40 U/µL	New England Biolabs, Ipswich, USA

[1] designed within this thesis

Table 7: Antibodies used for ELISA (Enzyme Linked Immunosorbent Assay)

Antibody	Code	Source	Use
Mouse monoclonal [2A11] to human IgG	ab7497	Abcam plc, Cambridge, UK	capture antibody
Anti-Human IgG (Fab specific)–Peroxidase antibody produced in goat	A0293	SIGMA-ALDRICH Handels GmbH, Vienna, Austria	detection antibody
Anti-Human IgG (Fab specific)–Alkaline Phosphatase antibody produced in goat	A8542	SIGMA-ALDRICH Handels GmbH, Vienna, Austria	detection antibody

Table 8: Antibiotics used for selective media

Name	Stock solution	Organism	Source
Ampicillin sodium salt	100 mg/mL	*E. coli*	Sigma-Aldrich Chemie GmbH, Schnelldorf, Germany
G-418 disulphate (geneticin)	100 mg/mL	*P. pastoris*	ForMedium™, Norfolk, UK
Geneticin disulphate (G418 Sulphate)	100 mg/mL	*P. pastoris*	Carl Roth GmbH, Karlsruhe, Germany
Kanamycin sulphate	100 mg/mL	*E. coli*	Carl Roth GmbH, Karlsruhe, Germany
Zeocin™ powder	100 mg/mL	*P. pastoris*	InvivoGen, San Diego, USA

Table 9: Primers used for the amplification of TF target genes and the pPUZZLE vector

Primer ID	Primer name	Used for	Sequence 5' – 3'
5WP-47	pPUZZLE_kan_*GAP*_rv	amplification of pPUZZLE vector backbone	CATTGTGTTTTGATAGTTGTTCAATTGATTG
5WP-48	pPUZZLE_kan_*CYC1*TT_fw	amplification of pPUZZLE vector backbone	CACGTCCGACGGCGGCCCAC
5WP-49	TF1_fw	amplification of PAS_chr4_0626	ATTTGTCCCTATTTCAATCAATTGAACAACTATCAAAACACAATGAAAGGGCATGAGCTGCC
5WP-50	TF1_rv	amplification of PAS_chr4_0626	GATCTCCGAGGCCTGGGACCCGTGGGCCGCCGTCGGACGTGTTAAAGAGCCATAGTCAGCCATTCC
5WP-51	TF2_fw	amplification of PAS_chr4_0271	ATTTGTCCCTATTTCAATCAATTGAACAACTATCAAAACACAATGCAAACGTACAATAGCAATAGTC

5WP-52	TF2_rv	amplification of PAS_chr4_0271	GATCTCCGAGGCCTGGGACCCGTG GGCCGCCGTCGGACGTGTCATCGG TCTTGCTCAAGCTC
5WP-53	TF3_fw	amplification of PAS_chr4_0540	ATTTGTCCCTATTTCAATCAATTGA ACAACTATCAAAACACAATGAAAG AGAACCAAGCCTCC
5WP-54	TF3_rv	amplification of PAS_chr4_0540	GATCTCCGAGGCCTGGGACCCGTG GGCCGCCGTCGGACGTGCTAGTGA ACAGTTGATTTGACAG
5WP-55	TF4_fw	amplification of PAS_chr4_0324	ATTTGTCCCTATTTCAATCAATTGA ACAACTATCAAAACACAATGAGTA ATGGGGGTGGACC
5WP-56	TF4_rv	amplification of PAS_chr4_0324	GATCTCCGAGGCCTGGGACCCGTG GGCCGCCGTCGGACGTGCTATACC CCTGCAGCCTTGATG
5WP-57	TF5_fw	PAS_chr4_0425	ATTTGTCCCTATTTCAATCAATTGA ACAACTATCAAAACACAATGCCGC ATGTCACAGAGGAC
5WP-58	TF5_rv	PAS_chr4_0425	GATCTCCGAGGCCTGGGACCCGTG GGCCGCCGTCGGACGTGTCATGCA GATCCAAATTCATTCACTAC
5WP-59	TF6_fw	amplification of PAS_chr2-1_0114	ATTTGTCCCTATTTCAATCAATTGA ACAACTATCAAAACACAATGGCTA ACCTAAAGATCCCTG
5WP-60	TF6_rv	amplification of PAS_chr2-1_0114	GATCTCCGAGGCCTGGGACCCGTG GGCCGCCGTCGGACGTGTTACTCA TCATATATACTACTGTGC
5WP-62	TF2_no intron_fw	amplification of PAS_chr4_0271 _no-intron	GTCCCTATTTCAATCAATTGAACAA CTATCAAAACACAATGCAAACGTA CAATAGCAATAGTCGACAAGAAGG ACTACGACTACCTTCCTTTGGAGAA TTAAGTGCTGC
5WP-63	TF5_short version_fw	amplification of PAS_chr4_0425 _short-version	GTCCCTATTTCAATCAATTGAACAA CTATCAAAACACAATGCGTGAAGC CTCAAAACAGAAACACG

Table 10: Primers used for amplification of the pPUZZLE-based expression cassettes

Primer ID	Primer name	Sequence 5' – 3'
5WP-66	pPuzzle_exp-cas_fw	AGATCTTTTTTGTAGAAATGTCTTGG
5WP-72	pPuzzle_expcas_kanrv	CAGTATAGCGACCAGCATTCAC

Table 11: Primers used for sequencing[2].

Primer ID	Primer name	Used for	Sequence 5' – 3'
5WP-7	TF1_seq 1_fw	PAS_chr4_0626	GACCATCAAGTTGAAGAACCAAGC
5WP-8	TF1_seq 2_fw	PAS_chr4_0626	GCAACCAGCATATTCATCGAATG
5WP-9	TF1_seq 3_fw	PAS_chr4_0626	GGCTCTGTACGACCATTATCATTG
5WP-10	TF1_seq 4_rv	PAS_chr4_0626	GAAGCTTTAAGAACAATCCACAAGC
5WP-11	TF1_seq 5_rv	PAS_chr4_0626	GCTGGGAGATGTCAAAGCTGG
5WP-12	TF1_seq 6_rv	PAS_chr4_0626	CCATGTCAGGTTTTCCATTCTGG
5WP-13	TF2_seq 1_fw	PAS_chr4_0271/ PAS_chr4_0271_no-intron	CCTTCCTTTGGAGAATTAAGTGC
5WP-14	TF2_seq 2_fw	PAS_chr4_0271/ PAS_chr4_0271_no-intron	CCAGAAAATACAGAGGATCGCTC
5WP-15	TF2_seq 3_fw	PAS_chr4_0271/ PAS_chr4_0271_no-intron	GCAGCCAGAATAATGCAATCACG
5WP-16	TF2_seq 4_rv	PAS_chr4_0271/ PAS_chr4_0271_no-intron	GGTGATACTTTCAGGGATATTGAC
5WP-17	TF2_seq 5_rv	PAS_chr4_0271/ PAS_chr4_0271_no-intron	GGTATCATTCTGAGGTGGGATTGG
5WP-18	TF2_seq 6_rv	PAS_chr4_0271/ PAS_chr4_0271_no-intron	GGCTCAGCACATGAGAGTAGC
5WP-19	TF3_seq 1_fw	PAS_chr4_0540	CCAAAGGGCTACACCAAGAATCTG
5WP-20	TF3_seq 2_fw	PAS_chr4_0540	GTTGATGGGTTCAGAAAGTATTTCG
5WP-21	TF3_seq 3_fw	PAS_chr4_0540	CACTGACAGTGATGAGCTCAGTG
5WP-22	TF3_seq 4_fw	PAS_chr4_0540	CCAAGCTCGCTTTTTGGAAGTTAC
5WP-23	TF3_seq 5_rv	PAS_chr4_0540	CGGGTTGATTGTTGGTTCTTGTTTG
5WP-24	TF3_seq 6_rv	PAS_chr4_0540	GAGAAATTAGCTTGGATCGCAGC
5WP-25	TF3_seq 7_rv	PAS_chr4_0540	GACAATAAAGCACTGTTCAAACTCG
5WP-26	TF3_seq 8_rv	PAS_chr4_0540	GAACTACGTGTCAGCCTGTCACTG
5WP-27	TF4_seq 1_fw	PAS_chr4_0324	CCATCCAAGCTTTCTAGAGAGACGG
5WP-28	TF4_seq 2_fw	PAS_chr4_0324	CCAATTGTTATATGCTGTGTTTGCC
5WP-29	TF4_seq 3_fw	PAS_chr4_0324	GGAATGCAATGCTCAAAGTAACAAC

[2] TF2 and TF5 sequencing primer were used for sequencing of TF2, TF5, TF2_no-intron and TF5_short-version

5WP-30	TF4_seq 4_fw	PAS_chr4_0324	GGTGTAGACATGTTGGATCCGAG
5WP-31	TF4_seq 5_rv	PAS_chr4_0324	CCACCATGATGATATTTGGAGCTTG
5WP-32	TF4_seq 6_rv	PAS_chr4_0324	GGTAATAAAGCATTGCTCAGATCGG
5WP-33	TF4_seq 7_rv	PAS_chr4_0324	CCACCTGAGACCTAAAATGAGAATC
5WP-34	TF4_seq 8_rv	PAS_chr4_0324	GCATCCCCTGATTGATCACCAAC
5WP-35	TF5_seq 1_fw	PAS_chr4_0425/ PAS_chr4_0425_short-version	GGTGCATTTTTAGCCTATATTTGGC
5WP-36	TF5_seq 2_fw	PAS_chr4_0425/ PAS_chr4_0425_short-version	GCTCTGAAAACTTAGAATCTGGTG
5WP-37	TF5_seq 3_rv	PAS_chr4_0425/ PAS_chr4_0425_short-version	CGTCACATTGAAATTCTTCGATGC
5WP-38	TF5_seq 4_rv	PAS_chr4_0425/ PAS_chr4_0425_short-version	GCAGAGTTGATAGAGTCCTCTGTG
5WP-39	TF6_seq 1_fw	PAS_chr2-1_0114	GCAGGAAAGGATGTACGACTTGC
5WP-40	TF6_seq 2_fw	PAS_chr2-1_0114	GGATTTTCCACGTTAAGGGAGC
5WP-41	TF6_seq 3_fw	PAS_chr2-1_0114	CCCAGTCTGGCCTTTTGGATAC
5WP-42	TF6_seq 4_rv	PAS_chr2-1_0114	CCTCCTCCTCCCGAATACTCG
5WP-43	TF6_seq 5_rv	PAS_chr2-1_0114	CGTAGGAGACGTAGAGCATCG
5WP-44	TF6_seq 6_rv	PAS_chr2-1_0114	GGTATTTCCGCTTGCCCTTGG
5WP-46	*CYC1*TT_seq_rv	*CYC1*-transcription terminator region	CTGTCAAGGAGGGTATTCTGGG
5WP-68	pGAP_seqnew_fw	P_{GAP} region	GGCTGATCAGGAGCAAGCTCG

Table 12: Instruments and devices

Instrument type	Instrument name	Source
Analytical balance	Electronic Balance ABS 220-4	Kern & Sohn GmbH, Balingen, Germany
Autoclave	V150	Systec GmbH, Wettenberg, Germany
Bench scale	FCB 3K0.1	Kern & Sohn GmbH, Balingen, Germany
Centrifuge	Centrifuge 5415 R	Eppendorf AG, Hamburg, Germany
Centrifuge	Centrifuge 5810 R	Eppendorf AG, Hamburg, Germany
Centrifuge (Rotor JA 10)	Avanti J-20XP Centrifuge	Beckman Coulter GmbH; Vienna, Austria
Certoclave	Certoclave	Certoclave Steriliser GmbH, Traun, Austria
Electrophoresis cell	Sub-Cell® GT	Bio-Rad Laboratories

		GmbH, Vienna, Austria
Electrophoresis instruments	PowerPac™ Basic Power Supply	Bio-Rad Laboratories GmbH, Vienna, Austria
Electroporator	MicroPulser™	Bio-Rad Laboratories GmbH, Vienna, Austria
Incubator (30 °C)	Incubator with mechanical control	Binder GmbH, Tuttlingen, Germany
Incubator (37 °C)	Type BVW 50	Memmert, Schwabach, Germany
Laminar flow	Biological safety cabinet	Clean Air Products, Minneapolis, USA
Magnetic stirrer	IKA® RCT basic safety control	IKA®-Werke GmbH & Co. KG, Staufen, Germany
Micro centrifuge	Rotilabo®-mini-centrifuge	Carl Roth GmbH, Karlsruhe, Germany
Microplate reader	Synergy Mx monochromator-based multi-mode microplate reader	BioTek Instruments, Winooski, USA
Mini centrifuge	Mini Centrifuge MCF-2360	LMS Co., Tokyo, Japan
Nanodrop	NanoDrop 2000c spectrophotometer	Peqlab Biotechnologie GmbH, Polling, Austria
PCR machine	Gene Amp® PCR Systems 2700	Applied Biosystems, Foster City, USA
PCR machine	2720 Thermal Cycler	Applied Biosystems, Foster City, USA
pH-electrode	Polyplast Temp Din	Hamilton Messtechnik GmbH, Höchst, Germany
pH-meter	inoLab pH 720	WTW GmbH, Weilheim, Germany
Photometer	Eppendorf Biophotometer	Eppendorf AG, Hamburg, Germany
Photometer	Eppendorf Biophotometer plus	Eppendorf AG, Hamburg, Germany
Platform rocker	Grant-Bio PMR-30 platform rocker	Grant Instruments, Cambridgeshire, UK
Precision balance	GP3202	Sartorius Austria GmbH, Vienna, Austria
Shaker	Certomat® BS-1	Sartorius BBI Systems GmbH, Melsungen, Germany
Shaker (28 °C and 37 °C)	Orbitron	Infors AG, Bottmingen, Switzerland
Shaker for DWPs (28 °C)	Multitron	Infors AG, Bottmingen,

		Switzerland
Thermomixer	Thermomixer comfort	Eppendorf AG, Hamburg, Germany
Titramax	Titramax 1000	Heidolph Instruments GmbH, Schwabach, Germany
Turntable for petridishes	Petriturn M-plus	schuett-biotec GmbH, Göttingen, Germany
Ultrapure Water System	arium ® basic T	Sartorius AG, Göttingen, Germany
UV lamp	Vilber Lourmat electronic ballast transilluminators ECX-F20.M	Sigma-Aldrich Handels GmbH, Vienna, Austria
UV-Transilluminator – Fisherbrand FT-28/312	Fisherbrand® UV-Transilluminator FT28/312	Fisher Scientific, GmbH, Schwerte, Germany
Vortex	Vortex-Genie2	Scientific Industries, New York, USA
Vortex (12 wells)	Vortex-Genie2	Scientific Industries, New York, USA

Table 13: Additional devices

Name	**Source**
Bacterial cell spreader	Carl Roth GmbH, Karlsruhe, Germany
Baffled flask (250 mL and 2000 mL)	Kavalierglass, Co.Ltd, Sázava, Czech Republic
Biohit optifit tip 1200 µL	Sartorius Biohit Liquid Handling OY, Helsinki, Finland
Cryo.S, 2 mL, PP, round bottom, external thread natural screw cap, sterile	Greiner Bio-One GmbH, Frickenhausen, Germany
Denville XL 3000i™ pipette (0.1 µL – 2 µL)	Denville Scientific Inc., South Plainfield, USA
Denville XL 3000i™ pipette (100 µL – 1000 µL)	Denville Scientific Inc., South Plainfield, USA
Denville XL 3000i™ pipette (2 µL – 20 µL)	Denville Scientific Inc., South Plainfield, USA
Denville XL 3000i™ pipette (20 µL – 200 µL)	Denville Scientific Inc., South Plainfield, USA
DURAN® baffled flask GL 45 (250 mL, 1.000 mL and 2.000 mL)	Duran Group GmbH, Wertheim/Main, Germany
DURAN® laboratory bottle GL 45 (100 mL, 500m, 1.000 mL and 2.000 mL)	Duran Group GmbH, Wertheim/Main, Germany
Electroporation cuvettes	Hanke Laboratory Products, Vienna, Austria
Finnpipette Novus (30 µL – 300 µL, 8 channel)	Thermo Fisher Scientific, New York, USA
Gas Permeable Adhesive Seals	Fisher Scientific - Austria GmbH, Vienna, Austria

GL 45 screw caps	Duran Group GmbH, Wertheim/Main, Germany
Glass beads	Retsch, Haan, Germany
Injekt® Solo 20 mL	B. Braun Austria GmbH, Maria Enzersdorf, Austria
Injekt® Solo 5 mL	B. Braun Austria GmbH, Maria Enzersdorf, Austria
Ino-Loop	Simport, Beloeil, Canada
MF™-membrane filter	Merck Millipore, Darmstadt, Germany
Micro tube 1.5 mL	Sarstedt AG & Co., Nümbrecht, Germany
Nalgene® labware 500 mL PPCO centrifuge bottle	Thermo Scientific, Rochester, USA
Nunc-Immuno™ MicroWell™ 96 well solid plates	SIGMA-ALDRICH Handels GmbH, Vienna, Austria
OmniTray w/lid, sterile, PS	Thermo Fisher Scientific, New York, USA
PCR – strip, 8 well, 0.2 mL	Greiner Bio-One GmbH, Kremsmünster, Austria
Peqlab peqPETTE 10E pipette (0.5 µL – 10 µL)	PEQLAB Biotechnologie GmbH, Erlangen, Germany
Petri dish	Greiner Bio-One GmbH, Kremsmünster, Austria
Picus electronic pipette (50 µL – 1200 µL, 8-channel)	Sartorius Biohit Liquid Handling OY, Helsinki, Finland
Pipetboy	Integra Biosciences GmbH, Fernwald, Germany
Pipette tip universal 200µL	Greiner Bio-One GmbH, Kremsmünster, Austria
Pipette with tip, sterile, 10 mL	Greiner Bio-One GmbH, St. Gallen, Switzerland
Pipette with tip, sterile, 25 mL	Greiner Bio-One GmbH, St. Gallen, Switzerland
Pipette with tip, sterile, 5 mL	Greiner Bio-One GmbH, St. Gallen, Switzerland
PP-microplate, 96 well, V-shape	Greiner Bio-One GmbH, Frickenhausen, Germany
PP-tube, sterile, 50 mL	Greiner Bio-One GmbH, Frickenhausen, Germany
PP-tube, sterile, cap, 12 mL	Greiner Bio-One GmbH, Frickenhausen, Germany
PP-tube, sterile, skirt, 50 mL	Greiner Bio-One GmbH, Frickenhausen, Germany
Proline electronic pipette	Sartorius Biohit Liquid Handling OY, Helsinki,

(50 µL – 1,200 µL, multichannel)	Finland
Proline plus mechanical pipette (30 µL – 300µL, multichannel)	Sartorius Biohit Liquid Handling OY, Helsinki, Finland
PS-microplate, sterile, 96 well, flat bottom	Greiner Bio-One GmbH, Frickenhausen, Germany
PS-semi-micro-cuvette, 1.6 mL	Greiner Bio-One GmbH, Kremsmünster, Austria
Replicator	Enzyscreen, Haarlem, the Netherlands
Rotilabo®-sealing films	Carl Roth GmbH, Karlsruhe, Germany
Rotilabo®-syringe filters, CME, sterile	Carl Roth GmbH, Karlsruhe, Germany
Scienceware® 96 deep-well plate	Best Lab Deals Inc, Garner, USA
SILVERseal™ aluminium film	Greiner Bio-One GmbH, Frickenhausen, Germany
Sterican® Ø 0.80 * 120 mm	B. Braun Austria GmbH, Maria Enzersdorf, Österreich
Toothpick flat and round	Decor Service GmbH, Bad Radkersburg, Austria
Trifill multi channel pipettor reservoir	CamLab, Cambridge, UK
Tube strips 0.2 mL with domed cap strips	Peqlab, Erlangen, Germany
Whatman® UNIPLATE microplates 24 well (10 mL)	Sigma-Aldrich, Chemie GmbH, Schnelldorf, Germany

Table 14: Kits used for plasmid isolation and DNA purification

Kit	**Source**
GeneJET™ Plamid Miniprep Kit	Thermo Scientific, Vienna, Austria
QIAquick® Gel Extraction Kit	Qiagen GmbH, Hilden, Germany
QIAquick® PCR Purification Kit	Qiagen GmbH, Hilden, Germany

Table 15: Software used for *in silico* cloning and data analysis

Software	**Source**
EXCEL	Microsoft Corp.
Gen5 1.11 – Data Analysis Software	BioTek
IDT Oligoanalyzer 3.1	http://eu.idtdna.com/analyzer/Applications/OligoAnalyzer/
Lasergene SeqBuilder	DNASTAR, Inc.
Launch Doc-ItLS – Image Analysis Software	UVP
Nanodrop 2000	Thermo Scientific
SnapGene	GSL Biotech LLC

Table 16: Reagents

Name	Source
1,4-Dithiothreitol (DTT)	Carl Roth GmbH, Karlsruhe, Germany
6x DNA Loading Dye	Thermo Scientific, Vienna, Austria
Acetic acid	Carl Roth GmbH, Karlsruhe, Germany
Albumin Fraktion V ≥98 %	Carl Roth GmbH, Karlsruhe, Germany
Ammonium acetate	Sigma-Aldrich Chemie GmbH, Schnelldorf, Germany
Aqua bidest. „Fresenius"	Fresenius Kabi Austria GmbH, Graz, Austria
Bacto™ agar	Becton, Dickinson and Company, Sparks, USA
Bacto™ peptone	Becton, Dickinson and Company, Sparks, USA
Bacto™ yeast extract	Becton, Dickinson and Company, Sparks, USA
Bicine	Carl Roth GmbH, Karlsruhe, Germany
Biotin (B)	Carl Roth GmbH, Karlsruhe, Germany
Biozym LE agarose	Biozym BioTech Trading GmbH, Vienna, Austria
Calciumchlorid ($CaCl_2 \cdot 2\ H_2O$)	Carl Roth GmbH, Karlsruhe, Germany
Citric acid monohydrate ($C_6H_8O_7 \cdot H_2O$)	Carl Roth GmbH, Karlsruhe, Germany
Deoxyadenosine triphosphate (dATP)	Carl Roth GmbH, Karlsruhe, Germany
Deoxycytidine triphosphate (dCTP)	Carl Roth GmbH, Karlsruhe, Germany
Deoxyguanosine triphosphate (dGTP)	Carl Roth GmbH, Karlsruhe, Germany
Deoxynucleotide triphosphate (dNTP Set)	Thermo Scientific, Vienna, Austria
Deoxythymidine triphosphate (dTTP)	Carl Roth GmbH, Karlsruhe, Germany
D-Glucose-monohydrate (D)	Carl Roth GmbH, Karlsruhe, Germany
Di-ammoniumhydrogenphosphate ($(NH_4)_2HPO_4$)	Carl Roth GmbH, Karlsruhe, Germany
di-Potassium hydrogen phosphate (K_2HPO_4)	Carl Roth GmbH, Karlsruhe, Germany
di-Sodium hydrogen phosphate (Na_2HPO_4)	Carl Roth GmbH, Karlsruhe, Germany
di-Sodium hydrogen phosphate dihydrate ($Na_2HPO_4 \cdot 2\ H_2O$)	Carl Roth GmbH, Karlsruhe, Germany
di-sodiumhydrogenphosphate-dihydrate ($Na_2HPO_4 \cdot 2\ H_2O$)	Carl Roth GmbH, Karlsruhe, Germany
D-Sorbitol	Carl Roth GmbH, Karlsruhe, Germany
Ethidium bromide	Carl Roth GmbH, Karlsruhe, Germany
Ethylene glycol	Carl Roth GmbH, Karlsruhe, Germany
Ethylenediaminetetraacetic acid (EDTA)	Carl Roth GmbH, Karlsruhe, Germany
FeedBeads® Glucose (Ø 12mm), pack of 25	Adolf Kühner AG, Basel, Switzerland

GeneRuler DNA ladder mix	Thermo Scientific, Vienna, Austria
Glycerol	Carl Roth GmbH, Karlsruhe, Germany
Hydrochloric acid (HCl)	Carl Roth GmbH, Karlsruhe, Germany
Isopropanol	Carl Roth GmbH, Karlsruhe, Germany
J. T. Baker ® Ethanol absolute	VWR International GmbH, Vienna, Austria
Liquid nitrogen	Air Liquide Austria GmbH, Graz, Austria
Magensiumsulphate-heptahydrate ($MgSO_4 \cdot 7\ H_2O$)	Carl Roth GmbH, Karlsruhe, Germany
Magnesium chloride ($MgCl_2$)	Carl Roth GmbH, Karlsruhe, Germany
Magnesium sulphate ($MgSO_4$)	Carl Roth GmbH, Karlsruhe, Germany
Methanol (MeOH)	Carl Roth GmbH, Karlsruhe, Germany
Nicotinamide adenine dinucleotide (NAD)	Carl Roth GmbH, Karlsruhe, Germany
PEG-8000	Sigma-Aldrich Chemie GmbH, Schnelldorf, Germany
Phosphatase substrate pNPP (4-Nitrophenyl phosphate) disodium salt hexahydrate [5 mg tablets]	Sigma-Aldrich Handels GmbH, Vienna, Austria
Potassium chloride (KCl)	Carl Roth GmbH, Karlsruhe, Germany
Potassium dihydrogen phosphate (KH_2PO_4)	Carl Roth GmbH, Karlsruhe, Germany
Potassium hydroxide (KOH)	Carl Roth GmbH, Karlsruhe, Germany
Purified Human Fab/Kappa [1 mg/mL]	Bethyl Laboratories, Inc., Montgomery, USA
Pyridoxal-5-phosphate (PLP)	Sigma-Aldrich Chemie GmbH, Schnelldorf, Germany
Roti®-Phenol/Chloroform/Isoamylalkohol (25:24:1)	Carl Roth GmbH, Karlsruhe, Germany
Rotilabo®-sealing film, microtest plates	Carl Roth GmbH, Karlsruhe, Germany
Sodium carbonate (Na_2CO_3)	Carl Roth GmbH, Karlsruhe, Germany
Sodium chloride (NaCl)	Carl Roth GmbH, Karlsruhe, Germany
Sodium dihydrogen phosphate (NaH_2PO_4)	Carl Roth GmbH, Karlsruhe, Germany
Sodium dodecyl sulphate (SDS)	Carl Roth GmbH, Karlsruhe, Germany
Sodium hydrogen carbonate ($NaHCO_3$)	Carl Roth GmbH, Karlsruhe, Germany
Sodium hydroxide (NaOH)	Carl Roth GmbH, Karlsruhe, Germany
TMB (3,3',5,5'-tetramethylbenzidine) One Component Substrate	Bethyl Laboratories, Inc., Montgomery, USA
TRIS	Carl Roth GmbH, Karlsruhe, Germany
Triton X-100	Carl Roth GmbH, Karlsruhe, Germany
Tween® 20	Carl Roth GmbH, Karlsruhe, Germany

Table 17: Solutions and buffers

Name	Components
10x D	220 g/L D-glucose-monohydrate
500x Biotin	200 mg/L biotin
Ammonium acetate, 4 M	308.32 g/L ammonium acetate
BEDS solution	1.632 g/L bicine-NaOH, pH 8.3, 3 % (v/v) ethylene glycol, 5 % (v/v) DMSO, 182 g/L D-sorbitol
Blocking-solution (ELISA protocol 1)	50 mM Tris, 0.14 M NaCl, 1 % BSA, pH 8
Coating-buffer (ELISA protocol 1)	0.05 M sodium carbonate – sodium hydrogen carbonate (Na_2CO_3, $NaHCO_3$), pH 9.6
Coating-buffer (ELISA protocol 2)	1.8 g/L $Na_2HPO_4 \cdot 2\ H_2O$, 0.24 g/L KH_2PO_4, 0.2 g/L KCl, 8.0 g/L NaCl
Detection-buffer (ELISA protocol 2)	8.4 g/L $NaHCO_3$, 4.0 g/L Na_2CO_3
Dilution-buffer (ELISA protocol 2)	1.8 g/L $Na_2HPO_4 \cdot 2\ H_2O$, 0.24 g/L KH_2PO_4, 0.2 g/L KCl, 8.0 g/L NaCl, 20 g/L BSA, 1 mL/L Tween20
Dilution-solution (ELISA protocol 1)	50 mM Tris, 0.14 M NaCl, 1 % BSA, pH 8, 0.05 % Tween 20
Dithiothreitol (DTT), 1 M	152.2 g/L DTT
Ethanol, 70 %	70 % (v/v) ethanol
Gibson assembly master mix	320 µL 5x ISO reaction buffer, 0.64 µL T5 exonuclease, 20 µL Phusion® high-fidelity DNA polymerase, 160 µL *Taq* DNA ligase, 699.36 µL ddH_2O ➔ aliquot 15 µL each into PCR tubes ➔ stored at – 20 °C
Glycerol, 10 %	100 g/L glycerol
Glycerol, 60 %	600 g/L glycerol
Isothermal reaction buffer (5x)	1.5 g PEG-8000, 3,000 µL 1 M Tris/HCl pH 7.5, 150 µL 2 M $MgCl_2$, 300 µL 1 M DTT, 60 µL 100 mM dATP, 60 µL 100 mM dCTP, 60 µL 100 mM dGTP, 60 µL 100 mM dTTP, 300 µL 100 mM NAD, up to 6 mL with ddH_2O ➔ aliquot 100 µL each into sterile tubes ➔ stored at – 20 °C
Sodium phosphate buffer pH 7.5 (SPB), 100 mM	21.76 g/L Na_2HPO_4, 2.6 g/L NaH_2PO_4, pH 7.5
Sorbitol, 1 M	182.18 g/L D-sorbitol

TE buffer	1.21 g/L TRIS-HCl, pH 7.5, 0.29 g/L EDTA, pH 8.0
Tris(hydroxymethyl)-aminomethan (TRIS), 1 M	121,14 g/L TRIS
TRIS-Acetat-EDTA buffer (TAE)	20 mL/L 50x TAE buffer
Washing-buffer (ELISA protocol 1)	50 mM Tris, 0.14 M NaCl, 0.05 % Tween 20, pH 8
Washing-buffer (ELISA protocol 2)	1.8 g/L $Na_2HPO_4 \cdot 2\ H_2O$, 0.24 g/L KH_2PO_4, 0.2 g/L KCl, 8.0 g/L NaCl, 1 mL/L Tween20
Yeast lysis buffer	20 mL Triton X-100, 100 mL 10 % SDS, 20 mL 5 M NaCl, 2 mL 0.5 M EDTA, 10 mL 1 M TRIS-HCl pH 8, distilled water to 1 L

Table 18: Media used for cultivation of bacteria and yeast strains

Medium name	**Components**
LB agar	5 g/L NaCl, 10 g/L tryptone/peptone, 5 g/L yeast extract, 15 g/L bacto agar
LB amp agar	5 g/L NaCl, 10 g/L tryptone/peptone, 5 g/L yeast extract, 15 g/L bacto agar, 100 μg/mL ampicillin
LB kan agar	5 g/L NaCl, 10 g/L tryptone/peptone, 5 g/L yeast extract, 100 μg/mL kanamycin
LB liquid medium	5 g/L NaCl, 10 g/L tryptone/peptone, 5 g/L yeast extract
M2	3.15 g/L $(NH_4)_2HPO_4$), 0.49 g/L $MgSO_4 \cdot 7\ H_2O$, 0.80 g/L KCl, 0.0268 g/L $CaCl_2 \cdot 2\ H_2O$, 22.0 g/L $C_6H_8O_7 \cdot H_2O$, 1.470 mL PTM1, 500x Biotin → dissolved in H_2O →pH 5 with KOH →filled up to 1000 g with H_2O →sterilized by filtration
M2D	3.15 g/L $(NH_4)_2HPO_4$, 0.49 g/L $MgSO_4 \cdot 7\ H_2O$, 0.80 g/L KCl, 0.0268 g/L $CaCl_2 \cdot 2\ H_2O$, 22.0 g/L $C_6H_8O_7 \cdot H_2O$, 1.470 mL PTM1, 500x Biotin, 22.0 g/L D-Glucose-monohydrate → dissolved in H_2O →pH 5 with KOH →filled up to 1000 g with H_2O →sterilized by filtration

PTM1	5.00 mL/L H_2SO_4 <95%, 65.00 g/L $FeSO_4 \cdot 7\ H_2O$, 20.00 g/L $ZnCl_2$, 6.00 g/L $CuSO_4 \cdot 5\ H_2O$, 3.36 g/L $MnSO_4 \cdot H_2O$, 0.820 g/L $CoCl_2 \cdot 6\ H_2O$, 0.20 g/L $Na_2MoO_4 \cdot 2\ H_2O$, 0.080 g/L NaI, 0.020 g/L H_3BO_3
SOC liquid medium	20 g/L tryptone, 0.58 g/L NaCl, 5 g/L yeast extract, 2 g/L $MgCl_2$, 0.18 g/L KCl, 2.46 g/L $MgSO_4$, 3.46 g/L D
YPD gen/zeo agar	10 g/L bacto yeast extract, 20 g/L bacto peptone, 15 g/L bacto agar, 100 mL/L 10x D, 450 μg/mL geniticin, 50 μg/mL zeocin
YPD liquid medium	10 g/L bacto yeast extract, 20 g/L bacto peptone, 100 mL/L 10x D
YPD agar	10 g/L bacto yeast extract, 20 g/L bacto peptone, 15 g/L bacto agar, 100 mL/L 10x D
YPD zeo agar	10 g/L bacto yeast extract, 20 g/L bacto peptone, 15 g/L bacto agar, 100 mL/L 10x D, 50 μg/mL zeocin

2.2.Methods

2.2.1. Cloning

2.2.1.1. Plasmid Isolation

The GeneJET™ kit from Thermo Scientific was used for plasmid isolation. Isolation was performed according to the manufacturer's manual except for the elution step, which was done with distilled deionized water (ddH_2O).

2.2.1.2. DNA Purification

DNA purification from preparative agarose gels was performed with the QIAquick Gel Extraction kit according to the manufacturer's protocol. DNA purification of PCRs and restriction enzyme approaches was performed with the QIAquick PCR Purification Kit according to the manufacturer's protocol. The isopropanol step was skipped for fragments with a size below 500 bp and over 4 kb.

2.2.1.3. Isolation of gDNA from *P. pastoris*

For the isolation of gDNA from *P. pastoris*, an adapted version from Hoffman and Winston (1987) was used[70].

The following steps were performed:

A 7 mL starter yeast culture (*P. pastoris* CBS 7435) was grown overnight in YPD at 28 °C. Cells were spun down at 1500 rpm at RT. The supernatant was decanted and the pellet was resuspended in 0.5 mL sterile distilled water. The cell suspension was transferred to a 1.5 mL Eppendorf tube and spun down at 13200 rpm for 5 s. The supernatant was decanted and

pellet was vortexed in residual water. Then, 200 µL Yeast lysis buffer, 200 µL phenol:chloroform:isoamyl alcohol (25:24:1) and 0.3 g of acid washed beads were added. The suspension was vortexed for 3-4 min. Then, 200 µL of TE buffer were added. The resulting suspension was spun down at 13,200 rpm for 5 min and aqueous phase was transferred to a new tube. Afterwards, 1 mL of EtOH was added and mixed by inversion. The solution was spun down for 1 min and supernatant was aspirated. The gained pellet was resuspended in 400 µL TE buffer and 5 µL RNAse A [10 mg/mL] and incubated for 4 to 5 h. Ten µL of 4 M ammonium acetate and 1 mL 100 % EtOH were added and mixed by inversion. The supernatant was discarded after 1 min of centrifugation. The obtained pellet was washed with 1 mL ice-cold 70 % EtOH and resuspended in 50 µL ddH_2O.

2.2.1.4. Polymerase Chain Reaction (PCR)

Phusion™ High Fidelity DNA Polymerase was use for all PCRs. Conditions depended on the used template and are shown in Table 19. For all PCRs a total volume of 50 µL was used. PCR cycling conditions and pipetting instructions were performed according to the Thermo Scientific Phusion™ High-Fidelity DNA Polymerase guidelines. Primer annealing temperature was calculated using IDT oligoanalyzer 3.1. Extension time depended on length and complexity of the template used for PCR. For plasmid DNA 10 s per 1 kb were used. For gDNA 20 s per 1 kb were used. Components and pipetting instructions for PCR reactions are shown in Table 20.

Table 19: PCR conditions for Phusion polymerase

Condition	Temperature	Time	Cycle number
Initial denaturation	98 °C	30 s	1
Denaturation	98 °C	10 s	35
Annealing	50-60 °C	20 s	
Extension	72 °C	15 – 30 s/kb	
Final extension	72 °C	3 min	1
Final hold	4 °C	∞	-

Table 20: Reaction mixture for PCR

Component	Volume / 50 µL reaction	Final Concentration
Template	10 – 20 ng plasmid DNA 100 – 200 ng gDNA	-
Phusion DNA polymerase [2 U/µL]	0.5 µL	0.02 U/µL (Phusion)
2 mM dNTPs	5 µL	200 µM
5 µM Primer forward	2.5 µL	0.5 µM
5 µM Primer reverse	2.5 µL	0.5 µM
5x HF Buffer	10 µL	1x HF Buffer
ddH_2O	up to 50 µL	up to 50 µL

2.2.1.5. DNA Restriction, Control and Preparative Gels

Digestion of DNA fragments was performed for 15 – 30 min at the temperature recommended in the respective enzyme manual. The inactivation step was not performed. Only Fast Digest enzymes were used (Table 5).

In order to determine the size of DNA fragments or PCR products the samples were visualised on an agarose gel. GeneRuler™ DNA ladder mix from Thermo Scientific was the used standard as shown in chapter Appendix 5.1 DNA Ladder. Agarose gels (1 %) were used for control as well as for preparative gels. Consequently, 2 g agarose were weighed into a flask and 200 mL 1x TAE buffer were added. The mixture was heated using a microwave until the agarose was molten (~ 4 min, highest power level) and cooled using tap water. Afterwards, two drops of ethidium bromide [1 mg/mL] were added. The solution was mixed and poured into a gel chamber. Control gels were run at 120 V for about 1 h. In order to determine the exact band sizes of linearized plasmid construct with sizes over 5 kb, performance time was extended up to 3 h at 80 V. For control gels, an aliquot of the samples (2 µL), was mixed with 10 µL 1x DNA loading dye. Alternatively, control restrictions for fast determination of fragment sizes were performed with 10X Fast Digest Green Buffer for direct loading of samples on the agarose gels. Preparative gels, from which the samples were further isolated, were run at 80 V for about 2 h to obtain a good separation of the DNA fragments. For the purification of DNA via a gel the whole PCR mixture (50 µL) was mixed with 10 µL of 6x mass ruler DNA loading dye and loaded onto. Gels were analysed under UV light. Desired bands were cut using a scalpel and tweezers under low intensity UV-light to avoid damage of the DNA. Cut bands were purified according to section 2.2.1.2 DNA Purification. After cutting, an image was taken from the gel using the UV-Transilluminator with the software Launch Doc-ItLS.

2.2.1.6. Preparation of Electrocompetent *E. coli* TOP10F' cells

For the preparation of electrocompetent *E. coli* cells, an in-house protocol was used.

- **Day 1: Growing the cells 1**

Two 30 mL overnight cultures (ONCs) from a single colony were inoculated in 100 mL flasks and incubated at 37 °C and 220 rpm overnight. Reaction tubes, 1 L sterile deionised water and 40 mL sterile 10 % glycerol and sterile 500 mL centrifuge bottles (2 per 500 mL main culture) were placed in the 4 °C room.

- **Day 2: Growing the cells 2**

500 mL LB medium were inoculated in a 2 L baffled flask to an OD_{600} of 0.1 and incubated under the same conditions. Centrifuge rotor and the centrifuge bottles were cooled to 4 °C. OD_{600} value was measured in the meantime. The cell suspension should reach an OD_{600} of 0.8 (harvest after 5 – 6 h): At this point work was continued on ice or at 4 °C. Cell cultures

were transferred from the baffled flasks to the centrifuge bottles (250 mL in each bottle) and were put on ice for 30 min at 4 °C.

- **Day 2: Harvesting and Washing the cells**

Cells were centrifuged at 2000 x g and 4 °C for 15 min. Supernatants were discarded and pellets resuspended in 250 mL sterile, ice-cold water. Last step was repeated 2 times ending up with discarding the supernatant. Cells were resuspended in one bottle in 35 mL cold, sterile 10 % glycerol using a pre-chilled, sterile 25 mL pipette and cell suspension was transferred to second bottle and resuspended again. Cells were centrifuged at 4000 x g and 4 °C for 15 min. The 10 % glycerol was decanted and tubes were placed on ice. Each cell pellet was resuspended in 1 mL cold, sterile 10 % glycerol. Cell suspensions were pooled.

- **Day 2: Aliquoting and storage of cells**

A liquid N_2 bath was prepared. Sterile Sarstedt Micro tubes were pre-chilled at 4 °C and 100 µL of cell suspension were aliquoted. Tubes were quickly frozen in liquid N_2. Frozen tubes were stored at -80 °C until use. In order to determine the transformation rate of electrocompetent *E. coli* TOP10F' cells, 1 µL of pUC19 [10 pg/µL] was transformed into 80 µL of electrocompetent cells and plated out on LB amp plates and incubated over night at 37 °C.

2.2.1.7. Construction of Plasmids using Gibson Cloning

The cloning of 8 *P. pastoris* TF genes into the pPUZZLE expression vector, which are listed in Table 21, was performed using Gibson cloning. The selection procedure of the target genes is described in section 1.4.1.

Table 21: TF target hit list

Abbrevation	Probe_ID	Annotation	Zinc Finger
TF1	PAS_chr4_0626	Gat1p	Yes
TF2	PAS_chr4_0271	Gat2p	Yes
TF3	PAS_chr4_0540	Cat8p (could also be Sit4p)	Yes
TF4	PAS_chr4_0324	NA (YRM1)	Yes
TF5	PAS_chr4_0425	NA	Yes
TF6	PAS_chr2-1_0114	Upc2p	Yes
TF2ni (no intron)	PAS_chr4_0271	Gat2p	Yes
TF5sv (short version)	PAS_chr4_0425	NA	Yes

Gibson cloning is a method to combine double stranded DNA fragments via overlapping sequences generated by PCR. The overlapping regions of 30 – 40 bp were created by PCR using primers with sizes over 60 bp. The reaction was performed in one step using a premixed Gibson-mastermix with T5 exonuclease, DNA polymerase and *Taq* ligase (Table 6 and 17). Exonuclease digests 5' ends of the fragments, which were vector and insert for this approach in order to allow pairing of complementary regions. The polymerase fills up

missing nucleotides before the ligase repairs the left nicks (Figure 2). According to the manual, vector concentrations lower than 100 ng decrease the transformation rate[71]. In total, 5 µL of vector and insert in a molecular ratio of 1:3 were added to a 15 µL Gibson assembly master mix and incubated at 50 °C for 60 min. All primers used for the design of the plasmids are listed in Table 9.

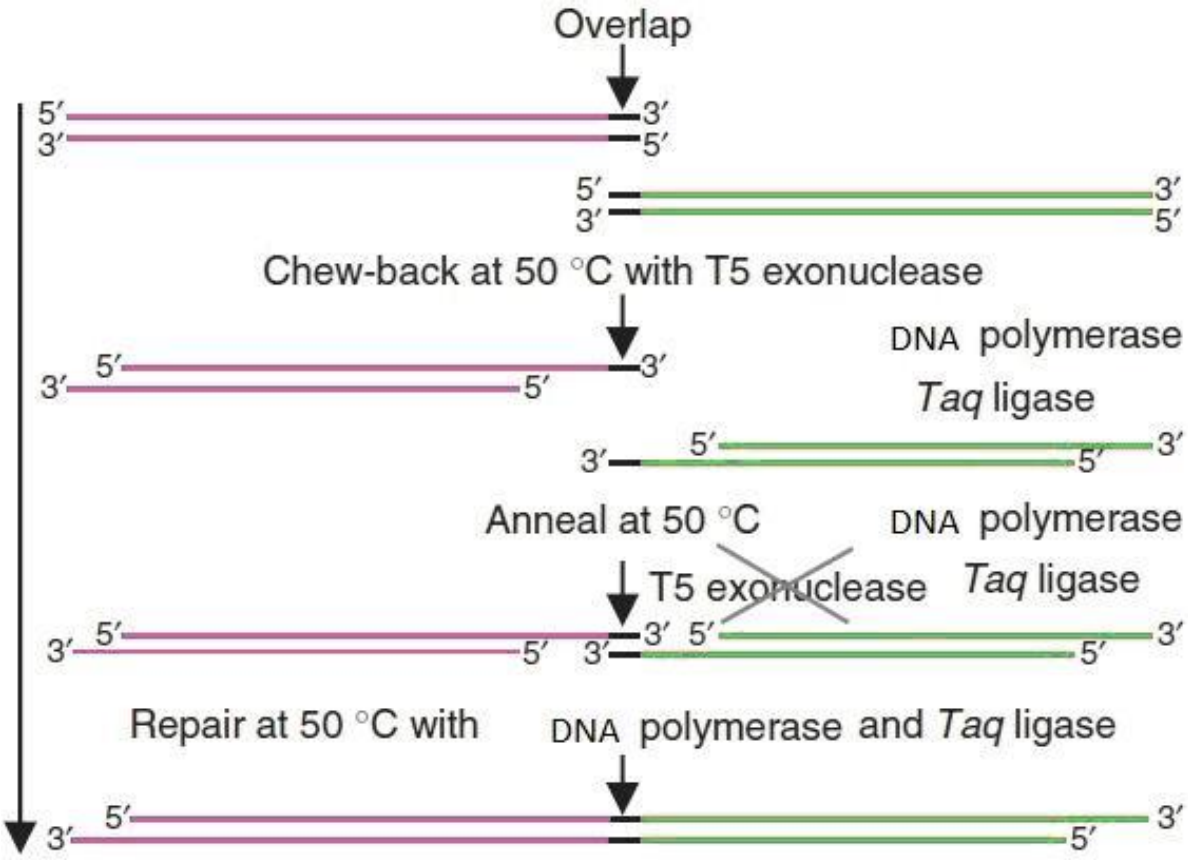

Figure 2: Reaction mechanism of Gibson cloning procedure. Exonuclease digests 5' ends of the fragments, which were vector and insert for this approach in order to allow pairing of complementary regions. The polymerase fills up missing nucleotides and the ligase seals nicks between vector and insert[71].

2.2.1.8. Transformation of Electrocompetent *E. coli* TOP10F' Cells

For the transformation of *E. coli* TOP10F' cells with pPUZZLE-constructs, electroporation cuvettes were precooled on ice. Eighty µL of electrocompetent *E. coli* TOP10F' cells were pipetted into the cuvette. Five µL of filter-desalted or 3 µl of Gibson assembly mixture were added to the competent cells without determination of concentration. The cell suspension was incubated on ice for approximately 15 min. EC-2 (2,000 V, 25 µF and 200 Ω) program was used for the electro transformation. Afterwards, 1 mL of SOC (Super Optimal broth with Catabolite repression) medium was added to the cells, which were regenerated for 1 h at 37 °C and 600 rpm. After regeneration, 20 µL and 120 µL were plated on LB Kan agar plates [100 µg/mL kanamycin]. Plates were then incubated at 37 °C overnight. Plasmids were isolated according to section 2.2.1.1. Isolated plasmids were sent for sequencing to Microsynth AG Austria (http://www.microsynth.ch/). Sequencing results were analysed with

Lasergene SeqMan and SeqBuilder software from DNASTAR. Correct plasmid constructs were stored in the IMBT culture collection (Table 4).

2.2.1.9. Linearization of pPUZZLE Plasmids for Transformation of *P. pastoris*

The *P. pastoris* parent strain P_{AOX} HyHEL-Fab-#8was transformed with linearized plasmids in order to allow effective integration via homologous recombination into the *P. pastoris* genome [17]. Fast Digest *Asc*I was used for linearization of the pPUZZLE plasmids. *Asc*I cuts in-between the *AOX*-TT, which then flanks the linearized plasmid for homologous recombination at the *AOX*-TT locus (Figure 3).

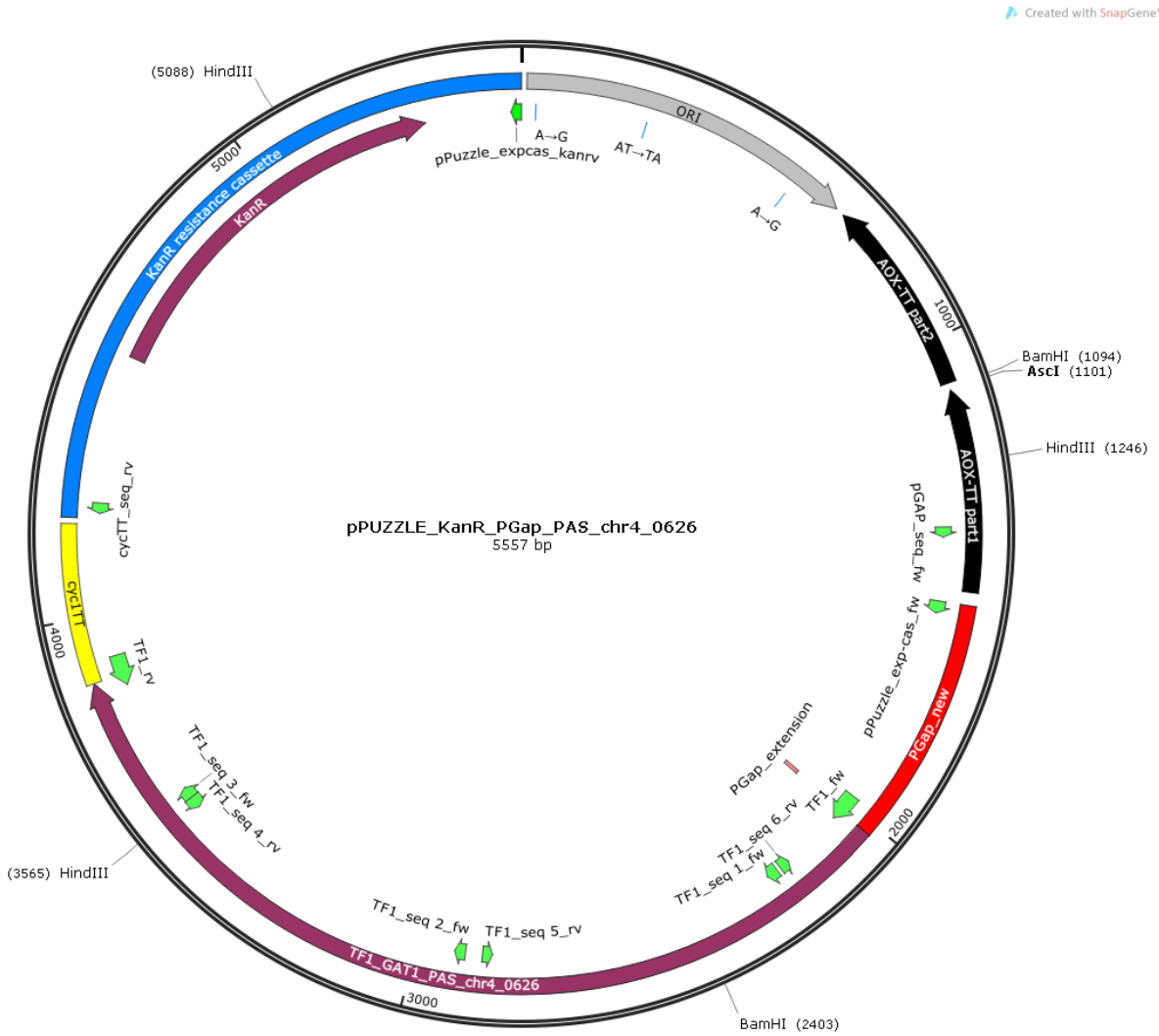

Figure 3: Plasmid map of pPUZZLE_KanR_*PGAP*_PAS_chr4_0626 with restriction sites of *Asc*I, *Bam*HI and *Hind*III. *Asc*I restriction site, which is necessary for linearization, is marked in bold letters. Open reading frames (ORF) of KanR (kanamycin resistance) and PAS_chr4_0626 (TF1): purple, P_{Gap}: red, AOX-TT regions: black, *CYC1*-TT in yellow, ORI in grey, primers in green and KanR expression cassette in blue. Re-sequencing of the vector-backbone revealed three alterations in the ORI marked with an arrow. The plasmid structure is the same for all other plasmid constructs listed in Table 4.

Linearization was performed with 1 FDU at 37 °C for 30 min in a final volume of 50 µL. Two µg to eight µg of plasmid were linearized per reaction. Linearized plasmids were directly purified out of the restriction mixture instead of using a preparative gel. Concentration was

measured with Nanodrop. Correct size of the linearization product was checked afterwards by a control agarose gel.

2.2.1.10. Amplification of Expression Cassettes for Transformation of *P. pastoris*

In a second approach the P_{AOX} HyHEL-Fab-#8 parent strain was transformed with a linear PCR-product of the pPUZZLE expression cassette. The expression cassette consisted of the P_{Gap} promoter, the ORF of the TF-gene, the *CYC1*-terminator and the kanamycin resistance cassette. PCRs were performed according to section 2.2.1.4. Used primers are listed in Table 10. PCR products were column purified instead of performing a preparative gel. Correct sizes of PCR products were analysed by parallel control gels of purified aliquots. The P_{AOX} HyHEL-Fab-#8 parent strain was transformed with 0.8, 2, 5 or 8 µg of the expression cassette.

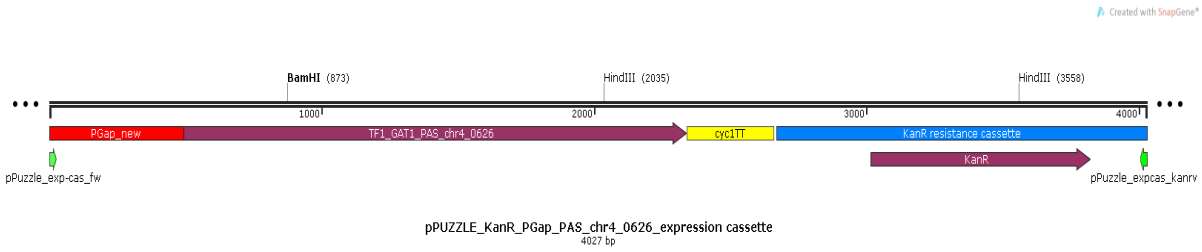

Figure 4: Map of pPUZZLE_KanR_*PGAP*_PAS_chr4_0626 expression cassette (TF1) without flanking AOX-TT regions for homologous recombination. All other features remain the same as describe above.

2.2.1.11. Preparation of Electrocompetent *P. pastoris* cells

An adapted version of the condensed protocol for competent cell preparation and transformation from Lin-Cereghino et al. (2005) was used[72]. Therefore, a 5 mL overnight culture of P_{AOX} HyHEL-Fab-#8 parent strain was grown in YPD Zeo at 30 °C and 120 rpm. A 50 mL main culture was inoculated to an OD_{600} of 0.2 and grown to an OD_{600} of 0.8 – 1. The culture was centrifuged at 4000 rpm and RT for 5 min and supernatant was discarded. The pellet was resuspended in 9 mL of ice-cold BEDS solution, supplemented with 1 mL of 1.0 M dithiothreitol (DTT). Work was done on ice. The cell suspension was shaken in the hand for 5 min. Afterwards, the cell suspension was centrifuged at 4000 rpm and RT for 5 min and pellet was resuspended in 1 mL of BEDS solution without DTT on ice. The competent cells were ready for transformation and small aliquots were stored at -20 °C for a short period of time (up to 1 month).

2.2.1.12. Transformation of *P. pastoris*

Electroporation cuvettes were cooled on ice. 0.8, 2, 5 and 8 µg of linearized plasmid DNA or linear PCR-product of the pPUZZLE expression cassette was mixed with 80 µL of electrocompetent P_{AOX} HyHEL-Fab-#8 parent strain cells. The mixture was incubated for 15 min on ice. The program PIC (1,500 V, 25 µF and 200 Ω) was used for electroporation. After electroshock, 1 mL of regeneration medium (1 M Sorbitol) was added and the suspension was transferred to a sterile 12 mL tube. The tube was incubated at 28 °C for 2 h without shaking. After the incubation, the cells were plated out onto selective YPD agar plates (Zeo 50/Gen 450) and incubated at 30 °C for 72 h to allow for growth of colonies that

harbour the integrated plasmid with the selection marker. 40-48 big to medium sized colonies of each transformation were picked into 96 DWP with YPD-antibiotic (Zeo 50/Gen 450) and grown over night at 28 °C and 320 rpm. On the next day colonies were pinned onto YPD (Zeo 50/Gen 450) plates and grown at 30 °C for approximately 48 h. The scheme of picking and pinning is depicted in Figure 5. Plates were re-pinned on fresh plates every month. Glycerol stocks were prepared by starting new ONCs from the pinning plates. Pool-screenings and early single-clone screenings in 24 DWP were inoculated form plates or fresh streak outs of these strains. Single-clone-screenings were directly inoculated in 24 DWP using single colonies from transformation plates in the late phase of the single-clone-screening procedure.

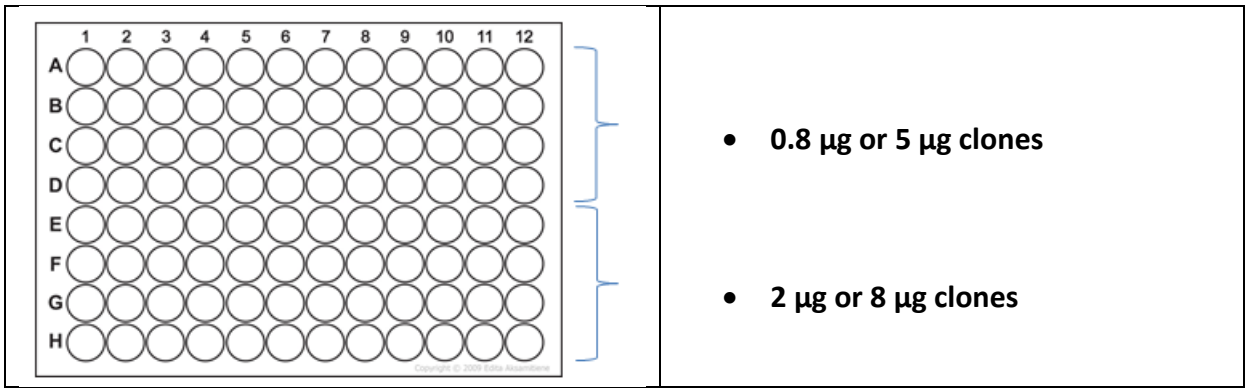

Figure 5: Picking and pinning scheme of clones transformed with 0.8, 2, 5 and 8 µg of linearized plasmid or expression cassette PCR-product. Up to 48 clones (half of the plate) were picked per transformation. One 96 DWP or pinning plate contained 40 – 48 clones from transformation with either 0.8 µg and 2 µg of or 5 µg and 8 µg of linearized plasmid.

2.2.1.13. Glycerol Stocks

P. pastoris glycerol stocks in cryogenic tubes:

A 10 mL ONC was spun down at 2500 rpm for 2 min. Supernatant was discarded and the pellet was resuspended in 2 mL of respective media of YPD Zeo/Gen or YPD Zeo. 600 µL of the yeast cell suspension and 300 µL of sterile 60 % glycerol were gently mixed. Two sterile cryogenic tubes were prepared per sample. Cells were directly stored at -80 °C.

P. pastoris glycerol stocks in 96 well microtiter plates:

160 µL of YPD grown cells in a 96 DWP (28 °C and 320 rpm) were transferred to a 96 well PS-microplate containing 80 µL of sterile 60 % glycerol and mixed. PS-microplates were sealed and stored at -80 °C.

2.2.2. 24 Deep Well Plate Cultivations

Pool-screenings and single-clone-screenings of P_{AOX} HyHEL-Fab-#8 transcription factor co-expressing strains were performed in 24 DWP.

2.2.2.1. Pool-Screenings in 24 DWP

Pool-screenings were performed in a 24 DWP cultivation procedure.

- 1st day: 10 am

Pre-cultures were grown in 96 DWP. Therefore, 200 µL of YPD (Zeo/Gen) per well were inoculated with clones from a pinning plate and cultivated at 320 rpm and 25 °C for 12 h. After 12 h, 30 µl of each clone were transferred to 8 mL fresh YPD (Zeo/Gen) in a 50 mL Greiner tube and incubated at 150 rpm and 25 °C for another 12 h. The pre-culture procedure for 0.8 µg clones is depicted in Figure 6. For a mixed pool of clones of all transformations (0.8, 2, 5 and 8 µg) 20 µL of each well were transferred in 12 mL fresh YPD (Zeo/Gen) and treated similar as described above.

- 2nd day: 8 am start of the batch cultures

OD_{600} of each pre-culture sample was measured as technical duplicate (dilution factor f=20). The batch culture (10 mL of M2D) was inoculated to OD_{600}=1 in 50 mL Greiner tubes. One Kuhner feed bead was added to each tube and the cultures were incubated at 150 rpm and 25 °C for 22 h.

- 3rd day: methanol induction

Kuhner feed beads were removed and cultures were spun down at 4000 rpm and RT for 5 min. Cells were resuspended in ~3 mL of M2M media (M2 media plus 0.5 % MeOH). OD_{600} of each sample was measured as technical duplicate (dilution factor f=50). Each well of the 24 DWP was filled with 2 mL of M2M medium, inoculated to OD_{600}=4 and incubated at 25 °C and 320 rpm. The 24-DWP was sealed with 2 air-permeable membranes. The cultures were induced with 1 % MeOH (20 µL per well), 6 h after the induction start.

- 4th day:

Cultures were induced with 1 % MeOH (20 µL per well) 22 h and 30 h of methanol induction

- 5th day: harvest

OD_{600} of each sample was measured as technical duplicate (dilution factor f=50). DWP were spun down at 4000 rpm and 4 °C for 5 min (from this time point work was performed on ice).

2 times 200 µL of supernatant were transferred into two separate 96 PS-microplates or in Sarstedt Micro tubes and frozen at -20 °C. In addition, 200 µL of supernatant were transferred to a 96 PS-microplate or in Sarstedt Micro tube were stored at 4 °C in the fridge.

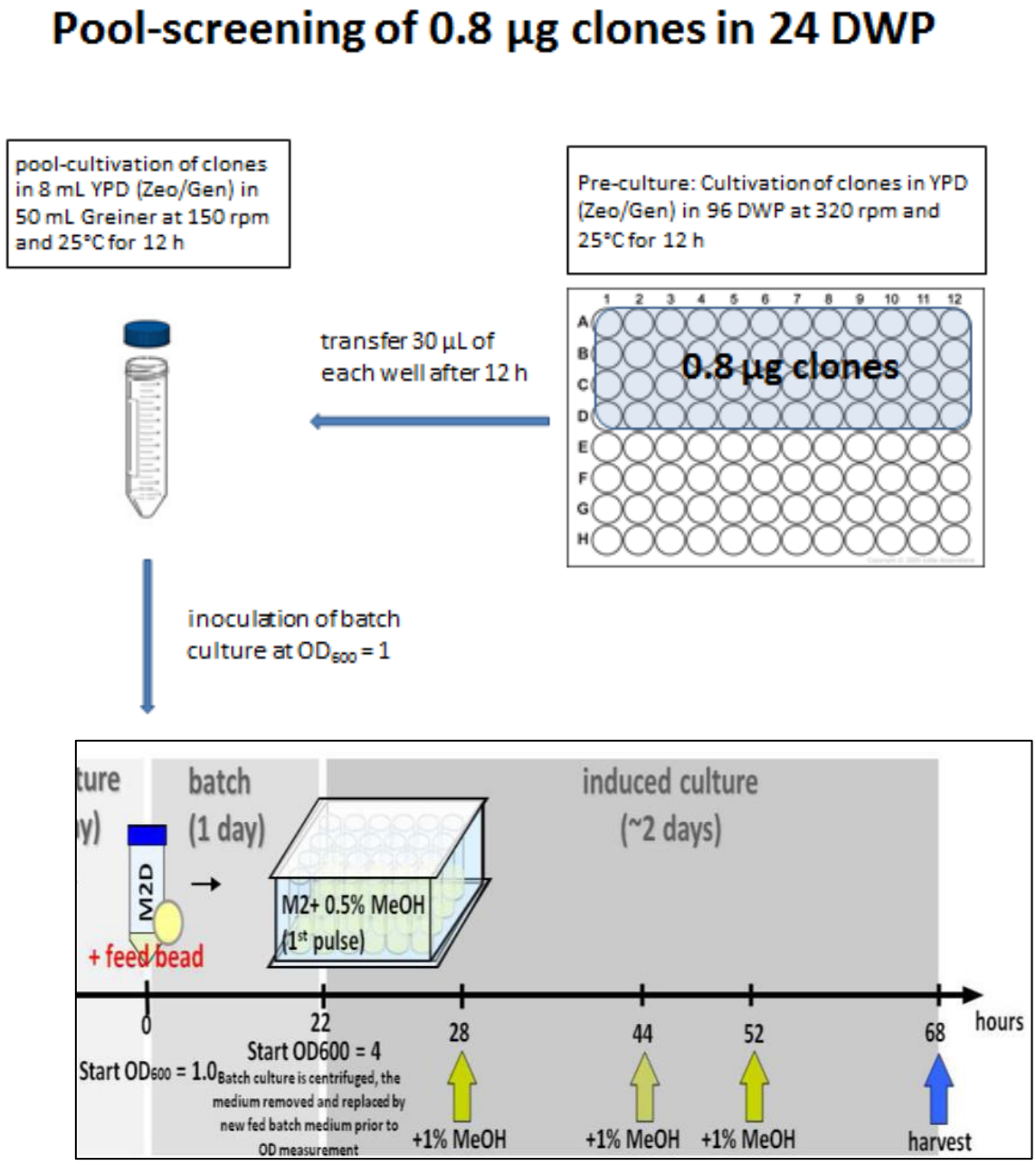

Figure 6: Workflow of the pool-screening procedure for 0.8 µg clones (same method for all other clones). Pre-culture was started in 96 DWP. After 12 h 48x 30 µL were transferred in a 50 mL Greiner tube. The clone-pool was again cultivated for 12 h before the start of the batch culture in M2D medium. Induction in M2M (M2 media plus 0.5 % Methanol (MeOH)) medium was started 22 h after inoculation of the batch culture and induced 3x to 1 % MeOH. Cultures were harvested 68 h after start of the M2D batch culture.

2.2.2.2. Single-Clone-Screenings in 24 DWP

Single-clone-screenings were performed in 24 DWP similar to the pool-screening procedure. Differences emerge in the pre-culture cultivation. For single-clone-screenings pre-cultures were performed in 50 mL Greiner tubes. Therefore, 10 mL of YPD (Zeo/Gen) were inoculated with a single clone and incubated for at 150 rpm and 25 °C for 22 h.

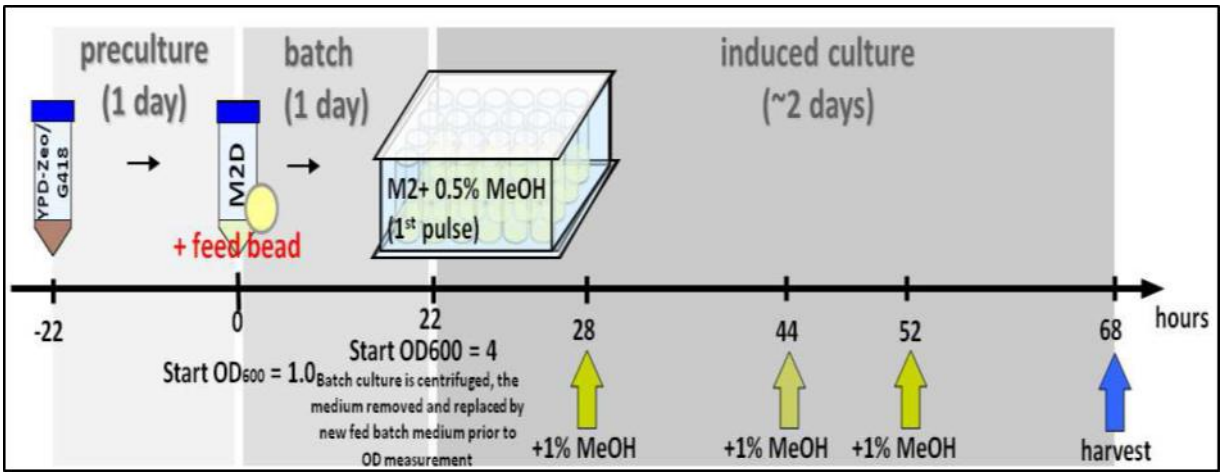

Figure 7: Workflow of the single-clone-screening procedure in 24 DWP. Pre-culture was grown in 50 mL Greiner tubes for 22 h before work was continued exactly like described in section 2.2.2.1 for the pool-screenings.

2.2.3. Screening

Secreted HyHEL-Fab was detected with a sandwich ELISA using the antibodies listed in Table 7. Two different ELISA protocols for HyHEL-Fab screenings were used within this thesis. The first ELISA protocol was used for the pool-screenings, and the second one was used for the single-clone-screenings. The change of protocols was a general project decision in order to standardise the ELISA protocol used in different working groups.

2.2.3.1. ELISA Protocol Used for the Pool-Screening

All incubations were carried out at 37 °C. The capture antibody (Abcam ab7497) was used in a freshly prepared 1:1000 dilution in coating buffer. The detection antibody (Sigma-Aldrich A0293) was used in a 1:10 000 dilution in dilution buffer, also freshly prepared. Prepared dilution buffer was only stored for a short period of time, i.e. 24 h. TMB (3,3',5,5'-tetramethylbenzidine, Bethyl laboratories) – one component substrate was used as substrate. All buffers are listed inTable 17. Samples were diluted in dilution-buffer (f=100). The standard (purified human fab-Kappa [1 mg/mL]),) was diluted to 200, 100, 50, 20, 10, 5, 1, 0.5 ng/mL. The used pipetting scheme is depicted in Table 22 and Table 23. All antibodies, buffers and the standard were stored at 4 °C.

Table 22: Pipetting scheme for ELISA plates with two technical replicates. 24 DWP samples are shown as numbers and are marked in green. Standard dilutions are marked in blue and are given in [ng/mL]. Blank is given as bl.

	1	2	3	4	5	6	7	8	9	10	11	12
A	1	5	9	13	17	21	200	200	bl			
B	2	6	10	14	18	22	100	100	bl			
C	3	7	11	15	19	23	50	50	bl			
D	4	8	12	16	20	24	20	20	bl			
E	1	5	9	13	17	21	10	10	bl			
F	2	6	10	14	18	22	5	5	bl			
G	3	7	11	15	19	23	1	1	bl			
H	4	8	12	16	20	24	0.5	0.5	bl			

Table 23: Pipetting scheme for ELISA plates with three technical replicates. 24 DWP samples are shown as numbers and are marked in green. Standard dilutions are marked in blue and are given in [ng/mL]. Blank is given as bl.

	1	2	3	4	5	6	7	8	9	10	11	12
A	1	5	9	13	17	21	1	5	9	13	17	21
B	2	6	10	14	18	22	2	6	10	14	18	22
C	3	7	11	15	19	23	3	7	11	15	19	23
D	4	8	12	16	20	24	4	8	12	16	20	24
E	1	5	9	13	17	21	200	10	200	10	bl	bl
F	2	6	10	14	18	22	100	5	100	5	bl	bl
G	3	7	11	15	19	23	50	1	50	1	bl	bl
H	4	8	12	16	20	24	20	0.5	20	0.5	bl	bl

An ELISA plate was coated with the capture antibody dilution for 1 h. Then, the plate was washed 3 times with 200 µL washing-buffer. Blocking was done with 200 µL of blocking-buffer for 30 min followed by 5 times washing with 250 µL washing-buffer. In protocol one, 100 µl of samples were applied in f=100 dilutions for 1 h. Afterwards, the plate was washed 5 times with 200 µL of washing buffer. Hundred µL of detection antibody were applied for 1 h followed by 5 times washing with 200 µL washing-buffer. 100 µL of TMB substrate were applied in a 1:2 dilution in H_2O. The blue colour development was followed at 370 nm with a platereader. Reaction was stopped with 100 µL of 0.2 M H_2SO_4. Finally, the yellow colour change was detected at 450 nm (background at 560 nm). Analysis of ELISA results: The absolute concentrations of HyHEL-Fab dilutions in each well were calculated using a linear regression model with a minimum of 4 standard points.

2.2.3.2. ELISA Protocol Used for the Single-Clone-Screenings

As described in 2.5.3.1, all incubations were done at room temperature. Dilutions of human fab-Kappa standards [1 mg/mL] were performed as shown in Table 24. Diluted standard stocks were stored in 600 µL aliquots at -20 °C. The samples of each 24 DWP were measured as technical duplicates on 2 ELISA plates. The capture AB (ab7497) was diluted 1:1000 in coating buffer. After that, 100 µL per well of this antibody dilution were applied on ELISA plates over night at RT on a rotary shaker. On the next day, the supernatant samples were pre-diluted in Eppendorf-tubes, using a dilution ratio of 1:25 and fresh dilution buffer. The blank wells were filled with dilution buffer only.

The dilution plate was pre-filled with 140 µL of dilution buffer in each well. 140 µL of dilution buffer, standard, and samples were applied on the dilution plate as depicted in Figure 8. 140 µL of dilution buffer were applied to well H1. 140 µL of diluted standard stock [200 ng/mL] were applied to the wells H2 and H3. 140 µL of sample dilutions (f=25) were applied to the columns 4, 7 and 10 consistently, the standards in H2 and H3 had a concentration of 100 ng/mL and the samples in columns 4, 7 and 10 were diluted 1:50 (Figure 8). After that, the samples in column 1, 2 and 3 were diluted from row H to A in 1:2 steps by transferring 140 µL from one well to the one above. Sample dilutions were performed in a similar manner. 140 µL were taken from column 4 and diluted 1:2 until row

6. The remaining 140 µL were discarded, tips were changed and the procedure was repeated for column 7 and column 10. Proper mixing of the dilutions was achieved by pipetting the solution up and down before the next dilution. The dilution procedure is shown in Figure 9.

Before adding the sample-dilutions, the pre-coated ELISA plates were washed 3 times with 200 µL/well of washing buffer. Hundred µL of each well of the dilution plate were applied on the ELISA plate and the plates were incubated on a rotary shaker for 2 h. After incubation plates were washed again as described previously. Then, 100 µL/well of the detection AB (Sigma Aldrich A8542) in a 1:1000 dilution were added and incubated for 1 h. Plates were washed as before and 100 µL/well of detection solution were applied. Therefore, 2 tablets of pNPP (4-Nitrophenyl phosphate, Sigma Aldrich) substrate per 11 mL of detection buffer were dissolved. The detection solution was prepared shortly before the measurement. After that, the plate was measured at 405 nm with a reference wavelength of 620 nm. Absorbance was measured with BioTek Synergy MX microplate reader and Gen5 analysis software was used for data depiction. The reaction was measured after ~5 min corresponding to an absorbance value of ~2 for the highest Fab standard. Data was analysed online using a four parameter logistic (4PL) regression model and MyAssays data analysis software (www.myassays.com).

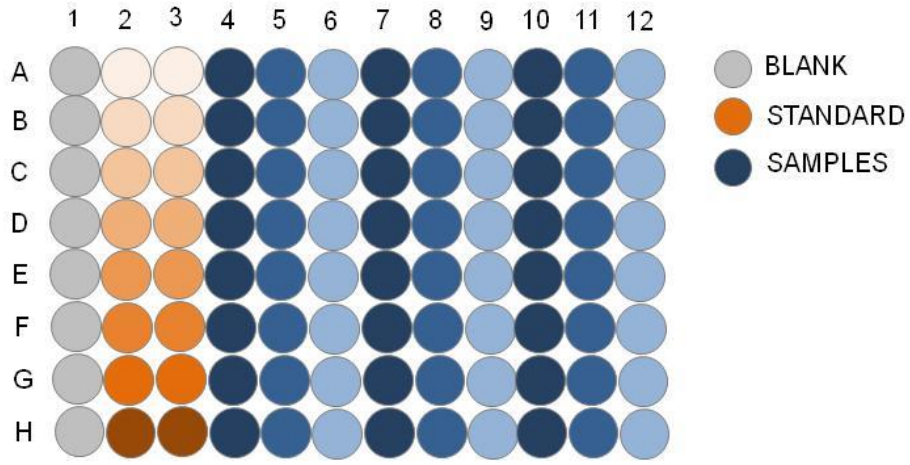

Figure 8: ELISA layout for 24 DWP single-clone-screening. 140 µL of dilution buffer were filled in every well of the ELISA plate. 140 µL dilution buffer were applied as blank in H1. 140 µL standard [200 ng/µL] were applied to the wells H2 and H3. 140 µL of sample dilutions (f=25) were applied in the row 4, 7 and 10 (see also Figure 9).

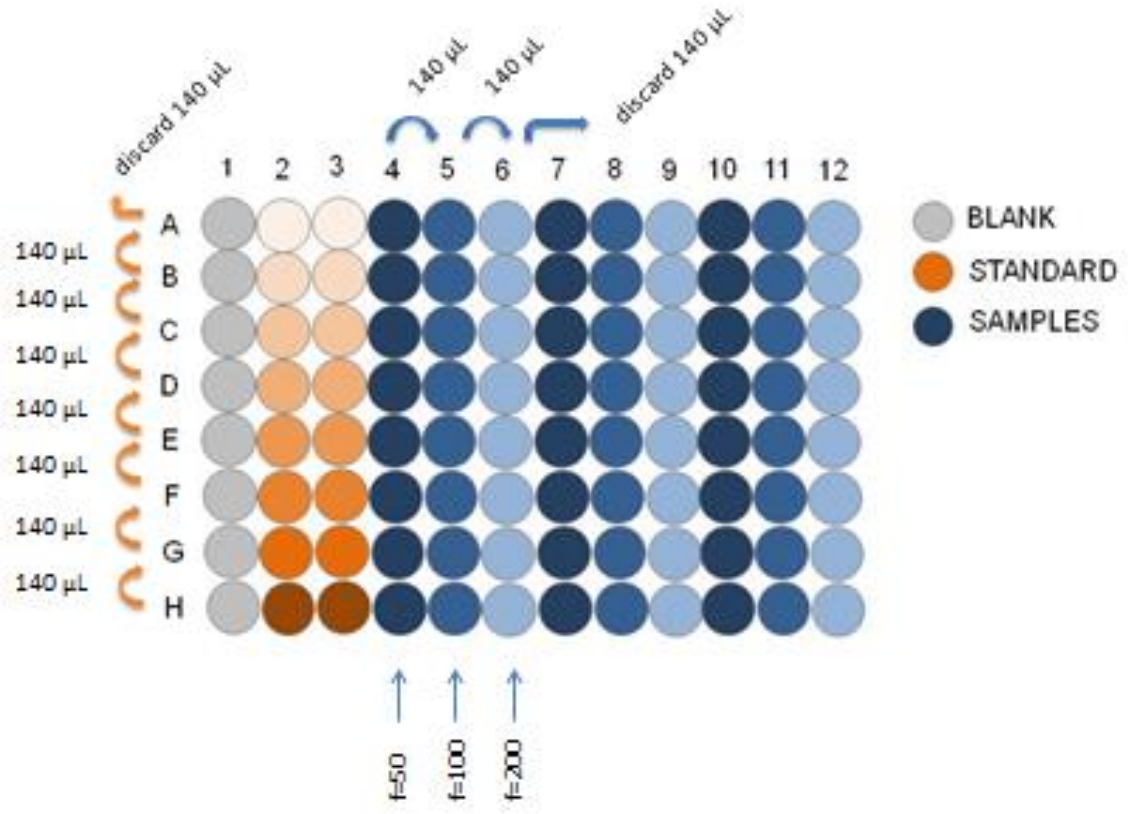

Figure 9: Dilution procedure for ELISA dilution plate. Blank and Standard dilution row: Starting at H1, H2 and H3, 140 µL were constantly transferred to the next row in direction H → A. The last 140 µL of a row A (A1, A2 and A3) were discarded. Sample dilutions: Starting in column 4, 140 µL were transferred to column 5. Then, 140 µL were transferred from column 5 to column 6. Remaining 140 µL were discarded. Dilution of column 7 and column 10 (other samples) was performed similarly. Proper mixing was achieved by pipetting up and down each well 5 times.

Table 24: Dilution steps for human fab-Kappa standard to achieve a stock concentration of 200 ng/mL

30 µL stock [1 mg/mL]	+	270 µL dilution buffer	=	300 µL [100 µg/mL]
200 µL [100 µg/mL]	+	1800 µL dilution buffer	=	2 mL [10 µg/mL]
1 mL [10 µg/mL]	+	49 mL dilution buffer	=	50 mL [200 ng/mL]

3. Results and Discussion

The effect of TF co-expression on *P. pastoris* HyHEL-Fab (P_{AOX} HyHEL-Fab-#8 parent strain) secretion was determined by measuring the level of secreted HyHEL-Fab model protein after 48 h of methanol induction in a 24 well plate by ELISA. To achieve this, the strain P_{AOX} HyHEL-Fab-#8 was transformed with linearized pPUZZLE_KanR_P_{GAP} plasmid (all plasmids generated within this thesis have been transformed into *E. coli* TOP10 F' and stored in the strain collection at the Institute of Molecular Biotechnology at Graz University of Technology;Table 4) or pPUZZLE_KanR_P_{GAP} expression cassette harbouring one of the TF target genes. Re-sequencing of the pPUZZLE_KanR_P_{GAP} plasmid revealed 3 alterations compared to the original sequence map, which were A to G at position 1722 (ORI), AT to TA at position 1954/1955 (ORI) and A to G at position 2274 (ORI) (Figure 3). The pPUZZLE_KanR_P_{GAP} vector was designed to integrate at the *AOX1* transcription termination region; however also ectopic integration by NHEJ is possible. To account for the effect of gene dosage, the parent strain was transformed with different amounts of linearized plasmid or expression cassette (0.8, 2, 5 and 8 µg). Effects of co-expression on the secretion level were compared to reference strains (parent and EVC). On the one hand, an empty vector control (EVC) was constructed by transforming P_{AOX} HyHEL-Fab-#8 with a linearized empty pPUZZLE_KanR_P_{GAP}, and on the other hand, the original parent strain (P_{AOX} HyHEL-Fab-#8) was used as reference. To narrow down the number of target TFs, a pool-screening procedure was performed. Single-clone-screening was performed to confirm the improvement of TF co-expressing strains compared to the reference strains and to choose single clones for bioreactor cultivation. Finally, interesting TFs will be investigated for their genomic TFBS by ChIP-Seq.

3.1. Pool-Screening of Clones Transformed with Linearized pPUZZLE_KanR_P_{Gap}_TF Plasmid

To assess the overall trend of a transcription factor for its ability to improve the secretion level of the HyHEL-Fab fragment, clones co-expressing a particular TF were cultivated as pools in a 24 DWP screening. A clone pool for a TF consisted of 40 – 48 (half of the 96 pinning plate) clones. Pools of clones transformed with 0.8, 2, 5 or 8 µg of DNA were studied separately and as a mixed pool (40 - 48 clones of each transformation). The pools of clones transformed with the respective amount of DNA were further termed as "X µg pool". Pool-screenings were performed for both, plasmid and expression cassette transformed clones. HyHEL-Fab secretion was compared to pools of clones transformed with the respective amount of empty vector and P_{AOX} HyHEL-Fab-#8 parent strain as a biological duplicate. After 48 h of methanol induction the supernatants of the respective pools were studied by ELISA. The layout for 24 DWP cultivation depicted in Figure 10 was used for all pool-screenings.

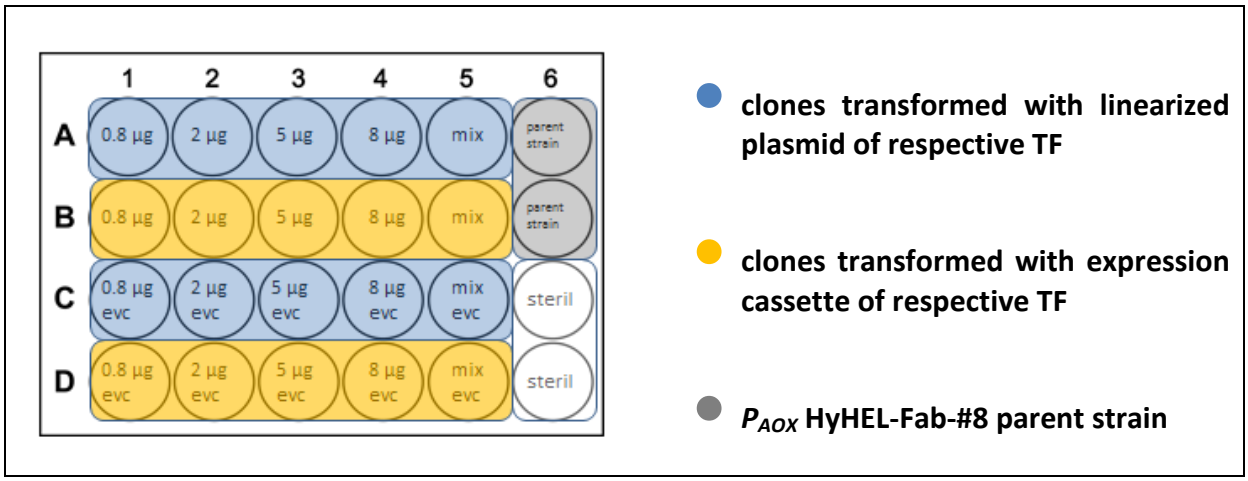

Figure 10: 24-well pool-screening layout. Clones transformed with linearized plasmid, expression cassette and EVC, as well as parent and reference strains were cultivated on one plate. One TF was analysed per plate. Wells C6 and D6 were sterile controls with media only.

TF1 co-expression resulted in an overall enhancement of Fab secretion. On average titers were 13.2 % higher than the corresponding EVC. Titers tended to be higher than the EVC and the parent strain except for the pool transformed with 5 µg of plasmid. Also the yields were far higher than the reference strains (parent strain and EVC), ranging between 8 and 147 %. The 8 µg pool showed the highest increase of HyHEL-Fab concentration reaching an improvement of 1.22-fold. Normalising to biomass (data not shown) the observed yields range from 1.57-fold for the 0.8 µg pool, 1.49-fold for the 2 µg pool and 1.45-fold for the 8 µg pool. The yield of the mixed pool was increased 2.47-fold, confirming the positive of TF1 co-expression on HyHEL-secretion (Table 25 and Figure 11).

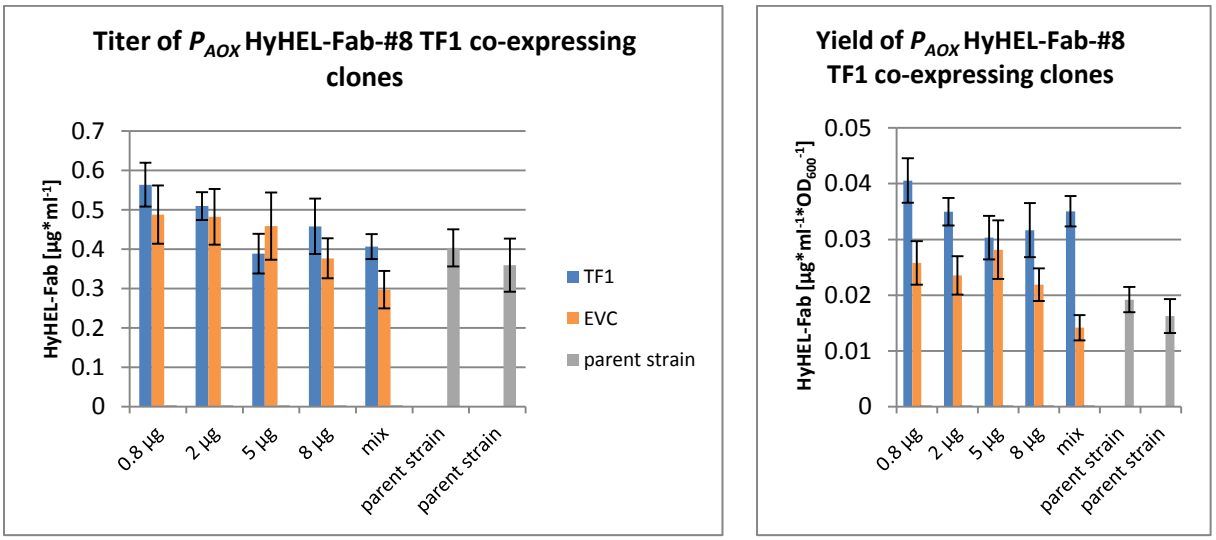

Figure 11: Titer and yield of P_{AOX} HyHEL-Fab-#8 TF1 co-expressing clones measured by ELISA. Data represents mean values of four technical replicates on two separate plates. EVC and recombinant P_{AOX} HyHEL-Fab-#8 parent strain were used as reference. Blue bars: pools of P_{AOX} HyHEL-Fab-#8 TF1 co-expressing clones; Orange bars: pools of P_{AOX} HyHEL-Fab-#8 EVC; Grey bars: P_{AOX} HyHEL-Fab-#8 parent strain.

Co-expression of TF2 also consistently increased HyHEL-Fab secretion (Table 25). The highest increase in titer was observed for the 8 µg pool with a 1.46-fold change compared to the EVC. Titers of the 0.8 µg and 5 µg pools were also higher than the EVC reaching a 6 % and 30 % improvement. In contrast, the HyHEL-Fab concentration of the 2 µg pool was below the

corresponding EVC (0.86-fold), however still higher than the parent strain as depicted in Figure 12.

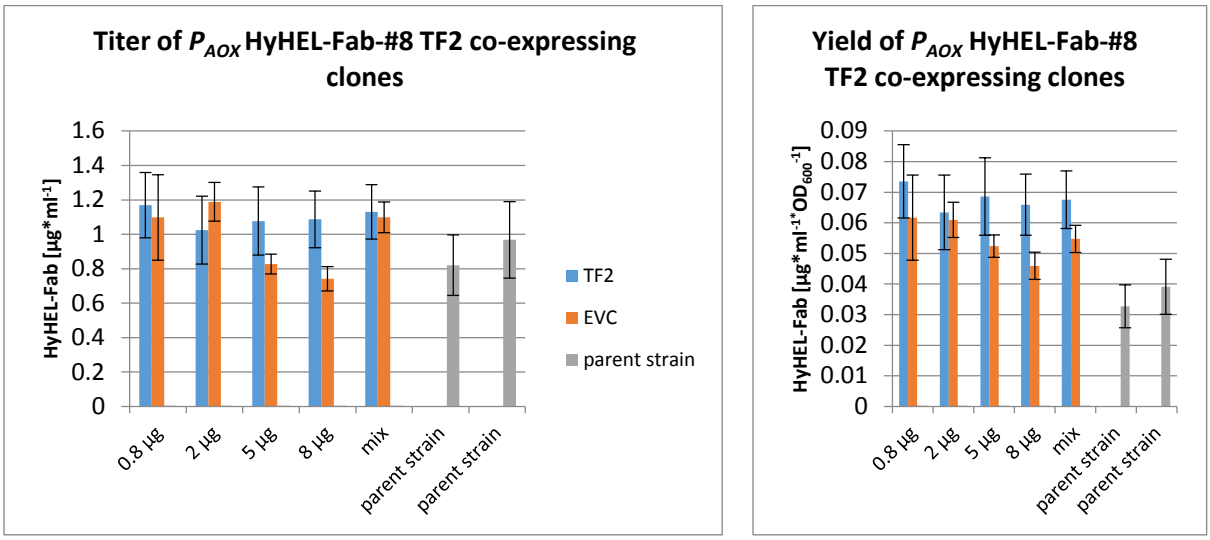

Figure 12: Titer and yield of P_{AOX} HyHEL-Fab-#8 TF2 co-expressing clones measured by ELISA. Data represents mean values of two technical replicates. EVC and recombinant P_{AOX} HyHEL-Fab-#8 parent strain were used as reference. Blue bars: pools of P_{AOX} HyHEL-Fab-#8 TF2 co-expressing clones; Orange bars: pools of P_{AOX} HyHEL-Fab-#8 EVC; Grey bars: P_{AOX} HyHEL-Fab-#8 parent strain.

Co-expression of TF3 had a negative impact on the secretion level of the HyHEL-fab model protein. Only the 8 µg pool showed a similar amount of secreted product compared to its corresponding EVC. The massive reduction in biomass formation of TF3 co-expressing clones increased the observed yields. The 0.8 µg pool showed a 1.17-, the 2 µg pool a 1.23- and the 8 µg pool a 1.53- fold-change in yield. The 5 µg pool showed a yield similar to the EVC strain. Due to the low titer levels, which were significantly below the EVC strain, TF3 was excluded from the subsequent single-clone-screening (Table 25 and Figure 13).

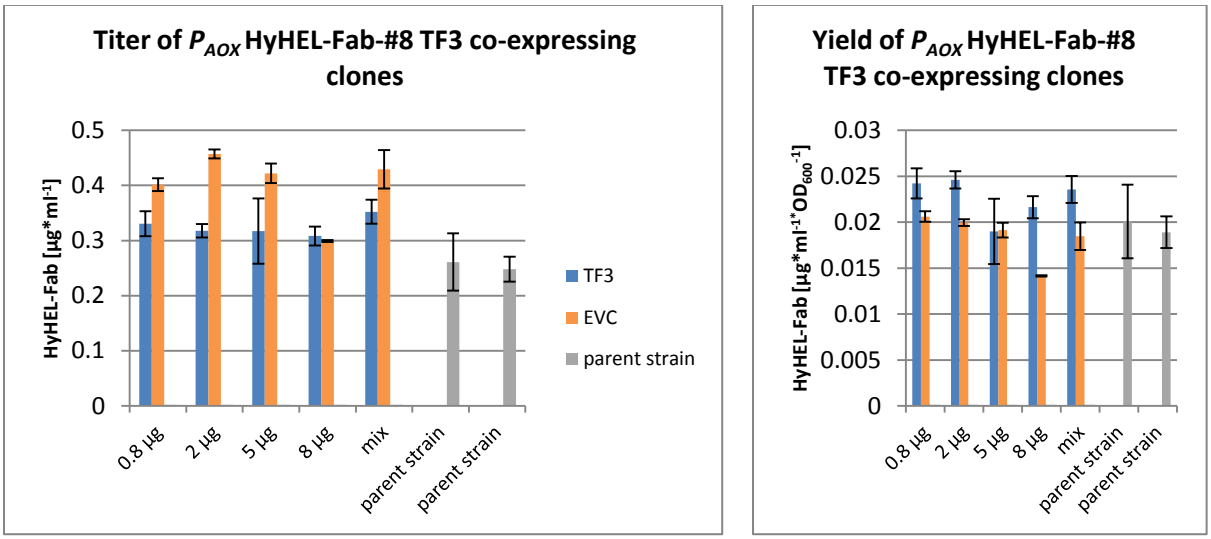

Figure 13: Titer and yield of P_{AOX} HyHEL-Fab-#8 TF3 co-expressing clones measured by ELISA. Data represents mean values of four technical replicates of two separate plates. EVC and recombinant P_{AOX} HyHEL-Fab-#8 parent strain were used as reference. Blue bars: pools of P_{AOX} HyHEL-Fab-#8 TF3 co-expressing clones; Orange bars: pools of P_{AOX} HyHEL-Fab-#8 EVC; Grey bars: P_{AOX} HyHEL-Fab-#8 parent strain.

TF4 had no significant impact on the secretion level. HyHEL-Fab concentrations stayed nearly the same compared to the EVC (Table 25). Clones of the 2 µg pool showed a ~20 % decrease of secreted product. The 46 % decrease of secreted product in the mixed pool might be a result of the very high standard deviation of the EVC strain (Figure 20 and Figure 21) and was not used for analysis (Figure 14). Generally, TF4 co-expression clones were characterized by an increased biomass production of nearly 25 % compared to the EVC strains resulting in a very low yield ranging from 0.63-fold (2 µg) to 0.87-fold (8 µg). As TF4 co-expression did not increase secretion per cell and rather influenced biomass production it was excluded from the single-clone-screening (Figure 14).

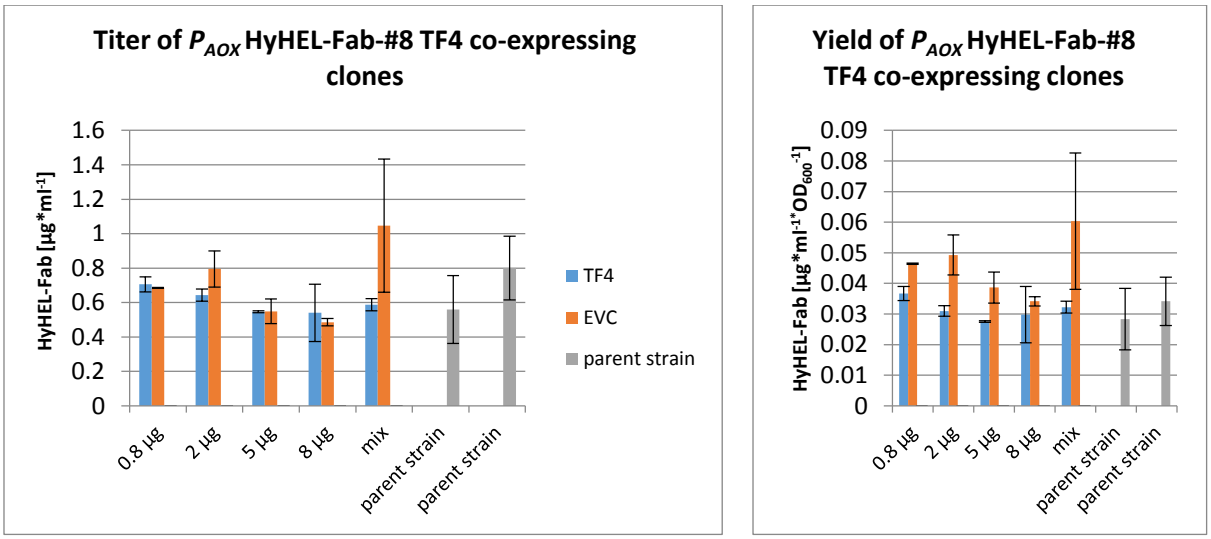

Figure 14: Titer and yield of P_{AOX} HyHEL-Fab-#8 TF4 co-expressing clones measured by ELISA. Data represents mean values of two technical replicates. EVC and recombinant P_{AOX} HyHEL-Fab-#8 parent strain were used as reference. Blue bars: pools of P_{AOX} HyHEL-Fab-#8 TF4 co-expressing clones; Orange bars: pools of P_{AOX} HyHEL-Fab-#8 EVC; Grey bars: P_{AOX} HyHEL-Fab-#8 parent strain.

Co-expression of TF5 in the parent strain lead to a decreased product concentration for clones of the 0.8, 2 and 5 µg pools (Table 25). Clones of the 8 µg pool showed a 13 % increase compared to the corresponding EVC. Yields of TF5 co-expressing clones were higher due to low biomass formation and reached levels from 1.08-fold (0.8 µg pool) to 1.53-fold (8 µg pool) of EVC. Though yields were improved TF5 was not further studied due to the low biomass formation of the clones (Figure 15).

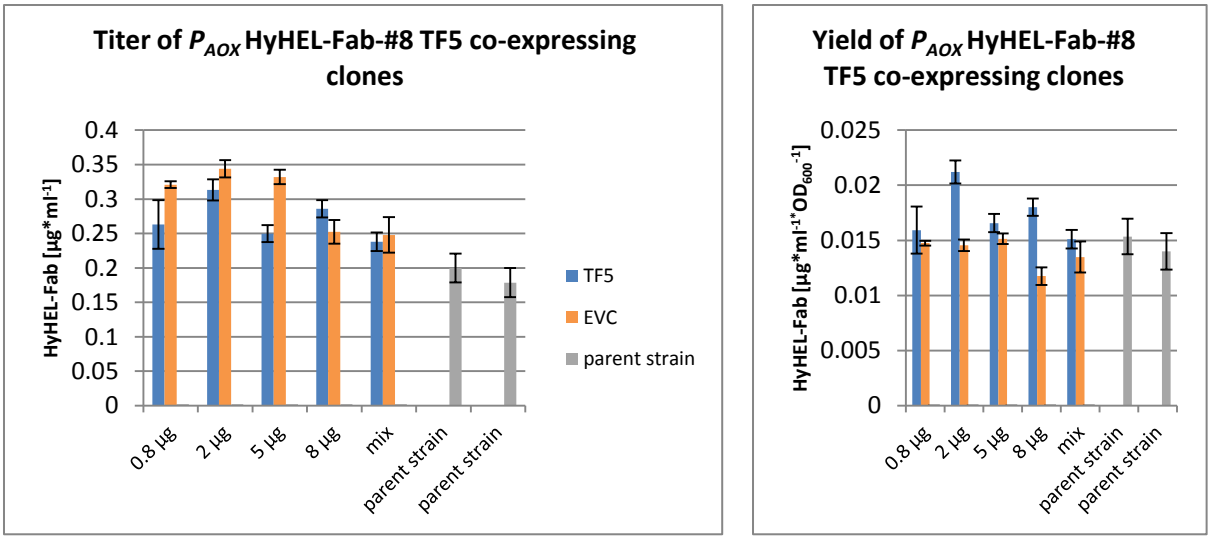

Figure 15: Titer and yield of P_{AOX} HyHEL-Fab-#8 TF5 co-expressing clones measured by ELISA. Data represents mean values of four technical replicates of two separate plates. EVC and recombinant P_{AOX} HyHEL-Fab-#8 parent strain were used as reference. Blue bars: pools of P_{AOX} HyHEL-Fab-#8 TF5 co-expressing clones; Orange bars: P_{AOX} HyHEL-Fab-#8 EVC; Grey bars: P_{AOX} HyHEL-Fab-#8 parent strain.

Reduced titers were also observed for TF6 co-expressing clones. Clones of the 0.8 µg pool showed a 29 % reduced, clones of the 2 µg and 5 µg pools a 20 % reduced and clones of the 8 µg pool a 5 % reduced concentration of HyHEL-Fab in the supernatant compared to the EVC. Again clones grew to lower biomass levels than the control clones, which resulted in a little higher yields (Figure 16). Nevertheless, yields were not significantly increased compared to the EVCs, ranging from a 0.97-fold decrease (0.8 µg), a 1.12-fold increase (2 µg), a 1.02-fold increase (5 µg) to a 1.13-fold increase (8 µg) (Table 25). This slight increase of secretion capacity was assessed no to be sufficient for a selection for the subsequent single-clone-screening.

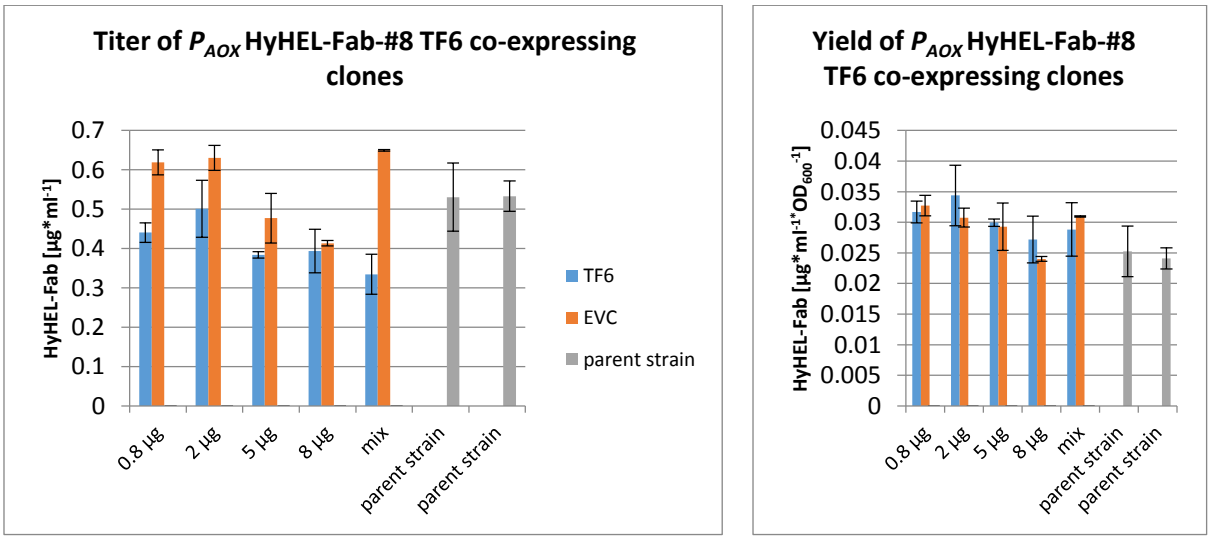

Figure 16: Titer and yield of P_{AOX} HyHEL-Fab-#8 TF6 co-expressing clones measured by ELISA. Data represents mean values of two technical replicates. EVC and recombinant P_{AOX} HyHEL-Fab-#8 parent strain were used as reference. Blue bars: pools of P_{AOX} HyHEL-Fab-#8 TF6 co-expressing clones; Orange bars: pools of P_{AOX} HyHEL-Fab-#8 EVC; Grey bars: P_{AOX} HyHEL-Fab-#8 parent strain.

Co-expression of TF2ni, which was lacking its intron-sequence in the gene sequence, resulted in an increased secretion of HyHEL-Fab for the clones of all transformations. Titer

concentrations were increased 1.15-fold for clones of the 0.8 µg pool, 1.03-fold for the clones of the 2 µg pool, 1.16-fold for the clones of the 5 µg pool and 1.40-fold for the clones of the 8 µg pool. The yields also showed an overall increase for all pools of 1.10-fold (0.8 µg), 1.30-fold (2 µg), 1.20-fold (5 µg) and 1.48-fold (8 µg) (Figure 17, Table 25). Despite these positive results for TF2ni, the native TF2 was chosen for further analysis by single-clone-screenings.

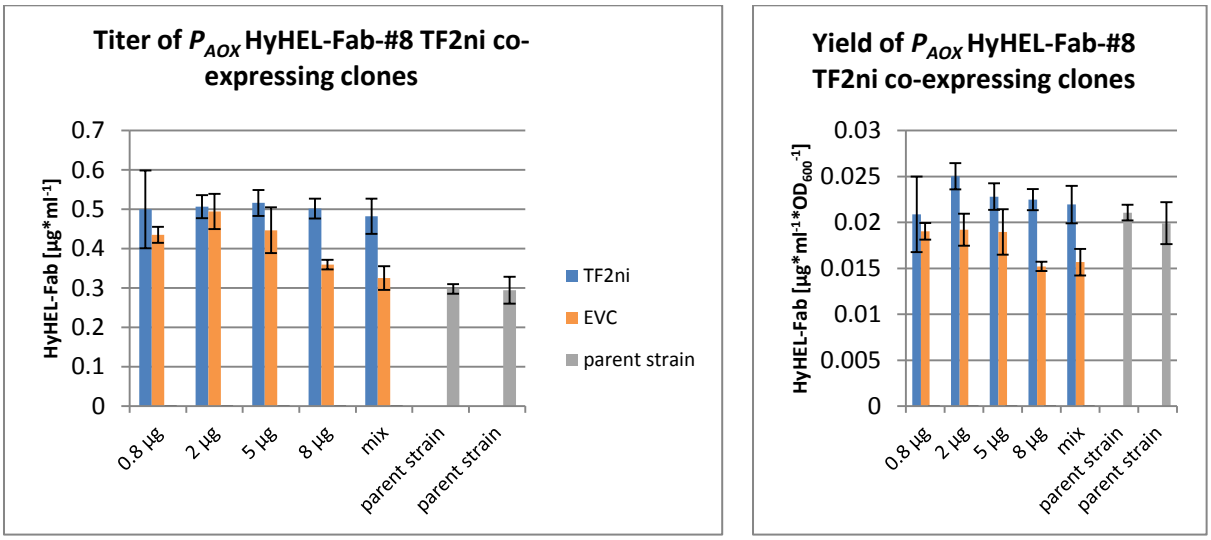

Figure 17: Titer and yield of P_{AOX} HyHEL-Fab-#8 TF2ni co-expressing clones measured by ELISA. Data represents mean values of four technical replicates of two separate plates. EVC and recombinant P_{AOX} HyHEL-Fab-#8 parent strain were used as reference. Blue bars: pools of P_{AOX} HyHEL-Fab-#8 TF2ni co-expressing clones; Orange bars: pools of P_{AOX} HyHEL-Fab-#8 EVC; Grey bars: P_{AOX} HyHEL-Fab-#8 parent strain.

HyHEL-Fab concentration was reduced to 40 % upon TF5sv co-expression for the clones of the 0.8 µg pool. Also the titers of the 2 µg-, the 5 µg - and the 8 µg pool were reduced by 47 %, 41 % and 18 %, respectively. Yields of the 0.8 µg, 2 µg and 5 µg transformations were slightly increased, but remained still below the threshold level of the corresponding EVCs. The best clones (8 µg pool) showed a 15 % increased yield (Figure 18).

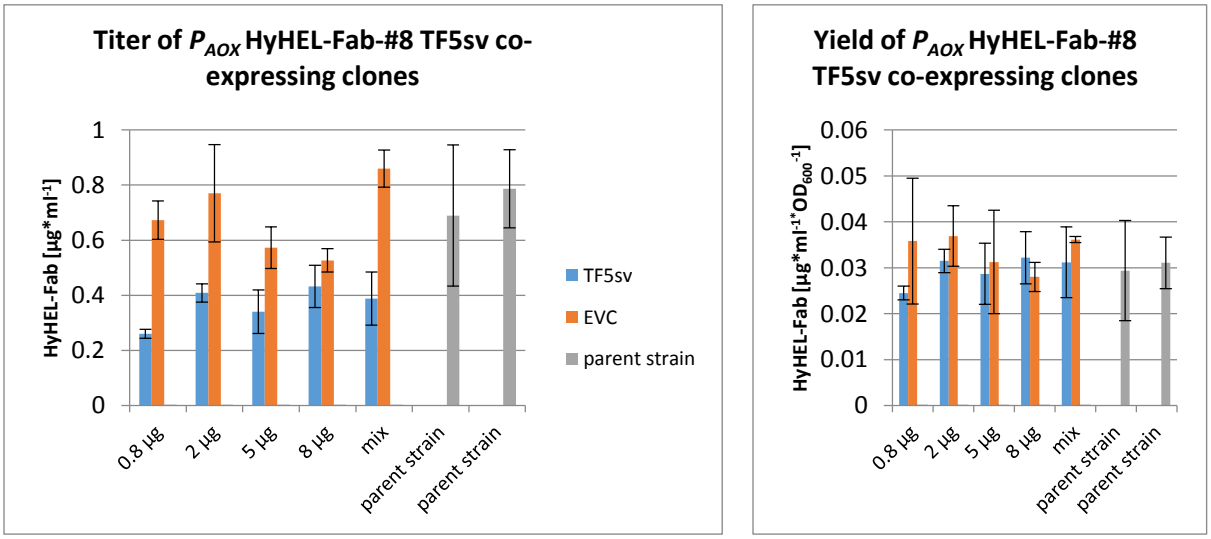

Figure 18: Titer and yield of P_{AOX} HyHEL-Fab-#8 TF5sv co-expressing clones measured by ELISA. Data represents mean values of four technical replicates of two separate plates. EVC and recombinant P_{AOX} HyHEL-Fab-#8 parent strain were used as reference. Blue bars: pools of P_{AOX} HyHEL-Fab-#8 TF5sv co-expressing clones; Orange bars: pools of P_{AOX} HyHEL-Fab-#8 EVC; Grey bars: P_{AOX} HyHEL-Fab-#8 parent strain.

In summary, increased titers were found for TF1, TF2 and TF2ni, while yields were improved for TF1, TF2, TF3, TF5 and TF2ni. TF3 and TF5were not further studied, due to their negative impact on HyHEL Fab secretion. In case of TF2 and TF2ni preference was given to the native TF2.

Constitutive co-expression of TF1, which is responsible for the regulation of genes required for the utilization of poor nitrogen sources, might be beneficial for growth on YPD, which contains several poor nitrogen sources such as proteins or amino acids. Though, a synthetic minimal medium was used for 24 well cultivation containing $(NH_4)_2HPO_4$ as a defined nitrogen source, nitrogen limitation might still have been a problem here. According to *S. cerevisiae*, TF1 is also involved in the regulation of genes coding for vacuolar proteases (*CPS1, PRP1, PRB1, PRC1 LAP4/APE1*)[73]. As reported previously, vacuolar proteases (*PEP4, CPS1*) were involved in the degradation of the secreted antibody fragment Fab3H6 recombinantly produced in *P. pastoris*[74]. Vacuolar degradation of heterologous proteins might help the cell to relieve the secretory pathway by eliminating misfolded proteins or an overcharge of heterologous proteins caused by overexpression. Heterologous expression of Hepatitis B surface antigen in *P. pastoris* GS115 also induced expression of vacuolar proteases and led to constitutive autophagic processes in the vacuole[75]. However, these findings were shown for vacuolar degradation of peroxisomes while growing on MeOH and it is questionable whether this can be attributed to recombinant protein secretion.

The role of TF2 is difficult to assess because of its unknown function in *S. cerevisiae* and *P. pastoris*. Homology is observed to *C. albicans* Brg1/Gat2, which is involved in biofilm formation, filamentous growth and virulence[61].

S. cerevisiae genes regulated or co-regulated by TF3 were reported in recent studies[76, 77]. TF3 acts as a transcriptional activator of genes responsible for ethanol utilization after a diauxic transition, i.e. when glucose is depleted. Energy metabolism is then shifted to oxidation of non-fermentable carbon sources. A total overlap of TF3 regulated genes in *S. cerevisiae* and *P. pastoris* might not be likely, because of general differences in metabolism and response to physiological and environmental changes like heterologous protein production or shift to another carbon source (e.g. methanol). Thus, one cannot speculate about the *P. pastoris* TF3 regulon. DNA binding studies like ChIP-Chip or ChIP-Seq could elucidate the pathways regulated by TF3 and their possible role in raising the secretion capacity of the HyHEL-Fab fragment in *P. pastoris*.

TF5 co-expression also showed positive effects on secreting recombinant HyHEL-Fab. Target genes regulated by this *P. pastoris* TF of unknown function are not known at this time point and are subject of future investigations.

TF4, TF6 and TF5sv did not or only slightly increase the secreted concentration of the HyHEL-Fab fragment compared to the EVC. Increased yields were only observed for clones of the 2 µg and 8 µg pool co-expressing TF6 and for the clones of the 8 µg pool co-expressing TF5sv. However, due to the bad growth behaviour of these clones they were not further studied.

The selection of the TFs studied was mainly based on up- and down-regulation of the TF genes while producing the HyHEL-Fab fragment. For down-regulated TFs, a knockout of the native genes would possibly influence the secretion capacity of the parent strain in a positive way and might be an interesting starting point for future studies.

Interestingly, the titers of the EVCs showed a clear trend in all 24 DWP cultivations. Secretion reached a maximum for 2 µg of transformed plasmid and decreased with higher amounts of transformed DNA, while yields stayed constant for the clones of the 0.8 µg, 2 µg, and 5 µg pool, but also decreased for clones of the 8 µg pool. Figure 19 showed the trend for EVCs for screening of TF2, TF4, TF5sv and TF6. The trend stayed the same for screening of TF1, TF3, TF5 and TFn2i. Seemingly, a high amount of transformed EVC DNA negatively influenced HyHEL-Fab secretion, possibly by excising copies of the original Fab expression cassette, which are integrated in the P_{AOX1} promoter region. This could also mask the effects of TF overexpression. Thus, analysis of 2 µg transformation seemed most reliable.

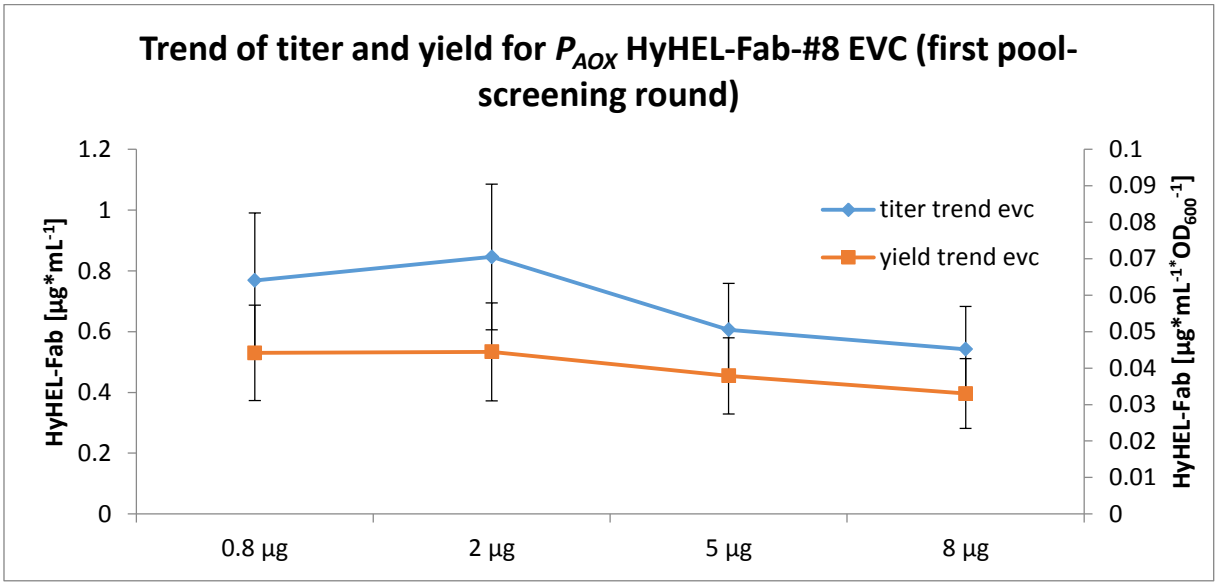

Figure 19: Trend of titer and yield depended on the amount of transformed linearized plasmid. Data of the 1st pool-screening round and mean values of 4 EVC-pools (each with 40 – 48 clones) were used. First screening round included screening of TF2, TF4, TF5sv and TF6.

EVCs also showed a wide distribution of secretion capacity. EVCs transformed with 2 µg of linearized plasmid were screened. Landscapes of secretion capacities (titer and yield) are depicted in Figure 20 and Figure 21.

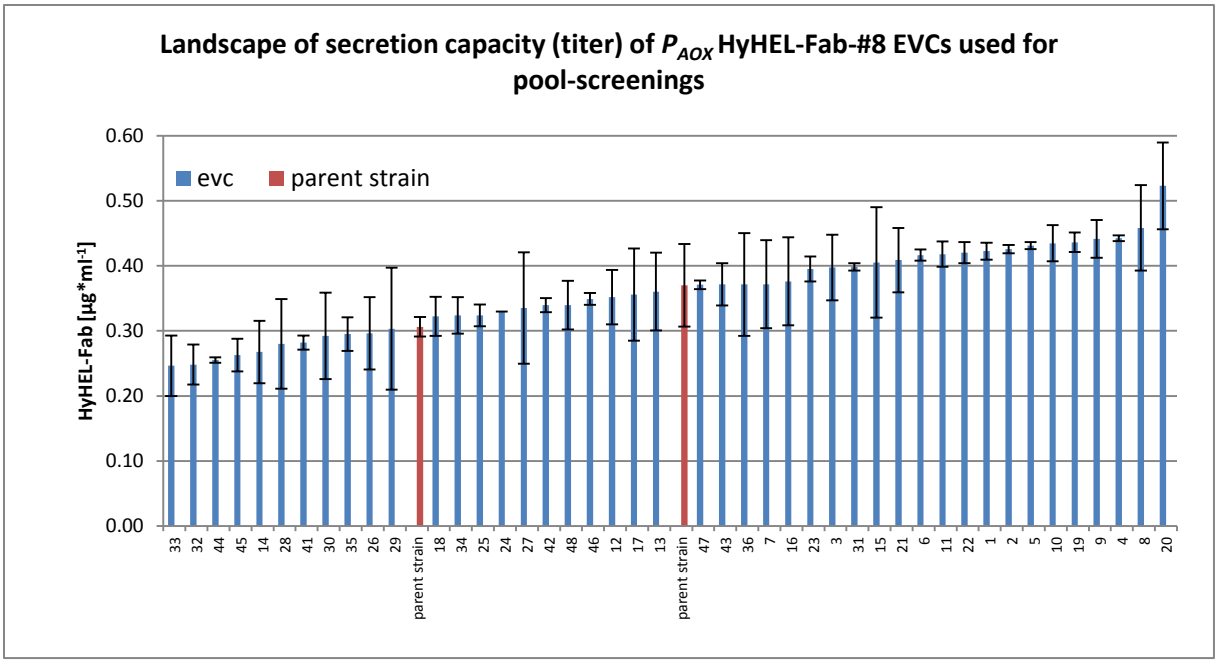

Figure 20: Landscape of secretion capacity (titer) of P_{AOX} HyHEL-Fab-#8 EVCs used for pool-screenings. 44 EVCs transformed with 2 µg linearized plasmid were used as reference for pool-screenings of TF clones also transformed with 2 µg of linearized plasmid.

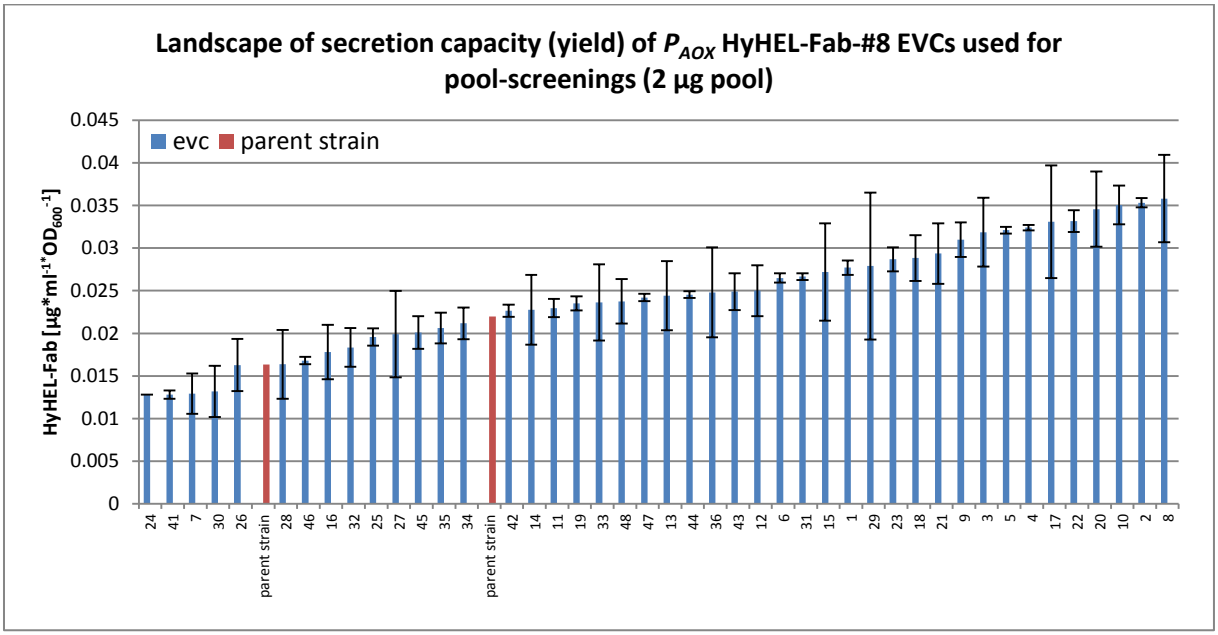

Figure 21: Landscape of secretion capacity (yield) of P_{AOX} HyHEL-Fab-#8 EVCs used for pool-screenings. 44 EVCs transformed with 2 µg linearized plasmid were used as reference for pool-screenings of TF clones also transformed with 2 µg of linearized plasmid.

Also notably, the absolute titer and yield values varied from the first (TF2, TF4, TF5sv and TF6) to the second (TF1, TF2ni, TF3 and TF5) pool-screening round. Observed values were up to 2-fold higher in the first screening round, which seemed to be a cultivation dependent phenomenon (compare Figure 11, Figure 13, Figure 15 and Figure 17 with Figure 12, Figure 14, Figure 16 and Figure 18).

Table 25: Results of pool-screening for linearized plasmid transfomations. Fold changes were compared to clone pools containing the P_{AOX} HyHEL-Fab-#8 parent strain transformed with the empty vector.

	Fold change titer						Fold change yield				
Co-expressed TF	**0.8 µg**	**2 µg**	**5 µg**	**8 µg**	**mix**		**0.8 µg**	**2 µg**	**5 µg**	**8 µg**	**mix**
TF1	**1.16**	**1.06**	0.85	**1.22**	**1.37**		**1.57**	**1.49**	**1.08**	**1.45**	**2.47**
TF2	**1.06**	0.86	**1.30**	**1.46**	**1.03**		**1.19**	**1.04**	**1.31**	**1.43**	**1.23**
TF3	0.82	0.69	0.75	**1.03**	0.82		**1.17**	**1.23**	0.99	**1.53**	**1.28**
TF4	**1.03**	0.81	1.00	**1.11**	0.56		0.79	0.63	0.71	0.87	0.53
TF5	0.82	0.91	0.75	**1.13**	0.96		**1.08**	**1.46**	**1.09**	**1.53**	**1.12**
TF6	0.71	0.80	0.80	0.95	0.52		0.97	**1.12**	**1.02**	**1.13**	0.93
TF2ni	**1.15**	1.03	**1.16**	**1.40**	**1.48**		**1.10**	**1.30**	**1.20**	**1.48**	**1.40**
TF5sv	0.39	0.53	0.59	0.82	0.45		0.68	0.85	0.92	1.15	0.86

3.2. Pool-Screening of Clones Transformed with pPUZZLE_KanR_P_{Gap}_TF Expression Cassette

To investigate locus-dependent effects, P_{AOX} HyHEL-Fab-#8 was also transformed with a PCR-product of the pPUZZLE_KanR_P_{Gap}_TF plasmid expression cassette, which consisted of the *GAP*-promoter, the TF-gene, *CYC1*-TT sequence and the Kanamycin-resistance, but lacking the *AOX1*-terminator sequences for homologous recombination at *AOX1*-terminator locus. Interestingly, results of the clones transformed with linearized plasmid and expression cassette did not exactly match. HyHEL-Fab concentration was constantly improved for the clones of the 2 µg pools of all TFs except TF6 and TF5sv. TF6 and TF2ni co-expressing clones showed an increased HyHEL-Fab titer in the 0.8 µg pool. Only co-expression of TF2ni led to a higher product concentration for clones of two different pools (0.8 µg and 2 µg). The yield was increased for nearly all TFs (except TF4), at least for clones of two pools. TF1, TF3 and TF6 co-expression led to a higher secretion capacity of clones in all transformations. Results of the expression cassette pool-screenings are depicted in Table 26, and Figure 22 - Figure 29.

Table 26: Results of pool-screenings of expression cassette transformations. Fold changes were compared to the P_{AOX} HyHEL-Fab-#8 parent strain transformed with empty vector.

	Fold change titer						Fold change yield				
Co-expressed TF	**0.8 µg**	**2 µg**	**5 µg**	**8 µg**	**mix**		**0.8 µg**	**2 µg**	**5 µg**	**8 µg**	**mix**
TF1	0.94	**1.44**	0.84	0.85	0.94		**1.51**	**1.89**	**1.21**	**1.28**	**1.20**
TF2	0.96	**1.05**	0.80	0.83	**1.13**		**1.25**	**1.36**	0.96	**1.46**	**1.18**
TF3	0.97	**1.14**	0.94	0.92	0.94		**1.31**	**1.35**	**1.23**	**1.23**	**1.21**
TF4	0.95	**1.28**	0.71	0.74	**1.05**		0.86	**1.17**	0.58	0.71	0.93
TF5	0.86	**1.35**	0.89	0.93	0.94		**1.06**	**1.63**	**1.17**	0.93	0.89
TF6	**1.06**	0.90	0.73	0.68	0.85		**1.71**	**1.18**	**1.04**	**1.02**	**1.09**
TF2ni	**1.42**	**1.30**	0.84	0.80	0.94		**1.39**	**1.47**	1.00	0.92	**1.03**
TF5sv	0.82	0.87	0.63	0.53	0.69		**1.22**	**1.34**	1.00	0.80	0.97

Interestingly, TF1 and TF2 did not show increased Fab concentrations in all transformations as it was shown for the linear plasmid. However, 2 µg pool was still improved for TF1 and TF2 by 44 % and 5 % (titer). Biomass dependent concentration was improved for TF1 and TF2 in all pools except the 5 µg pool of TF2. Highest yields were observed with 89 % improvement for the 2 µg pool of TF1 and with 46 % improvement for the 8 µg pool of TF2. Therefore, pool-screening results of transformed cassette indicated the potential as useful secretion helpers. The locus of integration of the cassette of both approaches needs to be evaluated in future by RT-PCR. Illegitimate recombination by NHEJ takes place between one or both ends of the transforming DNA with the chromosomal target by base pairing with micro-homology[20, 78]. Possible events of an ectopic integration of foreign DNA into the genome might be chromosomal deletions, duplications and translocations. A possible site of homologous recombination for this specific expression cassette could be the locus of the glyceraldehyd-3-phosphat-dehydrogenase (*GAP*) because of the flanking P_{GAP} region.

The idea of using an expression cassette with only one homologous end, was to prevent a putative loss of copy number of the HyHEL-Fab cassette integrated at the *AOX1* locus by gene replacement.

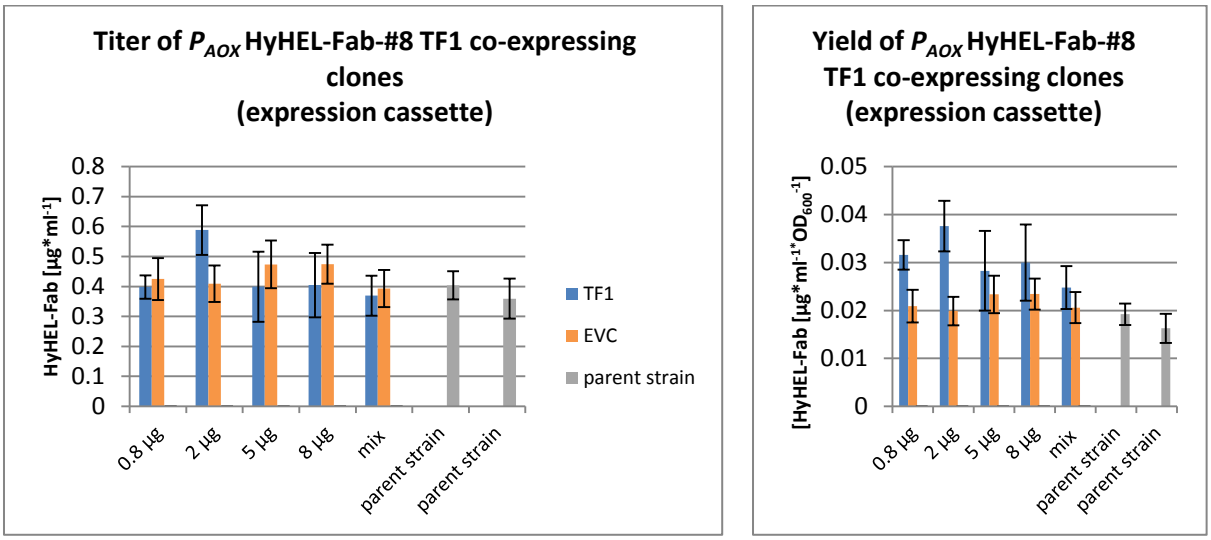

Figure 22: Titer and yield of P_{AOX} HyHEL-Fab-#8 TF1 co-expressing clones (expression cassette) measured by ELISA. Data represents mean values of four technical replicates of two separate plates. EVC and recombinant P_{AOX} HyHEL-Fab parent strains were used as reference. Blue bars: pools of P_{AOX} HyHEL-Fab-#8 TF1 co-expressing clones; orange bars: pools of P_{AOX} HyHEL-Fab-#8 EVC; grey bars: P_{AOX} HyHEL-Fab-#8 parent strain.

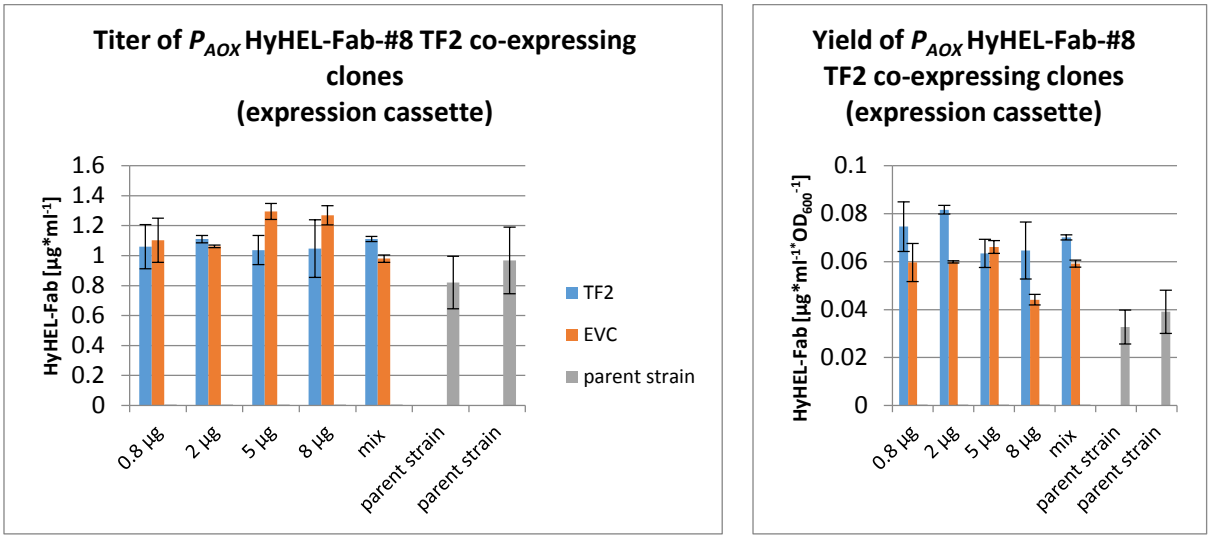

Figure 23: Titer and yield of P_{AOX} HyHEL-Fab-#8 TF2 co-expressing clones (expression cassette) measured by ELISA. Data represents mean values of four technical replicates of two separate plates. EVC and recombinant P_{AOX} HyHEL-Fab parent strains were used as reference. Blue bars: pools of P_{AOX} HyHEL-Fab-#8 TF2 co-expressing clones; orange bars: pools of P_{AOX} HyHEL-Fab-#8 EVC; grey bars: P_{AOX} HyHEL-Fab-#8 parent strain.

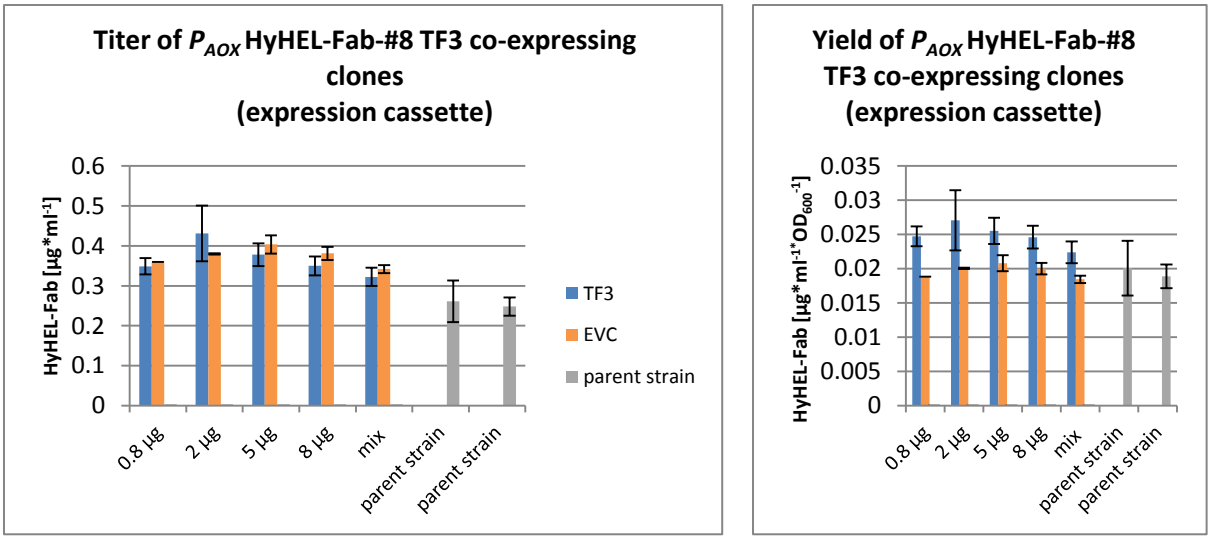

Figure 24: Titer and yield of P_{AOX} HyHEL-Fab-#8 TF3 co-expressing clones (expression cassette) measured by ELISA. Data represents mean values of four technical replicates of two separate plates. EVC and recombinant P_{AOX} HyHEL-Fab parent strains were used as reference. Blue bars: pools of P_{AOX} HyHEL-Fab-#8 TF3 co-expressing clones; orange bars: pools of P_{AOX} HyHEL-Fab-#8 EVC; grey bars: P_{AOX} HyHEL-Fab-#8 parent strain.

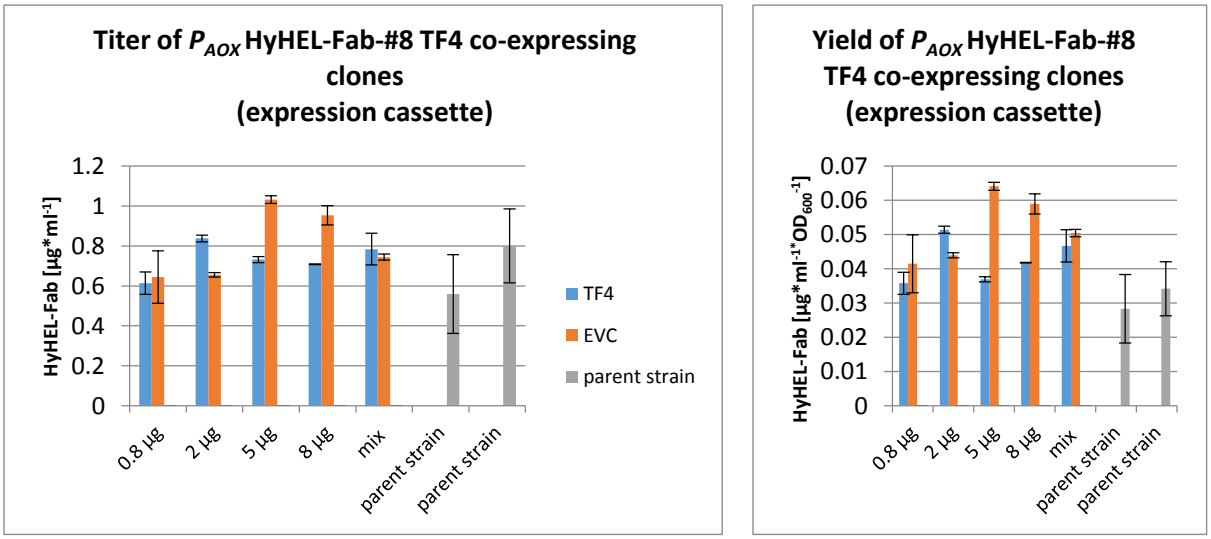

Figure 25: Titer and yield of P_{AOX} HyHEL-Fab-#8 TF4 co-expressing clones (expression cassette) measured by ELISA. Data represents mean values of four technical replicates of two separate plates. EVC and recombinant P_{AOX} HyHEL-Fab parent strains were used as reference. Blue bars: pools of P_{AOX} HyHEL-Fab-#8 TF4 co-expressing clones; orange bars: pools of P_{AOX} HyHEL-Fab-#8 EVC; grey bars: P_{AOX} HyHEL-Fab-#8 parent strain.

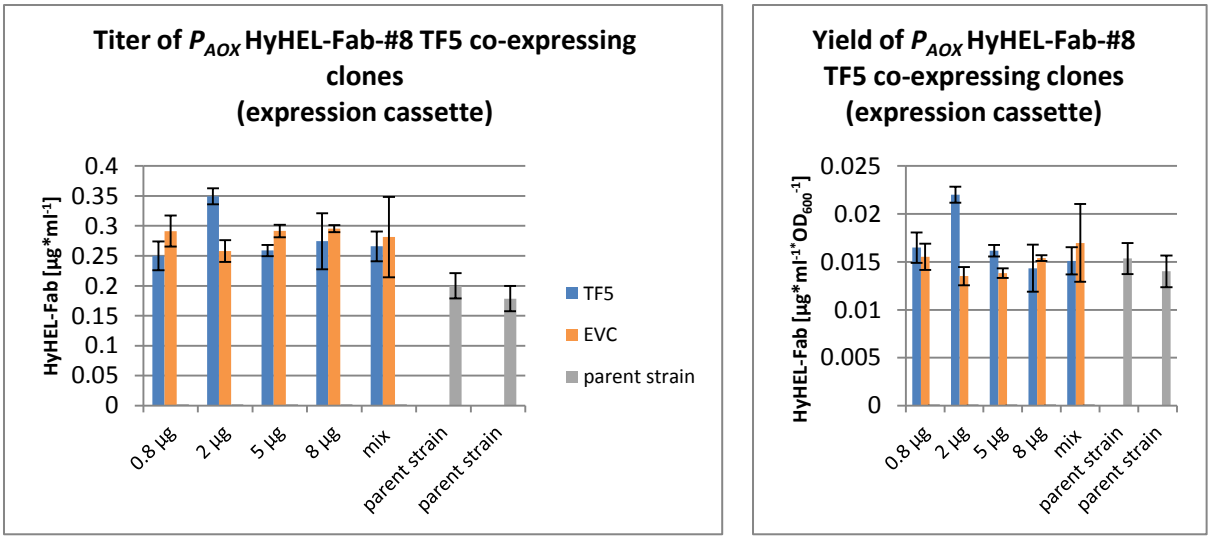

Figure 26: Titer and yield of P_{AOX} HyHEL-Fab-#8 TF5 co-expressing clones (expression cassette) measured by ELISA. Data represents mean values of four technical replicates of two separate plates. EVC and recombinant P_{AOX} HyHEL-Fab parent strains were used as reference. Blue bars: pools of P_{AOX} HyHEL-Fab-#8 TF5 co-expressing clones; orange bars: pools of P_{AOX} HyHEL-Fab-#8 EVC; grey bars: P_{AOX} HyHEL-Fab-#8 parent strain.

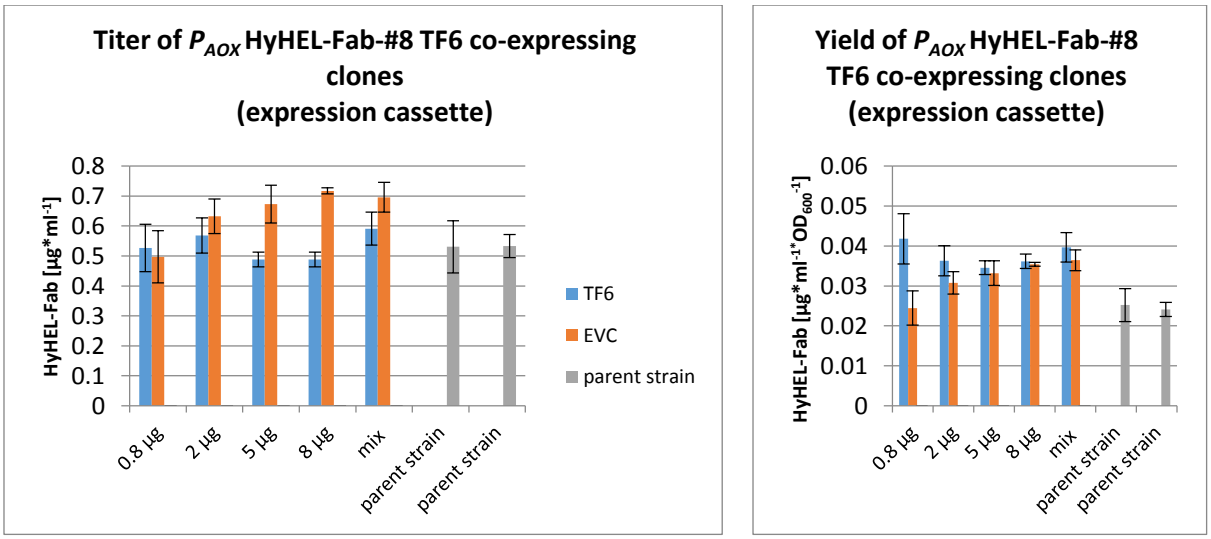

Figure 27: Titer and yield of P_{AOX} HyHEL-Fab-#8 TF6 co-expressing clones (expression cassette) measured by ELISA. Data represents mean values of four technical replicates of two separate plates. EVC and recombinant P_{AOX} HyHEL-Fab parent strains were used as reference. Blue bars: pools of P_{AOX} HyHEL-Fab-#8 TF6 co-expressing clones; orange bars: pools of P_{AOX} HyHEL-Fab-#8 EVC; grey bars: P_{AOX} HyHEL-Fab-#8 parent strain.

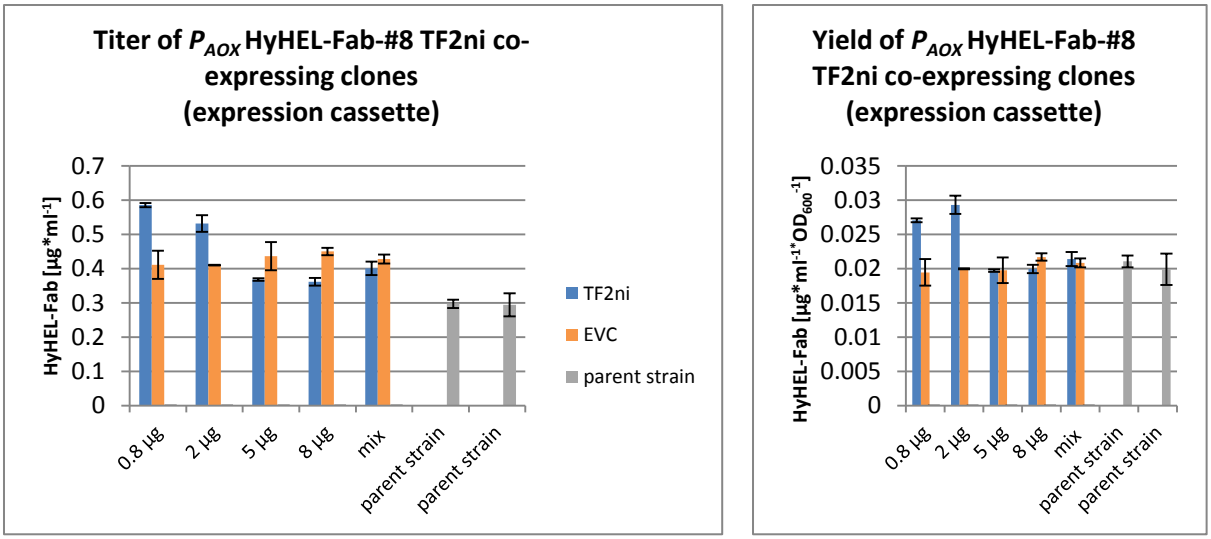

Figure 28: Titer and yield of P_{AOX} HyHEL-Fab-#8 TF2ni co-expressing clones (expression cassette) measured by ELISA. Data represents mean values of four technical replicates of two separate plates. EVC and recombinant P_{AOX} HyHEL-Fab parent strains were used as reference. Blue bars: pools of P_{AOX} HyHEL-Fab-#8 TF2ni co-expressing clones; orange bars: pools of P_{AOX} HyHEL-Fab-#8 EVC; grey bars: P_{AOX} HyHEL-Fab-#8 parent strain.

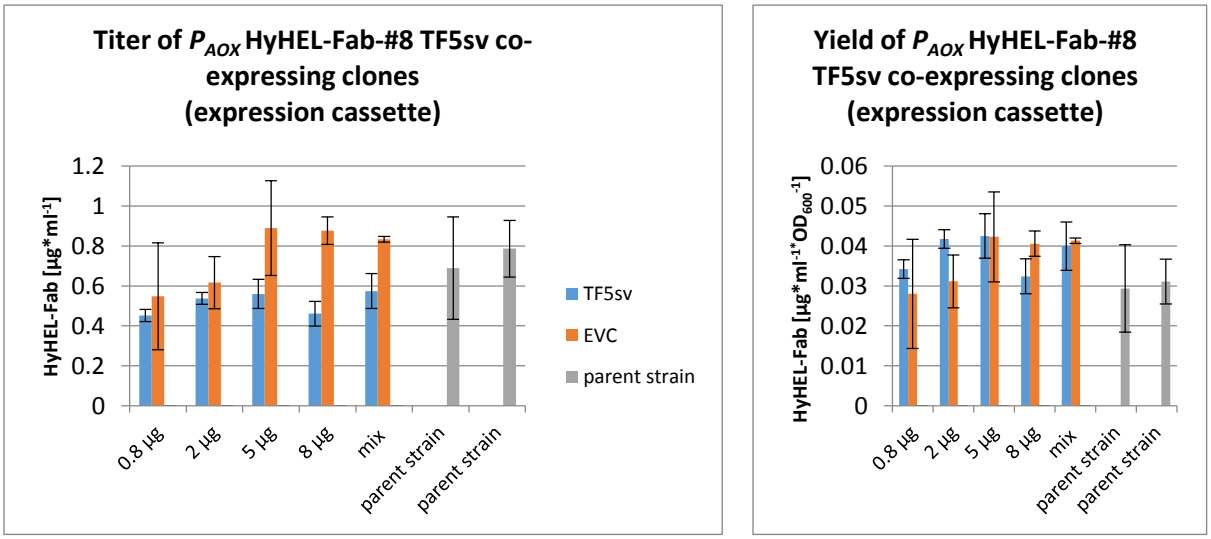

Figure 29: Titer and yield of P_{AOX} HyHEL-Fab-#8 TF5sv co-expressing clones (expression cassette) measured by ELISA. Data represents mean values of four technical replicates of two separate plates. EVC and recombinant P_{AOX} HyHEL-Fab parent strains were used as reference. Blue bars: pools of P_{AOX} HyHEL-Fab-#8 TF5sv co-expressing clones; orange bars: pools of P_{AOX} HyHEL-Fab-#8 EVC; grey bars: P_{AOX} HyHEL-Fab-#8 parent strain.

EVCs transformed with the expression cassette (cas), which was a PCR-product containing the P_{GAP}, gene of interest (TF), *CYC1*-TT and KanR (Figure 4), showed a different trend for titer and yield, dependent on the amount of transformed PCR-product. Compared to the EVCs transformed with linearized plasmid, this time secretion increased with higher amounts of transformed PCR-product. Analysis was again split in 1st and 2nd pool-screening, because of cultivation dependent absolute values of titer and yield. The first cultivation round showed a significant increase of titer between 2 µg cas and 5 µg cas and an overall increase of titer with higher amount of transformed expression cassette, while yields showed only a slight increase with higher amounts of transformed expression cassette reaching a maximum for 5 µg cas (Figure 30). The second cultivation-round confirmed these results (data not shown).

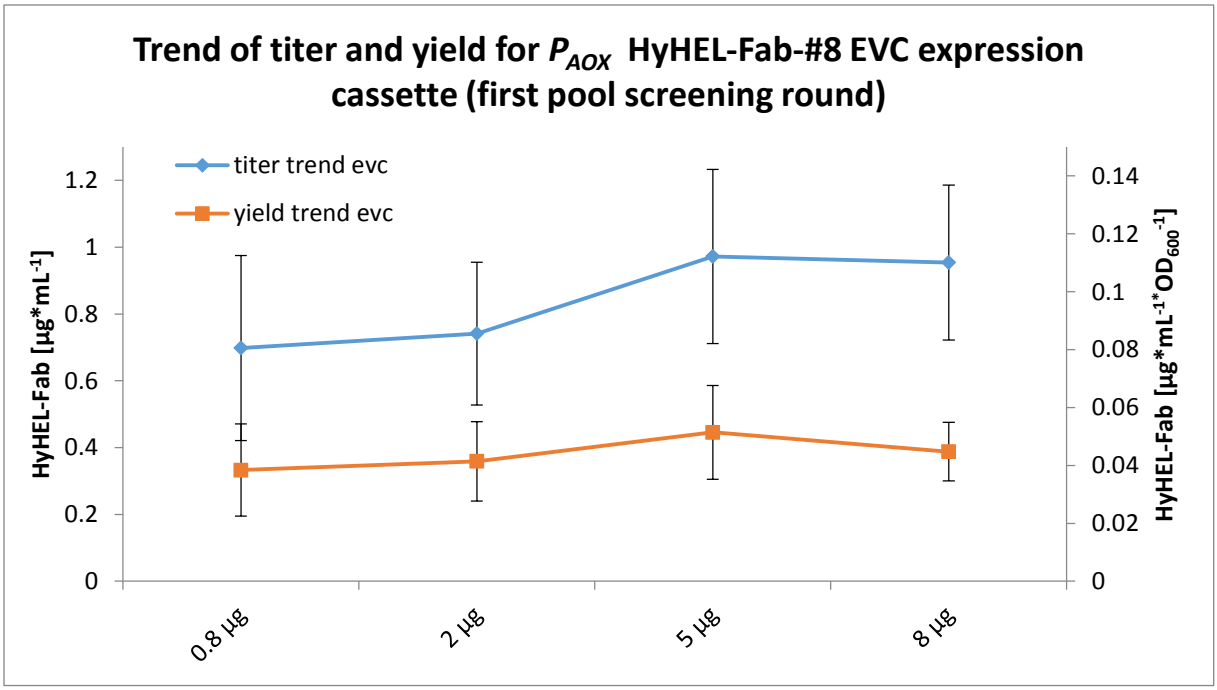

Figure 30: Trend of titer and yield depended on transformed amount of expression cassette. Diagram comprises summed up data of the 1st pool-screening round and represents mean values of 4 EVC-pools (each with 40 – 48 clones) with their ±SD (standard deviation).

Fold change levels of TF3 and TF5 co-expressing clone pools were compared upon transformation with linearized plasmid or expression cassette (Figure 31 - Figure 34).

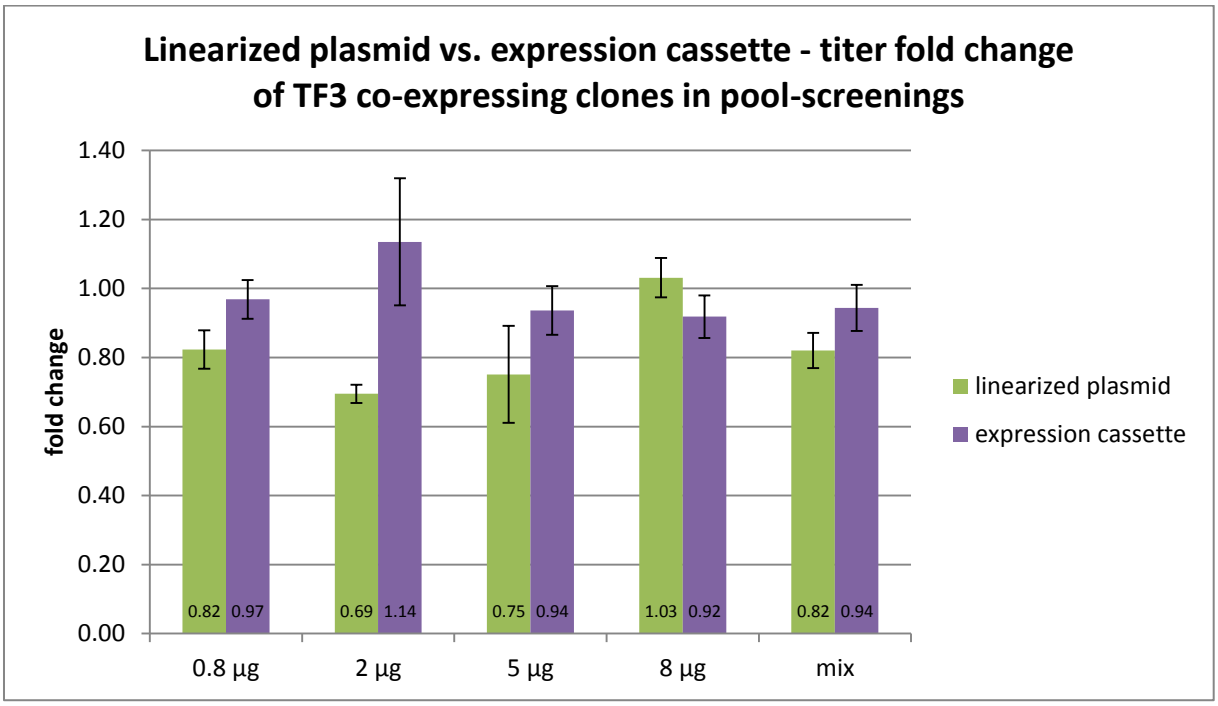

Figure 31: Comparison of titer fold changes of pools co-expressing TF3 transformed with linearized plasmid or expression cassette. Titers were normalized to corresponding EVC-pools.

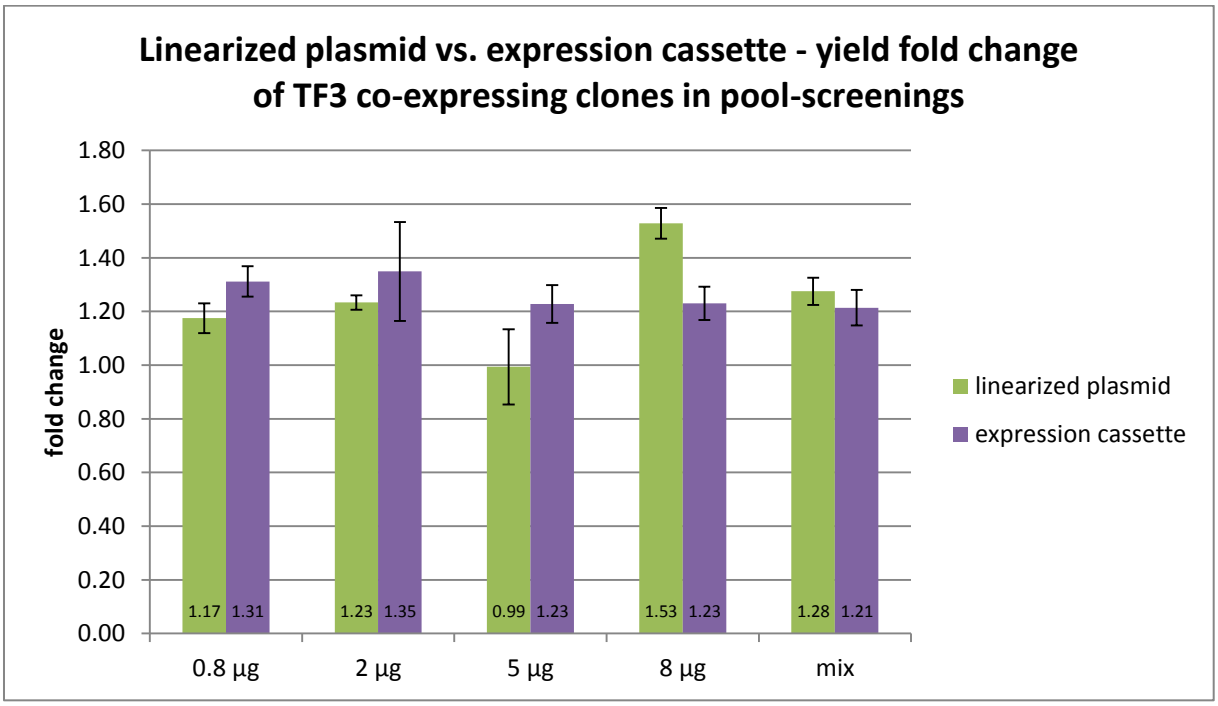

Figure 32: Comparison of yield fold changes of pools co-expressing TF3 transformed with linearized plasmid or expression cassette. Yields were normalized to corresponding EVC-pools.

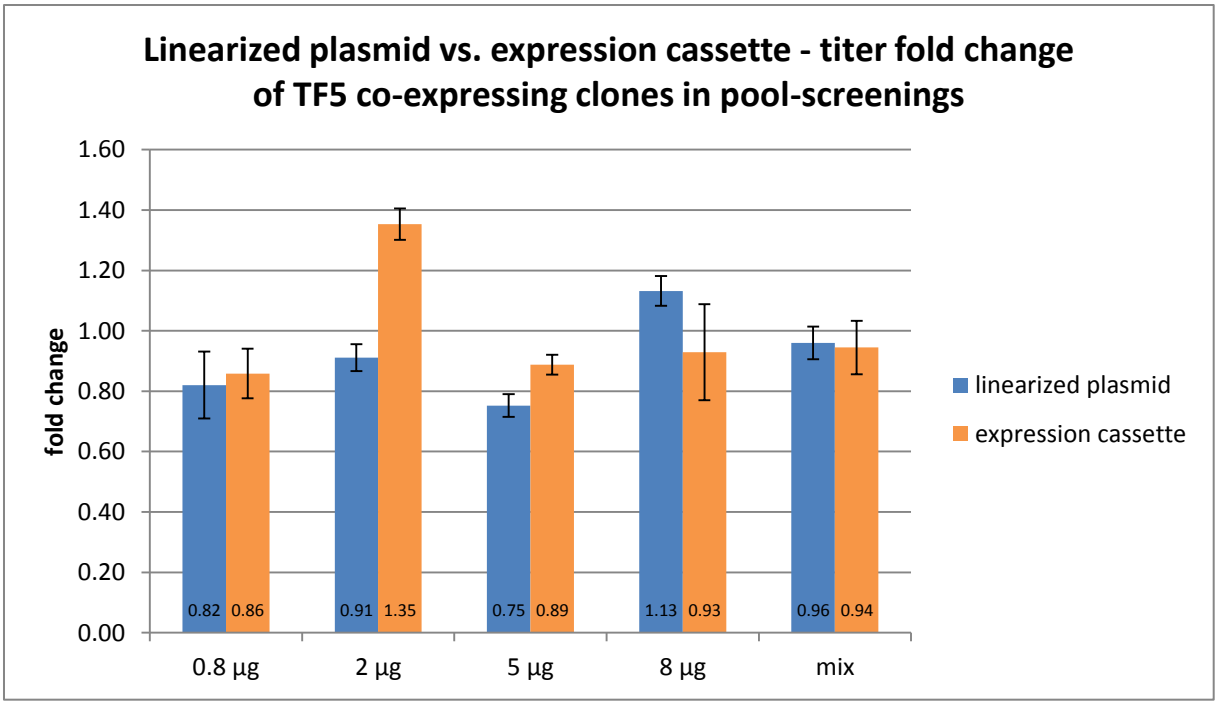

Figure 33: Comparison of titer fold changes of pools co-expressing TF5 transformed with linearized plasmid or expression cassette. Titers were normalized to corresponding EVC-pools.

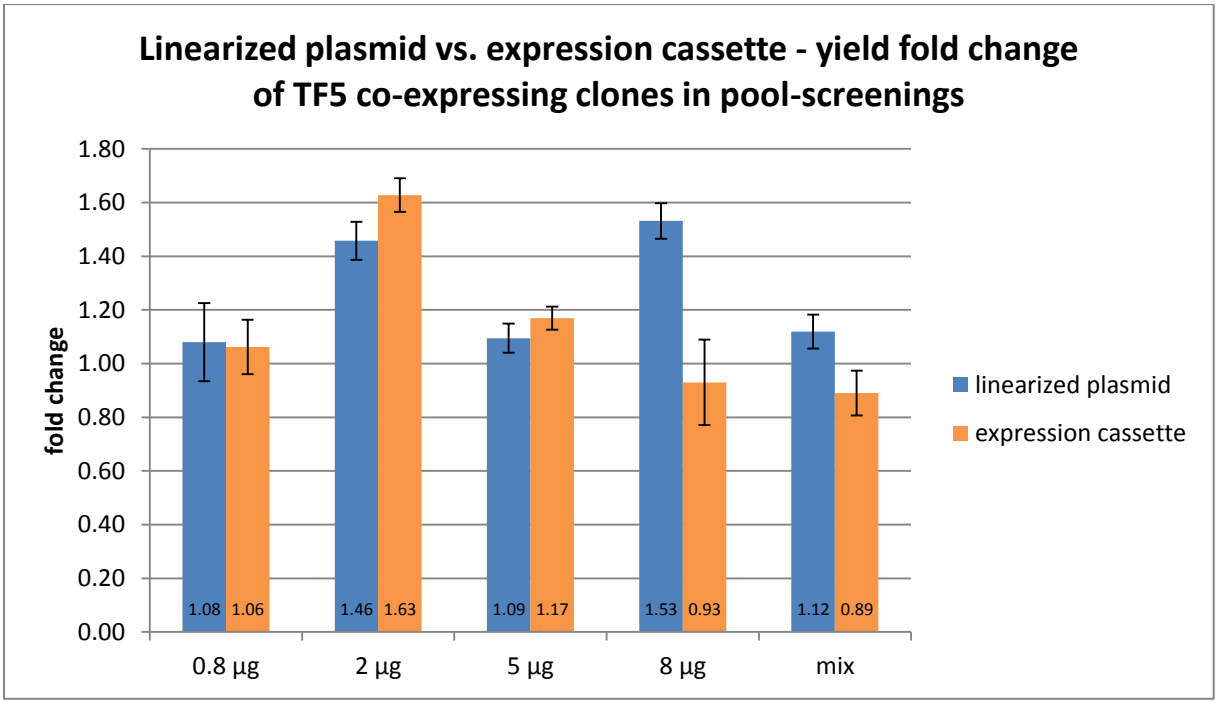

Figure 34: Comparison of yield fold changes of pools co-expressing TF5 transformed with linearized plasmid or expression cassette. Yields were normalized to corresponding EVC-pools.

3.3. Single-Clone-Screenings of TF1 and TF2 Co-Expressing Clones

Based on the results of the pool-screenings, TF1 and TF2 co-expressing clones were chosen to be tested in a single-clone-screening. Clones of the 2 µg pool were selected to be screened and tested against the best performing EVCs, which were derived from the 2 µg pool. Single-clone-screenings were also performed in 24 DWP and studied after 48 h of

methanol induction. To prove the results statistically valid, 12 TF co-expressing clones were cultivated together with 12 single EVC clones. Student's t-test (two-tailed test for unmatched pairs) was used to calculate the statistical significance of TF1 and TF2 co-expressing clones versus the EVCs (p-value ≤ 0.05 → ++ / p-value ≤ 0.01 → +++). Promising single clones were then selected for an in-kind bioreactor cultivation.

3.3.1. Screening of the Clones 1-12 Transformed with 2 µg Linearized Plasmid

First, 12 single clones (clones 1 to 12 of the 2 µg pool) co-expressing TF1 and TF2, were screened against 12 EVCs. For this purpose, clones were streaked out on YPD plates (Zeo 50/ Gen 450) and stored at 4 °C (Figure 35).

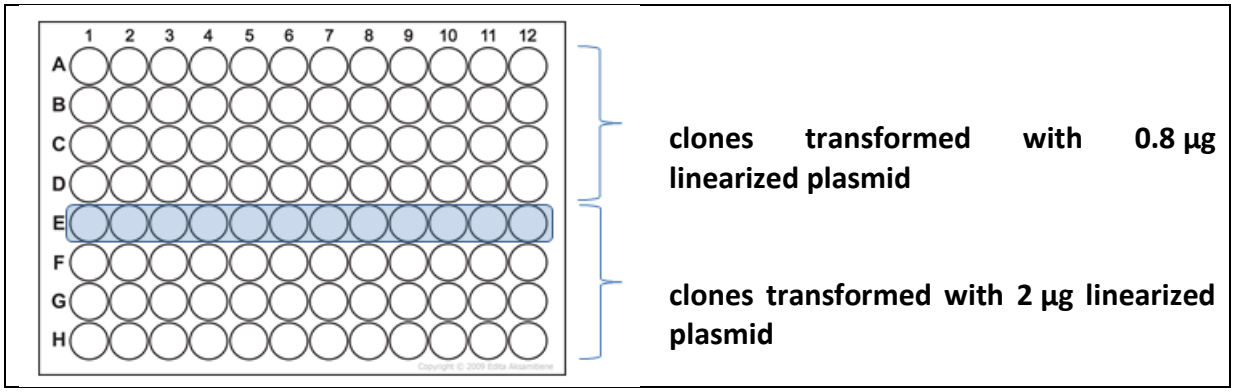

Figure 35: Clones selected for first single-clone-screening are marked in blue. Same layout was used for TF clones and EVC.

The titer of TF1 co-expressing clones was higher than the average of the EVCs for 8 of 12 clones with a maximum of 23 % improvement for clone 1. The p-value of 0.785 indicated a 78.5 % chance, that the obtained results for TF1 co-expression were not significantly different to EVC and not an effect of TF1 co-expression (Figure 36). However, analysis of the yields led to a totally different p-value of 0.019, indicating a statistical difference between the two sets of clones, i.e. 98.1 % chance of a positive impact of TF1. Accordingly, 10 of 12 clones showed an improved yield compared to the average EVC. For example clone 11, 8 and 6 had 48 %, 51 % and 59 % improved yields compared to the average EVC, respectively.

Also TF2 co-expression raised the HyHEL-Fab concentration in the supernatant of 6 of 12 screened clones above the average EVC titer-level. The highest titers were observed for clone 4 and clone 6 with a 57 – 60 % improvement compared to the average EVC. However, the high p-value of 0.425 suggested that the improvement was likely not an impact of TF2 co-expression (Figure 38). Analysing yields, 4 clones showed an over 2-fold improvement compared to the average EVC. But, the p-value of the yield was still high at 0.345 and significantly higher than the 0.05 limit for biological significance (Figure 39). Copy number and colony size might have influenced the results. therefore, 12 randomly chosen clones were cultivated and screened in addition to eliminate any influence of the colony size.

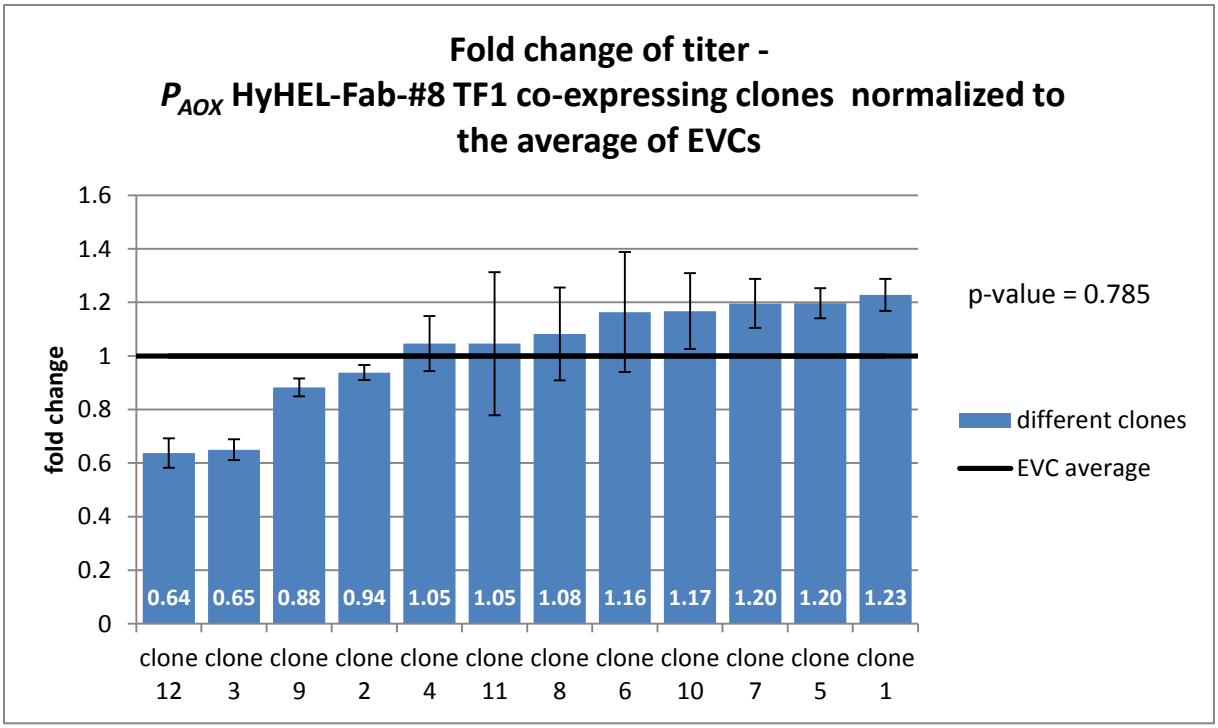

Figure 36: Results of single-clone-screening of TF1 co-expressing clones normalised to average of EVCs. Fold change of titer of 12 P_{AOX} HyHEL-Fab-#8 TF1 co-expressing clones obtained from single-clone-screening. Titer levels of 12 P_{AOX} HyHEL-Fab-#8 TF1 co-expressing clones were normalized to the average of 12 EVCs. Data represents mean values and ±SD of 3 technical replicates on a single ELISA plate. The p-value was calculated using a two – tailed test for unmatched pairs.

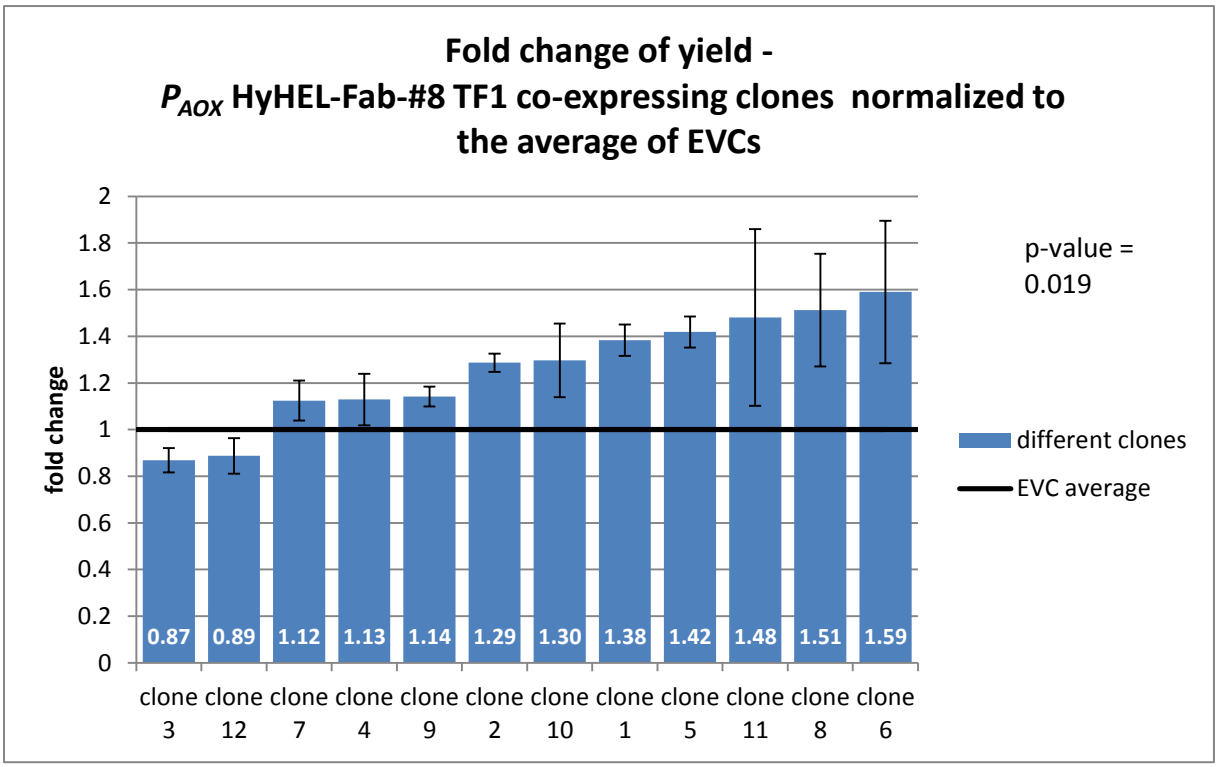

Figure 37: Results of single-clone-screening of TF1 co-expressing clones normalised to average of EVCs. Fold change of yield of 12 P_{AOX} HyHEL-Fab-#8 TF1 co-expressing clones obtained from single-clone-screening. Yield levels of 12 P_{AOX} HyHEL-Fab-#8 TF1 co-expressing clones were normalized to the average of 12 EVCs. Data represents mean values and ±SD of 3 technical replicates on a single ELISA plate. The p-value was calculated using a two – tailed test for unmatched pairs.

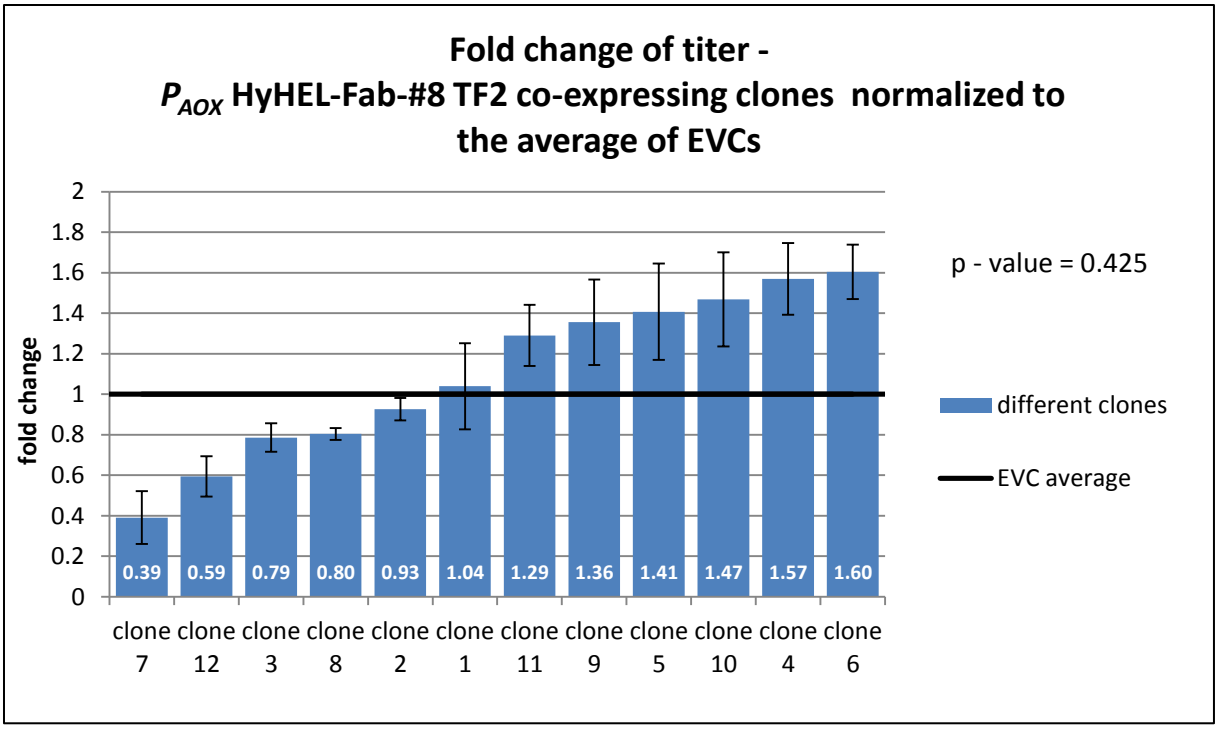

Figure 38: Results of single-clone-screening of TF2 co-expressing clones normalised to average of EVCs. Fold change of titer of 12 P_{AOX} HyHEL-Fab-#8 TF2 co-expressing clones obtained from single-clone-screening. Titer levels of 12 P_{AOX} HyHEL-Fab-#8 TF2 co-expressing clones were normalized to the average of 12 EVCs. Data represents mean values and ±SD of 3 technical replicates on a single ELISA plate. The p-value was calculated using a two – tailed test for unmatched pairs.

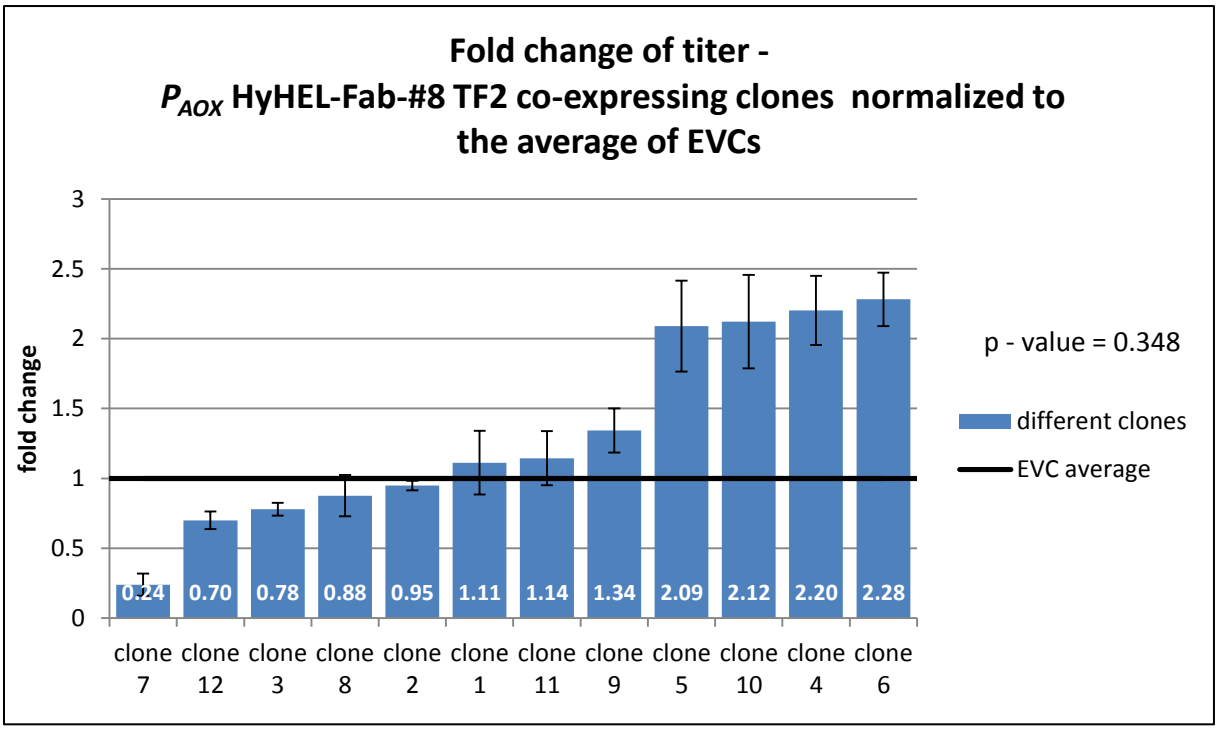

Figure 39: Results of single-clone-screening of TF2 co-expressing clones normalised to average of EVCs. Fold change of yield of 12 P_{AOX} HyHEL-Fab-#8 TF2 co-expressing clones obtained from single-clone-screening. Yield levels of 12 P_{AOX} HyHEL-Fab-#8 TF2 co-expressing clones were normalized to the average of 12 EVCs. Data represents mean values and ±SD of 3 technical replicates on a single ELISA plate. The p-value was calculated using a two – tailed test for unmatched pairs.

3.3.2. Screening of Randomly Selected Clones

12 clones randomly selected from the pinning plate were screened in addition to exclude a possible influence of the colony size on the secretion behaviour. Again 12 single clones co-expressing TF1 or TF2 were cultivated in a 24 DWP and compared to a random selection of EVCs. The Clones number 4, 9, 10, 13, 14, 18, 23, 28, 37, 40 and 44 were chosen (Figure 40).

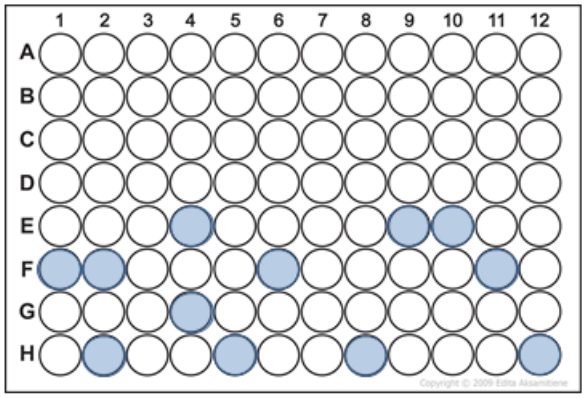

clones transformed with 0.8 µg of linearized plasmid

clones transformed with 2 µg of linearized plasmid

Figure 40: Randomly selected clones of the pinning plate for single-clone-screening. Selected clones are marked in blue. Same scheme is used for TF clones and EVC. Marked clones are: 4, 9, 10, 13, 14, 18, 23, 28, 37, 40 and 44.

Co-expression of TF1 revealed that 10 of 12 randomly selected clones secreted the HyHEL-Fab fragment in a higher concentration than the average EVC. Clone 44 showed the highest improvement of 67 %. Clone 13 and clone 10 still secreted the product in a 28 % and 30 % higher concentration. A p-value of 0.014 (++) was calculated, which indicated clearly a positive impact of TF1 co-expression on the secretion capacity (Figure 41). The yield of TF1 co-expressing randomly selected clones was also increased for nearly all screened clones over the average EVC. Clone 44 had a 2.47-fold improvement of yield, while clone 13 secreted 43 % more product per biomass. The calculated p-value of 0.008 (+++) indicated the significantly positive effect (Figure 42).

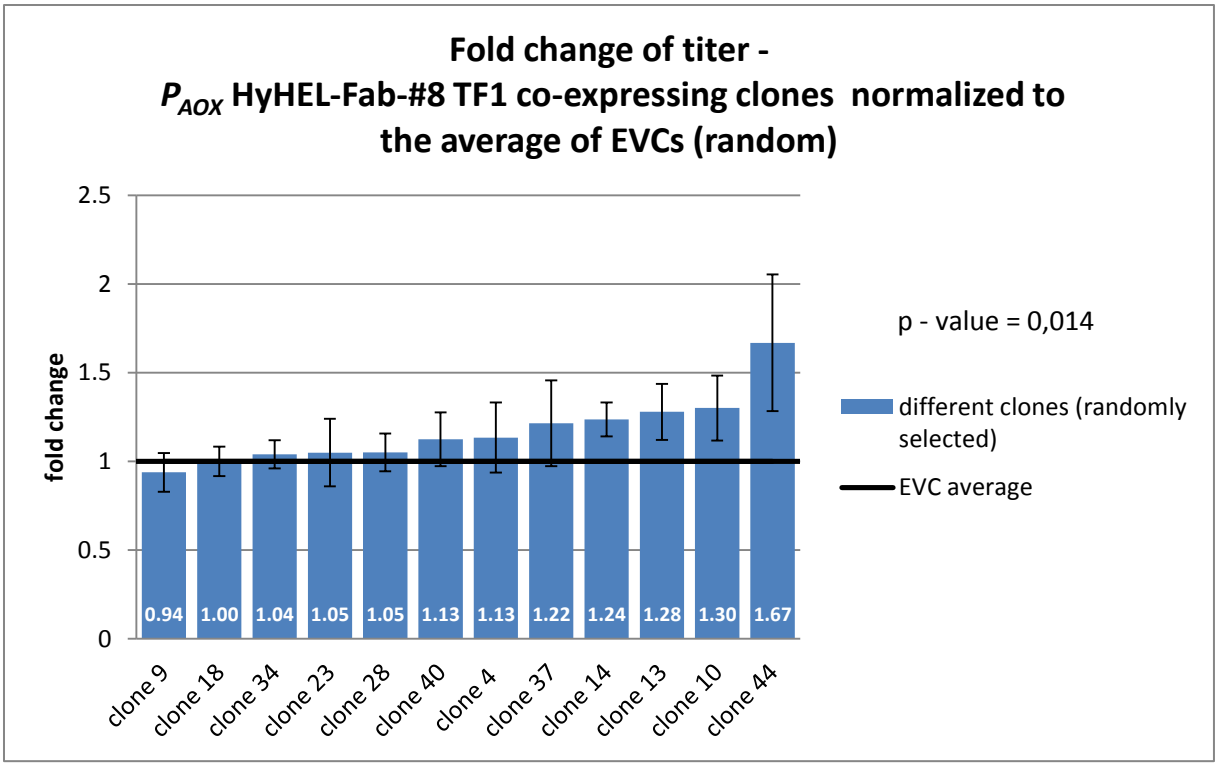

Figure 41: Results of single-clone-screening of randomly selected TF1 co-expressing clones and normalised to average of EVCs. Fold change of titer of 12 randomly selected P_{AOX} HyHEL-Fab-#8 TF1 co-expressing clones obtained from single-clone-screening. Titer levels of P_{AOX} HyHEL-Fab-#8 TF1 co-expressing clones were normalized to the average of 12 EVCs. Data represents mean values and ±SD of 3 technical replicates on a single ELISA plate. The p-value was calculated using a two – tailed test for unmatched pairs.

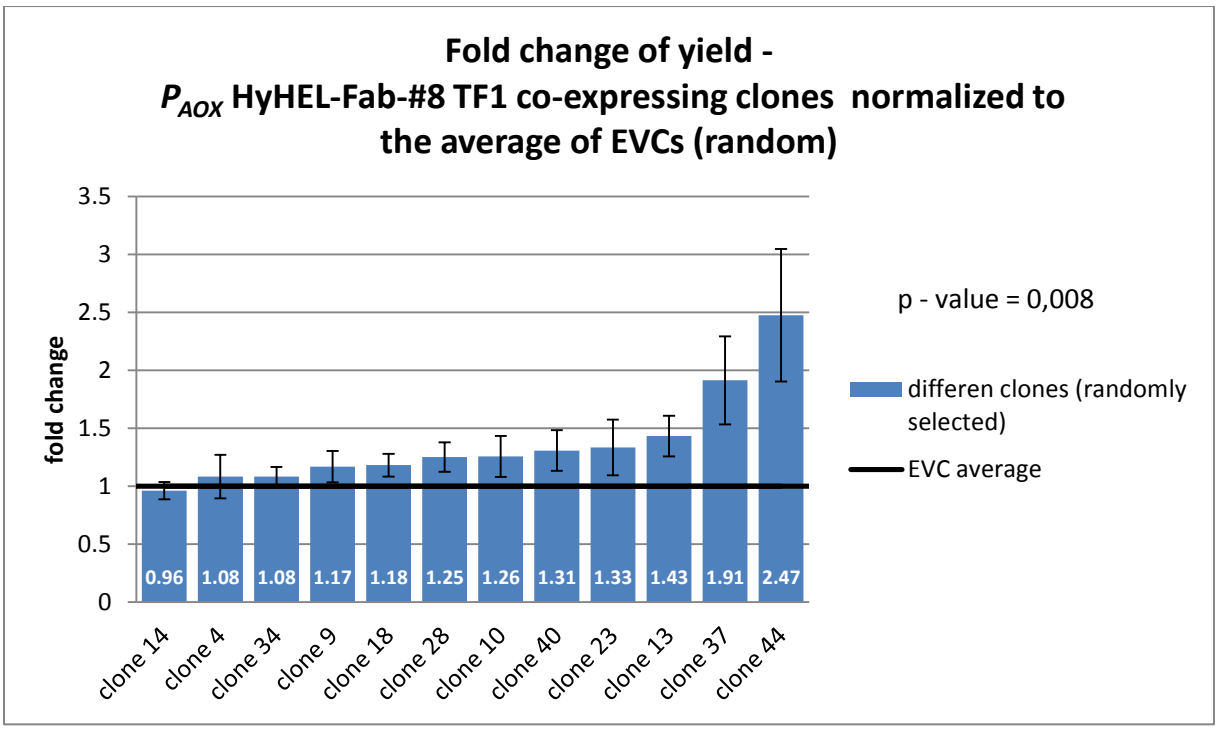

Figure 42: Results of single-clone-screening of randomly selected TF1 co-expressing clones and normalised to average of EVCs.Fold change of yield of 12 randomly selected P_{AOX} HyHEL-Fab-#8 TF1 co-expressing clones obtained from single-clone-screening. Yield levels of P_{AOX} HyHEL-Fab-#8 TF1 co-expressing clones were normalized to the average of 12 EVCs. Data represents mean values and ±SD of 3 technical replicates on a single ELISA plate. The p-value was calculated using a two – tailed test for unmatched pairs.

Seven clones with a higher titer than the average EVC were obtained for TF2 co-expression. Clone 18 and clone 13 showed an improvement of 55 % and 59 % for the product concentration. The p-value of 0.153 indicated only a chance of 15.3 % that the observed titer levels were not the effect of TF2 co-expression (Figure 43). Co-expression of TF2 increased the yield of 11 clones over the average EVC level. Clone 18 showed the highest improvement of yield of 87 %. Clones 9, 13 and 4 also had over 50 % increased yields of 59 %, 64 % and 73 %, respectively. The influence of the biomass formation reduced the p-value to 0.002 (+++), which indicated a positive effect of TF2 co-expression on the secretion capacity (Figure 44). The screening of randomly selected clones confirmed the positive effect of T1 and TF2 co-expression on HyHEL Fab secretion. Especially the p-values of the obtained yield values stated high biological significance (+++). Also the fact that more than half of the screened clones showed higher titer and yield levels for both TFs confirmed the positive influence of TF1/2 co-expression on Fab secretion. Colony size is presumably related to gene dosage after transformation with linearized pPUZZLE_KanR_P_{Gap}_TF. Bigger colonies most probably have a higher number of integrated plasmid, which was indicated by the faster growth on YPD (Zeo 50/ Gen 450) compared to small and medium colonies. Some studies showed a direct relationship between the copy number and the secretion capacity (mini-proinsulin)[21]. However, others stated the relationship only for low gene copy numbers and in particular cases (porcine insulin receptor) an optimum of the gene copy number was observed. Thus, big colonies with possibly higher copy numbers must not inevitably be the best secreters. The strategy to screen for randomly selected clones with various colony sizes, which potentially harbour various quantities of gene copies seems best.

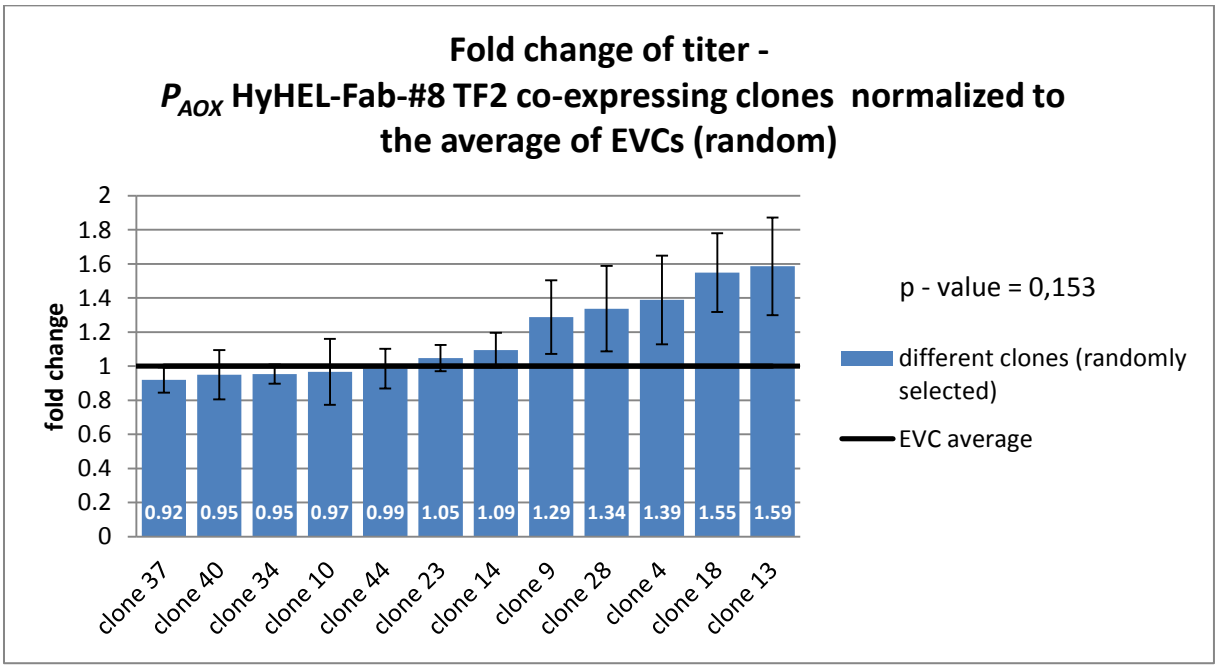

Figure 43: Results of single-clone-screening of randomly selected TF2 co-expressing clones and normalised to average of EVCs. Fold change of titer of 12 randomly selected P_{AOX} HyHEL-Fab-#8 TF2 co-expressing clones obtained from single-clone-screening. Titer levels of P_{AOX} HyHEL-Fab-#8 TF2 co-expressing clones were normalized to the average of 12 EVCs. Data represents mean values and ±SD of 3 technical replicates on a single ELISA plate. The p-value was calculated using a two – tailed test for unmatched pairs.

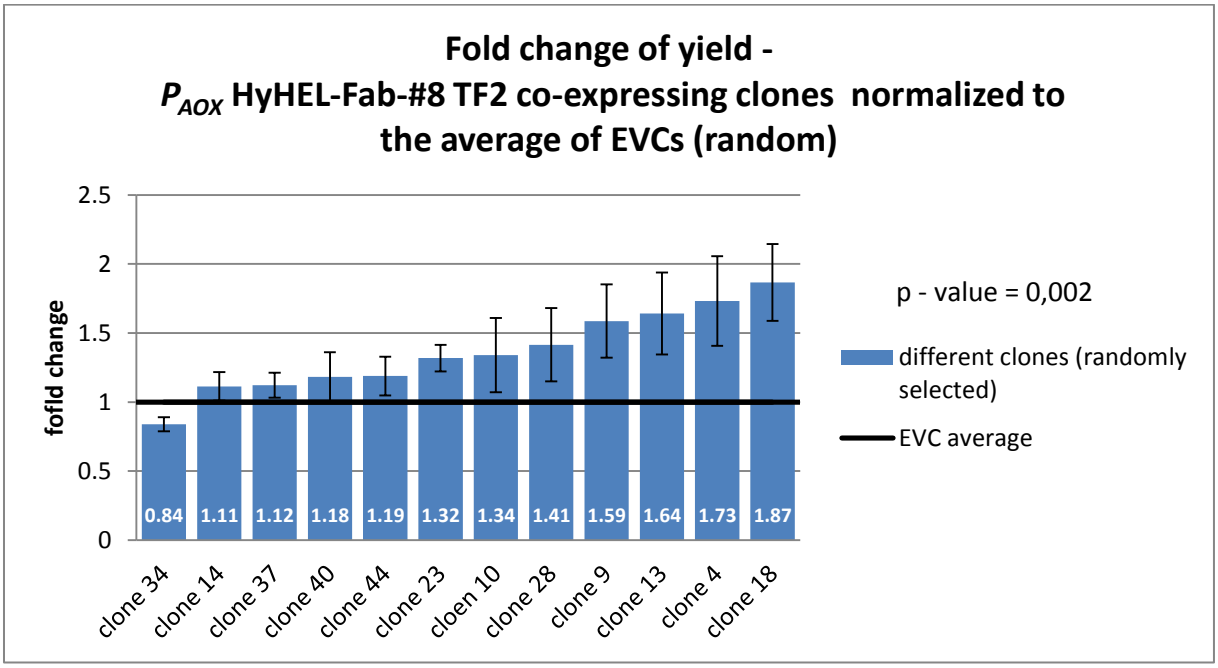

Figure 44: Results of single-clone-screening of randomly selected TF2 co-expressing clones and normalised to average of EVCs. Fold change of yield of 12 randomly selected P_{AOX} HyHEL-Fab-#8 TF2 co-expressing clones obtained from single-clone-screening. Yield levels of P_{AOX} HyHEL-Fab-#8 TF2 co-expressing clones were normalized to the average of 12 EVCs. Data represents mean values and ±SD of 3 technical replicates on a single ELISA plate. The p-value was calculated using a two – tailed test for unmatched pairs.

3.3.2.1. Change to ELISA Protocol for Single-Clone-Screening

At this point the ELISA procedure was changed. The change of protocols was a general project decision in order to standardise the ELISA protocol used in different working groups. We repeated the ELISA measurement of Figure 41 and Figure 42 to prove the reproducibility of these two different ELISA protocols. Though clone 44 was best in both ELISA methods, also divergent results of the two ELISA protocols were found (Table 27 and Table 28). Using the new protocol, clone 37 and clone 44 showed an increased product concentration of 2.07-fold and 2.18-fold, respectively (old protocol). However, the p-value was 0.126, questioning the biological significance of a positive TF1 impact (Figure 45). Six of twelve clones showed a yield level higher than the average EVC. But, four of these six clones were only slightly increased to an extent of maximal 14 %. Clone 37 and clone 44 were also the best secreters when taking the biomass formation into account, showing a yield improved by 31 % and 46 % (Figure 46). In summary, both methods showed that pipetting errors or incomplete mixing can significantly influence results and must be prevented. Despite the observed differences, the new protocol for single-clone-screenings has been shown applicable in other workpackages in this ACIB project (3.2) and was for this reason used as the standard protocol for all subsequent screening procedures.

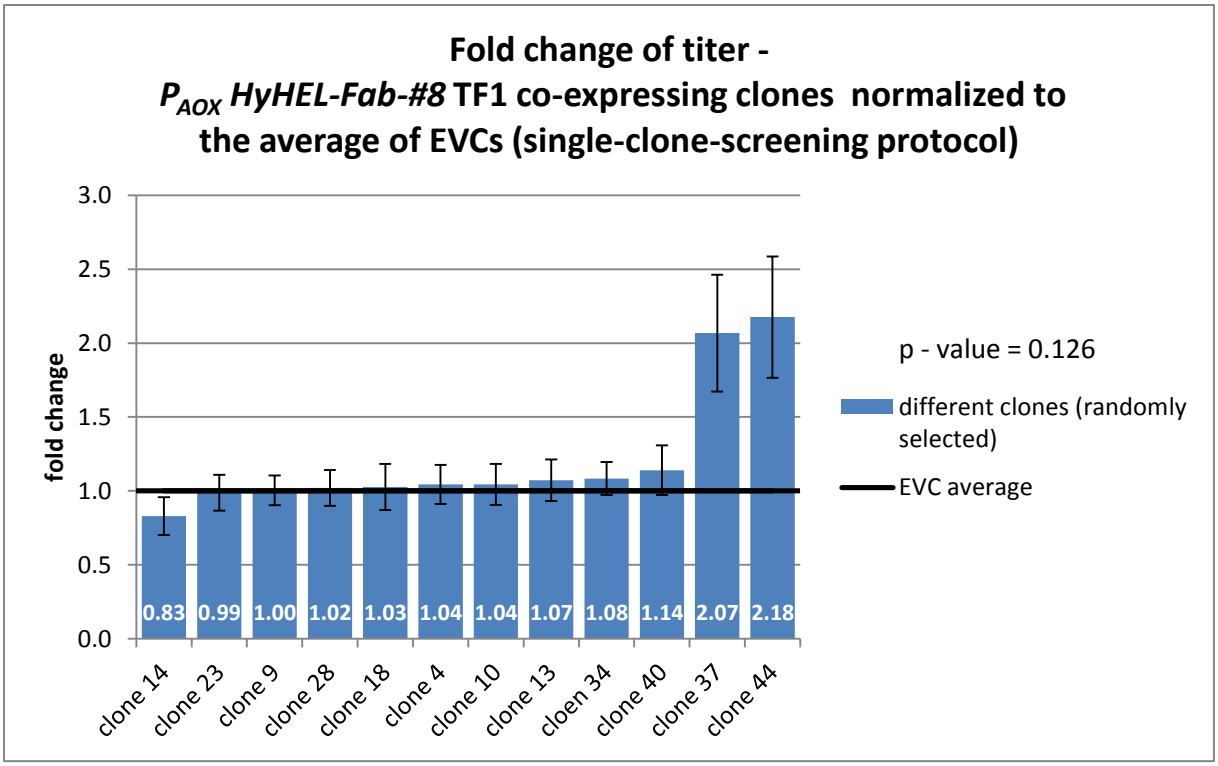

Figure 45: Fold change of titers of 12 randomly selected P_{AOX} HyHEL-Fab-#8 TF1 co-expressing clones (obtained from single-clone-screening). Titers were normalized to the average of 12 EVCs. Data represents mean values of 3 technical replicates according to the new ELISA protocol for single-clone-screenings. The p-value was calculated using a two – tailed test for unmatched pairs.

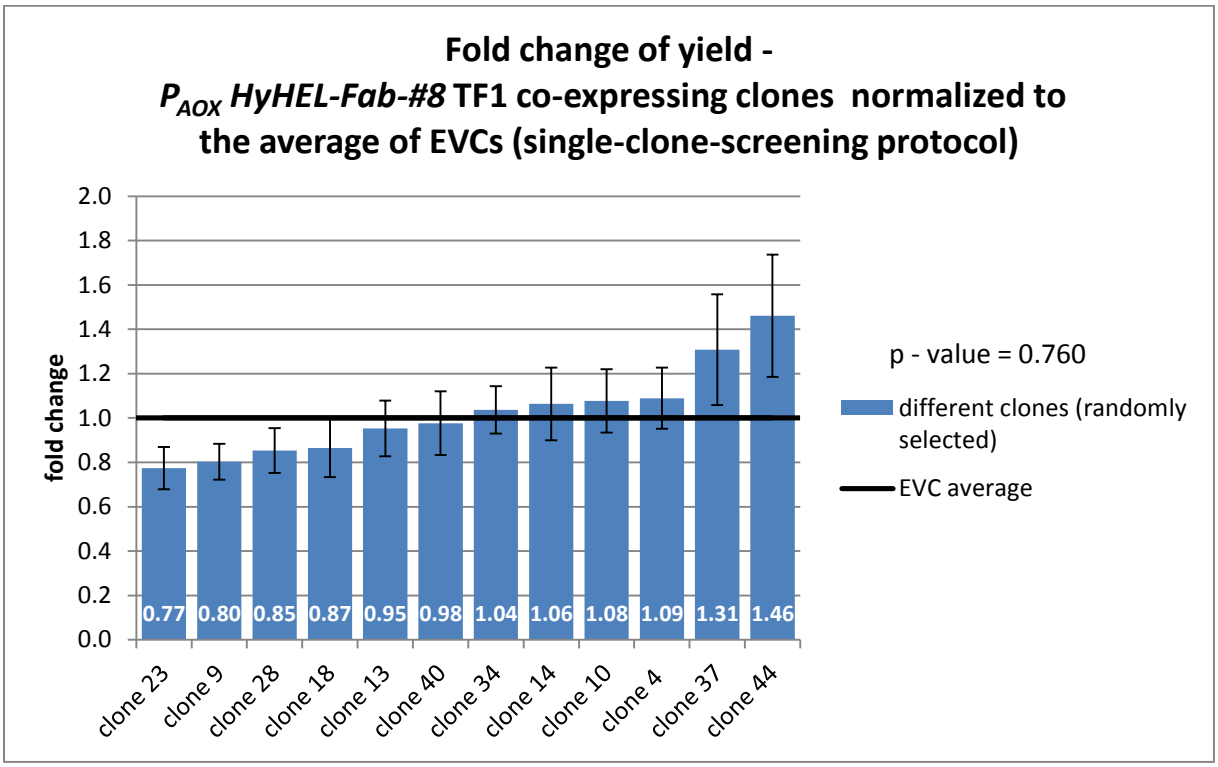

Figure 46: Fold change of yields of 12 randomly selected P_{AOX} HyHEL-Fab-#8 TF1 co-expressing clones (obtained from single-clone-screening). Yields were normalized to the average of 12 EVCs. Data represents mean values of 3 technical replicates according to the new ELISA protocol for single-clone-screenings. The p-value was calculated using a two – tailed test for unmatched pairs.

Table 27: Titer hierarchy of clones obtained with ELISA protocol for pool-screening and single-clone-screening. From bad to good secretors.

	titer hierarchy of clones												
ELISA protocol for pool-screenings	9	18	34	23	28	40	4	37	14	13	10	44	absolute match
ELISA protocol for single-clone-screenings	14	23	9	28	18	4	10	13	34	40	37	44	1 position different 2 positions different

Table 28: Yield hierarchy of clones obtained with ELISA protocol for pool-screening and single-clone-screening. From bad to good secretors.

	yield hierarchy of clones												
ELISA protocol for pool-screenings	14	4	34	9	18	28	10	40	23	13	37	44	absolute match
ELISA protocol for single-clone-screenings	23	9	28	18	13	40	34	14	10	4	37	44	1 position different 2 positions different

3.3.3. Screening of TF1 and TF2 Newly Transformed Clones

A third single-clone-screening round was performed in order to confirm the reproducibility of the TF1 or TF2 effect on co-expression and that it can be obtained with every new transformation of the P_{AOX} HyHEL-Fab-#8 parent strain. The parent strain was again transformed with 2 µg of linearized pPUZZLE_KanR_P_{GAP} harbouring TF1 or TF2 and the empty vector. Twelve clones co-expressing TF1 and nine clones co-expressing TF2 were picked for 24 DWP cultivation. Supernatants were analysed with ELISA according to the protocol for single-clone-screenings. Co-expression of TF1 showed an increase of titer for 10 of 12 clones of the new transformation. Clone 12 had a 6-fold improvement of titer compared to the average EVC, but is believed to be an outlier because of its tremendous improvement of 6-fold. Other improvements ranged from 28 % up to 246 %. A p-value of 0.0056 (+++) indicated the significantly positive effect of TF1 co-expression on secretion capacity significantly (Figure 47). An overall enhancement in yield was obtained for 11 of 12 newly transformed clones co-expressing TF1. Clone 12 showed again the highest improvement, which was 3-fold. The p-value of 0.0004 (+++) also revealed the positive impact of TF1 co-expression on secretion capacity (Figure 48).

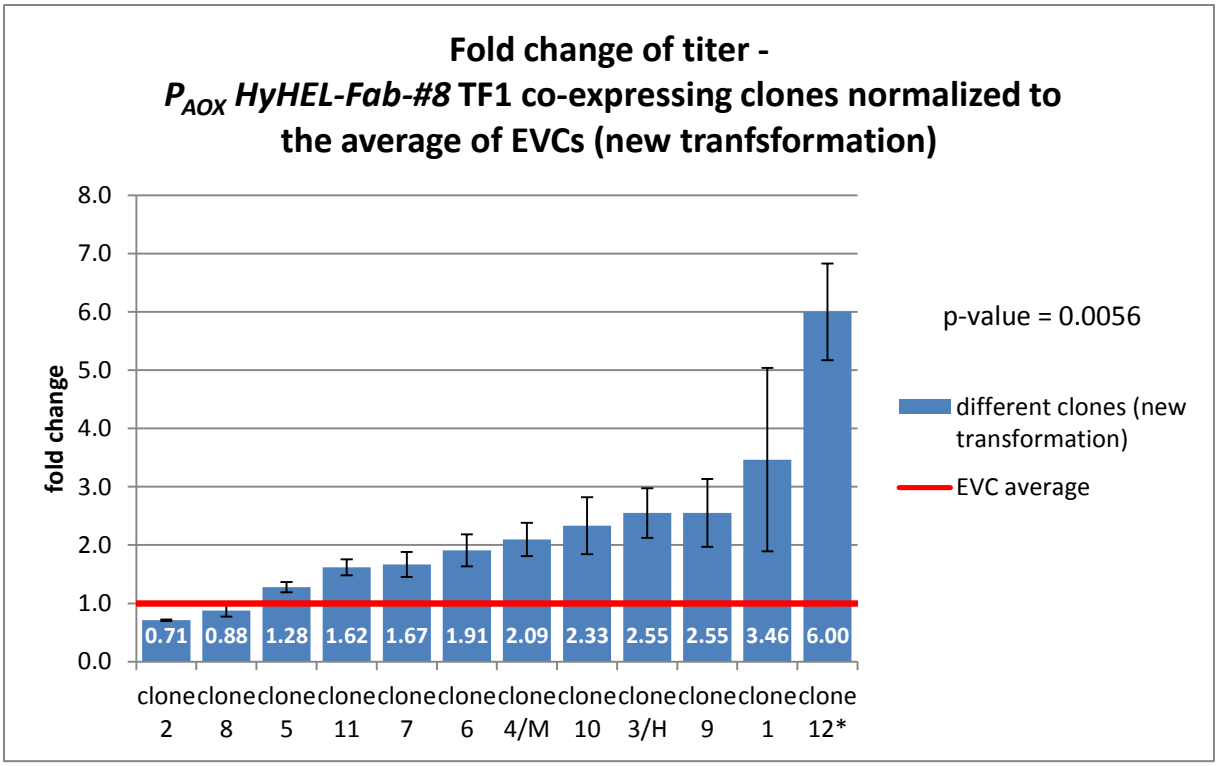

Figure 47: Fold change of titer of 12 newly transformed P_{AOX} HyHEL-Fab-#8 TF1 co-expressing clones obtained from single-clone-screening, normalized to the average of 12 EVCs. Data represented mean values of 6 technical replicates measured in two separate plates. The p-value was calculated with a two – tailed test for unmatched pairs.

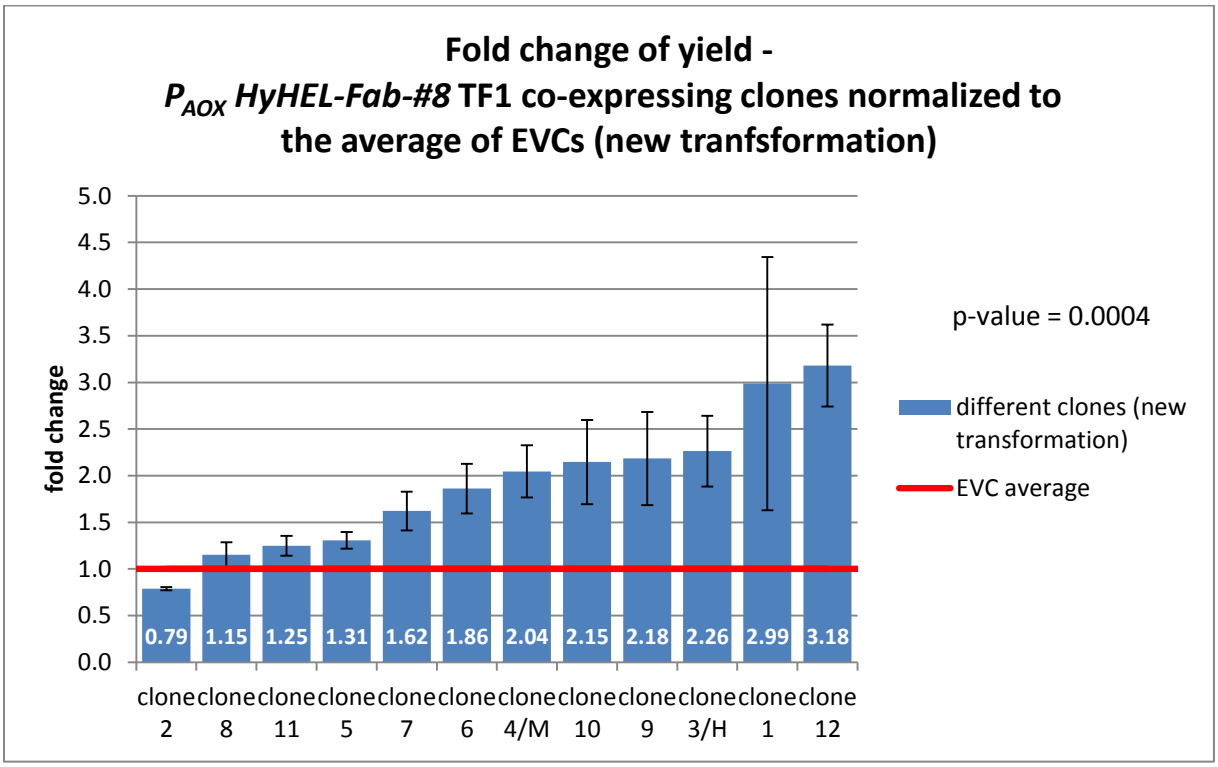

Figure 48: Fold change of yield of 12 newly transformed P_{AOX} HyHEL-Fab-#8 TF1 co-expressing clones obtained from single-clone-screening, normalized to the average of 12 EVCs. Data represented mean values of 6 technical replicates measured in two separate plates. The p-value was calculated with a two – tailed test for unmatched pairs.

Co-expression of TF2 improved the titer of 8 clones compared to the average EVC. Clone 8 showed a 3.77-fold improvement of product concentration in the supernatant. A p-value of 0.008 (+++) pointed towards the positive impact of TF2 co-expression (Figure 49). The yield was increased for 6 clones compared to the average EVC. Clone 8 performed again best (compare with titer) with a 2.2-fold improvement. A p-value of 0.0016 (+++) again confirmed the positive effect of TF2 co-expression (Figure 50).

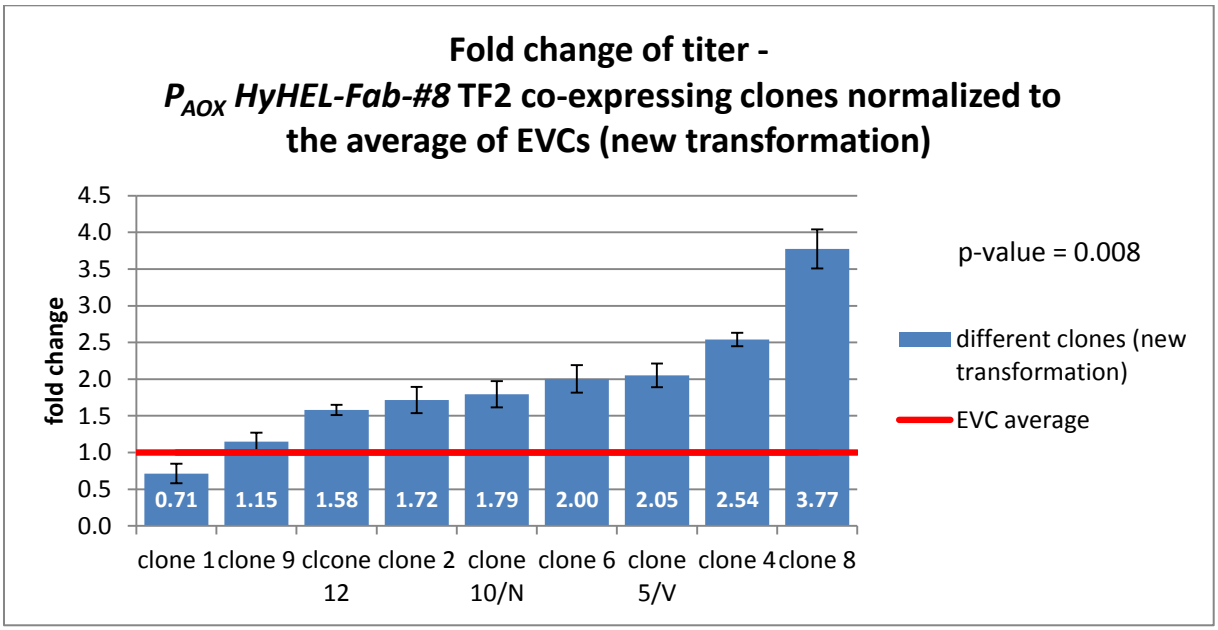

Figure 49: Fold change of titer of 9 newly transformed P_{AOX} HyHEL-Fab-#8 TF2 co-expressing clones obtained from single-clone-screening, normalized to the average of 9 EVCs. Data represented mean values of 6 technical replicates measured in two separate plates. The p-value is calculated with a two – tailed test for unmatched pairs.

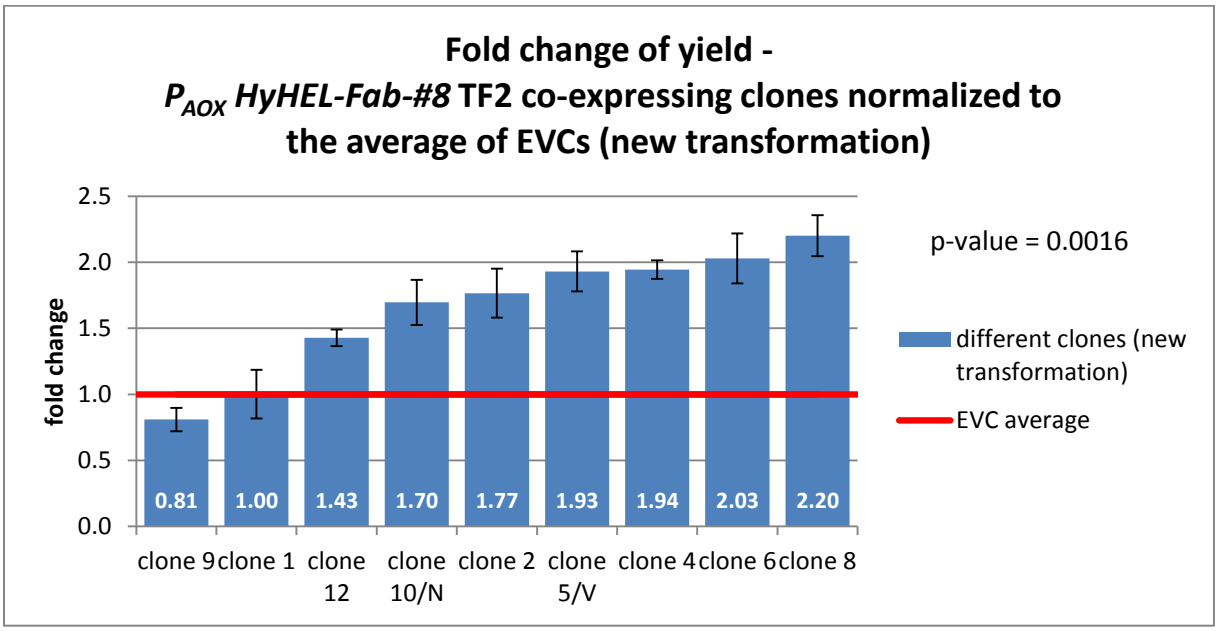

Figure 50: Fold change of yield of 9 newly transformed P_{AOX} HyHEL-Fab-#8 TF2 co-expressing clones obtained from single-clone-screening, normalized to the average of 9 EVCs. Data represented mean values of 6 technical replicates measured in two separate plates. The p-value is calculated with a two – tailed test for unmatched pairs.

At this time point two clones of each TF were selected for bioreactor cultivation performed by VTU (In-kind). A high and a medium secretor were chosen per construct. Clone 3 and clone 4 co-expressing TF1 were selected and renamed as clone H and clone M. Clone H was characterised by a 2.55-fold improvement in titer and 2.26-fold in yield. Clone M showed a 2.09-fold improvement in titer and 2.04-foldin yield. Clone 5 and clone 10 co-expressing TF2 were selected and renamed as clone V and clone N. Clone V is characterised by a 2.05-fold increase of titer and 1.96-fold increase of yield, while clone N showed values of 1.78-fold 1.70-fold for titer and yield respectively. (Table 29).

Table 29: Secretion characteristics of clone H and M co-expressing TF1 and clone V and clone N co-expressing TF2. Fold change of titer and yield is normalized to the average of EVC (24 DWP cultivation).

	Ø titer [µg*mL^{-1}]		Ø yield [µg*mL^{-1}*OD$_{600}$$^{-1}$]		Ø fold change titer		Ø fold change yield
Clone H (TF1 co-expressing)	0.998		0.069		2.26		2.55
Clone M (TF1 co-expressing)	0.902		0.057		2.09		2.04
Clone V (TF2 co-expressing)	0.883		0.059		2.05		1.93
Clone N (TF2 co-expressing)	0.776		0.051		1.79		1.70
EVC (for TF1 co-expression)	0.441		0.027		1.00		1.00
EVC (for TF2 co-expression)	0.457		0.028		1.00		1.00

3.3.4. Re-Screening of Clone H and M Co-Expressing TF1 and Clone V and N Co-Expressing TF2

Clones H, M, V and N were cultivated again in a 24 DWP re-screening experiment to prove their enhanced secretion capacity for the subsequent in-kind bioreactor cultivation performed by VTU. This time a standardized EVC termed P_{AOX} HyHEL-Fab-#8 EVC #1 was used as reference. This particular EVC had been used as a benchmark reference in all VTU bioreactor cultivations. Four biological replicates of each clone and 4 biological replicates of the EVC #1 were cultivated. Increased secretion capacity was confirmed for clone H co-expressing TF1 and clone N co-expressing TF2 compared to the new benchmark EVC #1. It was possible to reproduce the secretion capacity of clone H with a 2.25-fold increase for titer and a 1.18-fold increase for yield compared to the average of the benchmark EVC #1. Titer and Yield of clone N were increased to 1.66-fold and 1.04-fold extent (Table 30).

Table 30: Secretion characteristics of clone H, clone M, clone V and clone N cultivated as 4 biological replicates. Fold change of titer and yield was normalized to average P_{AOX} HyHEL-Fab-#8 EVC-#1, which is derived from 4 biological replicates. Changes of titer and yield compared to the average EVC-#1 benchmark reference were written in bold.

	Ø titer [µg*mL^{-1}]		Ø yield [µg*mL^{-1}*OD$_{600}$$^{-1}$]		Ø fold change titer		Ø fold change yield
Clone H (TF1 co-expressing)	1.376		0.058		**2.25**		**1.18**
Clone M (TF1 co-expressing)	0.589		0.026		0.96		0.52
Clone V (TF2 co-expressing)	0.765		0.042		**1.25**		0.86
Clone N (TF2 co-expressing)	1.018		0.051		**1.66**		**1.04**
EVC	0.612		0.049		**1.00**		**1.00**

Clone M and clone V were below expectations. While clone M showed a titer and yield even below the EVC #1 level, clone V still had an increased titer compared to EVC #1, but showed high deviations between the replicates. The yield of clone V could hardly reach the EVC #1 level. Clone M showed no improvement with a 4 % decreased titer and even 48 % decreased yield. Clone V showed only a titer improvement of 1.25-fold but also a 14 % decreased yield. (Figure 51 - Figure 54).

The reasons for the bad performance of the clones M (TF1) and V (TF2) were difficult to elucidate. The secretion capacity of the new P_{AOX} HyHEL-Fab-#8 EVC #1 obtained from VTU was not significantly higher compared to the average EVC used in the previous single-clone-screenings (data not shown).

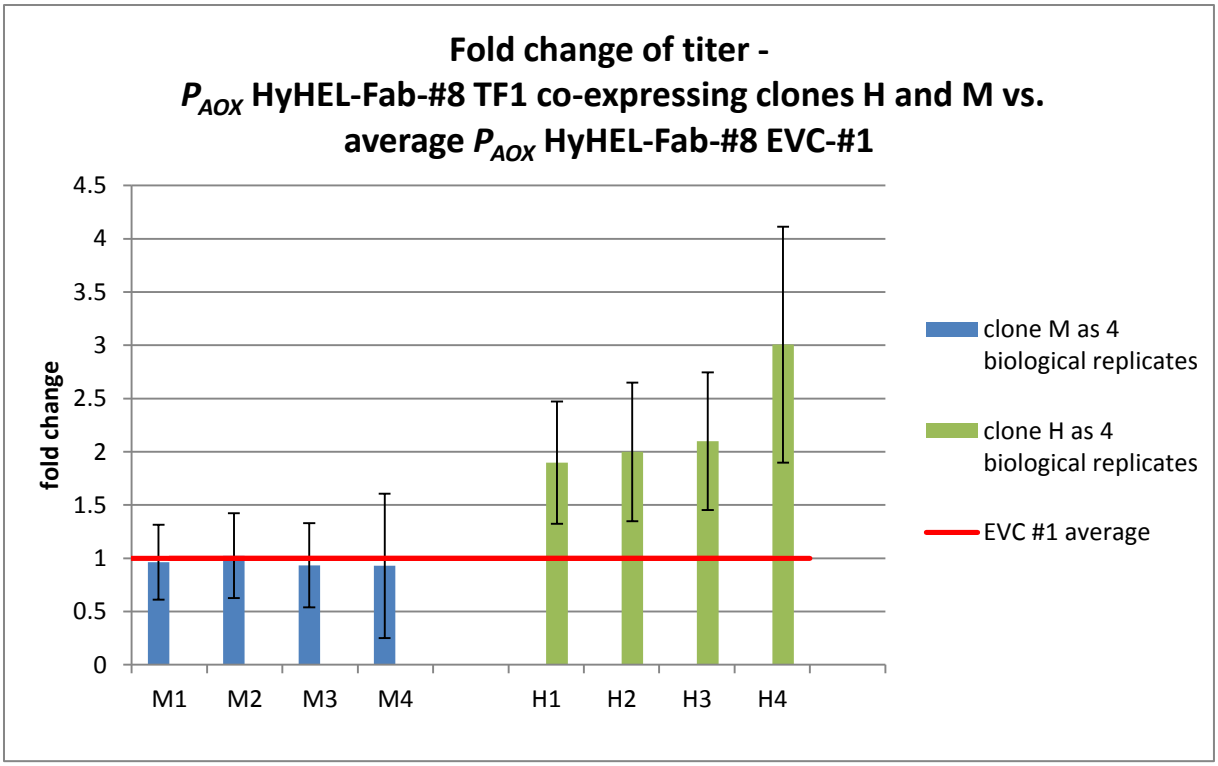

Figure 51: Titer fold change of clone H (green) and clone M (blue) co-expressing TF1 re-screened as 4 biological replicates. Titer was normalized to the average of 4 biological replicates of P_{AOX} HyHEL-Fab-#8 EVC-#1 obtained from VTU. Data represented mean values and ±SD of 6 technical replicates derived from 2 separate ELISA measurements.

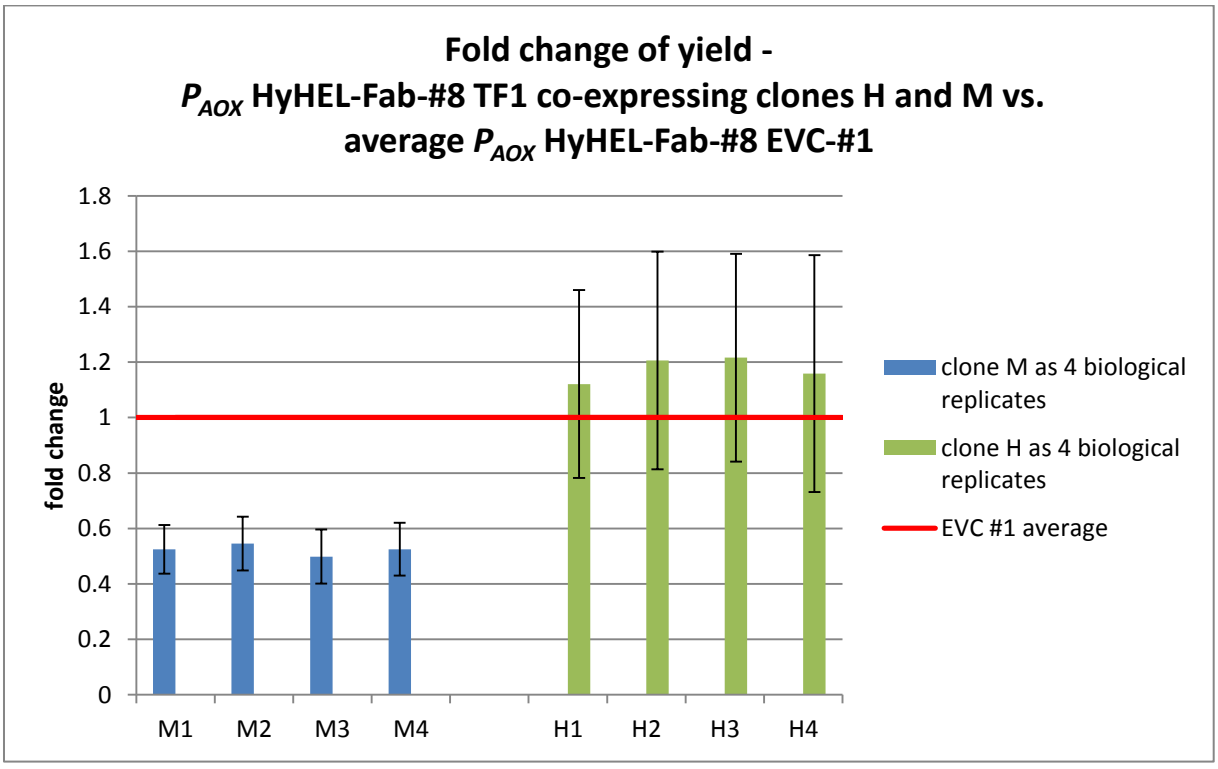

Figure 52: Yield fold change of clone H (green) and clone M (blue) co-expressing TF1 re-screened as 4 biological replicates. TF1. Yield was normalized to the average of 4 biological replicates of P_{AOX} HyHEL-Fab-#8 EVC-#1 obtained from VTU. Data represented mean values and ±SD of 6 technical replicates derived from 2 separate ELISA measurements.

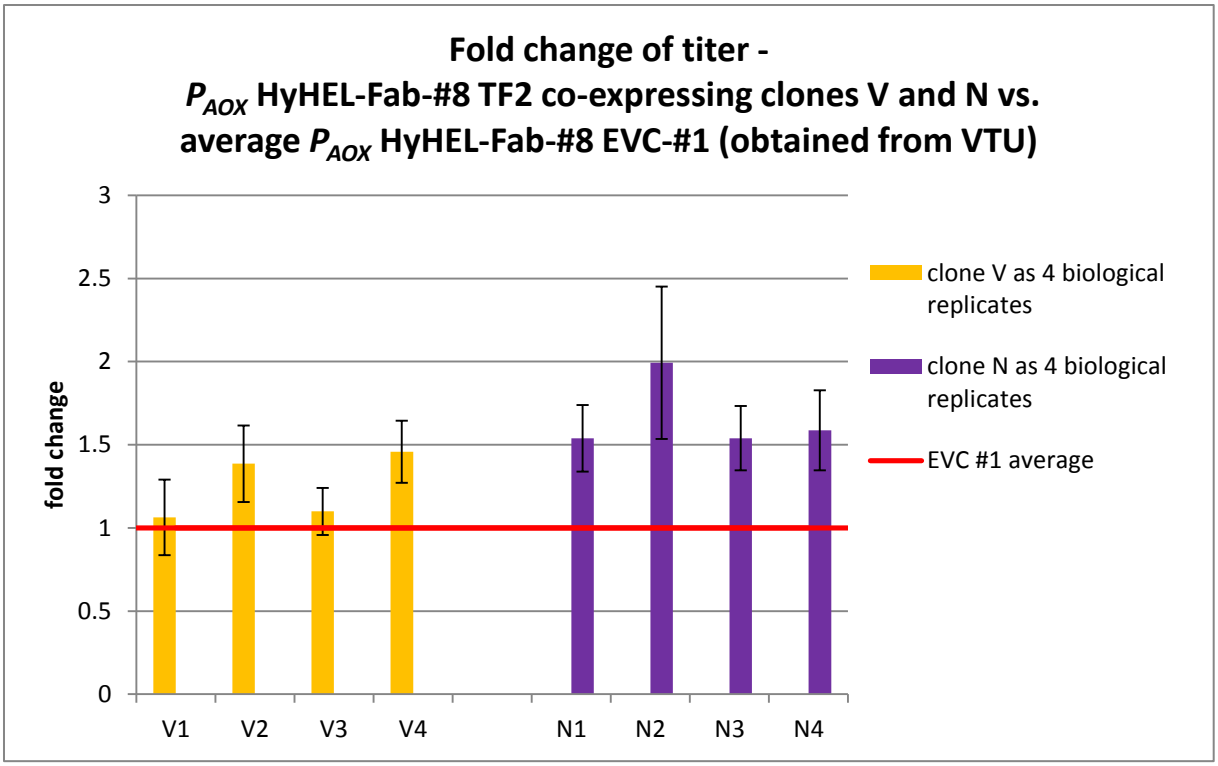

Figure 53: Titer fold change of clone V (orange) and clone N (violet) co-expressing TF2 re-screened as 4 biological replicates. Titer was normalized to the average of 4 biological replicates of P_{AOX} HyHEL-Fab-#8 EVC-#1 obtained from VTU. Data represented mean values and ±SD of 6 technical replicates derived from 2 separate ELISA measurements.

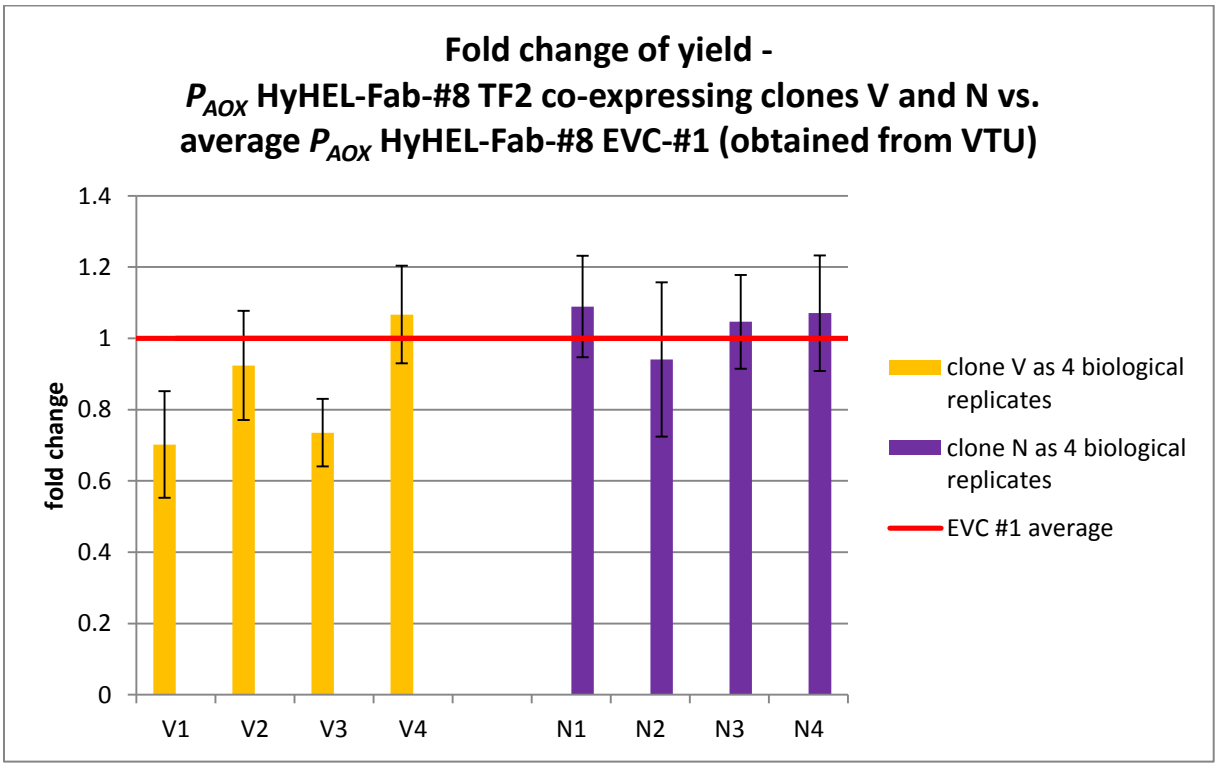

Figure 54: Yield fold change of clone V (orange) and clone N (violet) co-expressing TF1 re-screened as 4 biological replicates. Yield was normalized to the average of 4 biological replicates of P_{AOX} HyHEL-Fab-#8 EVC-#1 obtained from VTU. Data represented mean values and ±SD of 6 technical replicates derived from 2 separate ELISA measurements.

3.4. VTU (In-kind) Bioreactor Cultivation of Clones H and M Co-Expressing TF1 and Clones V and N Co-Expressing TF2

VTU ELISA results of samples from the bioreactor cultivation showed no improvement of secretion capacity for the clones H, M and N. Clone V had a 16 % increased titer at the last sampling point (110 h) and a 12 % increased yield (110 h). All other clones stayed at least 44 % (clone M) behind the titer level of the EVC-#1. Yield was decreased to an extent of 36 % for clone N co-expressing TF2 and even to 50 % and 52 % for clones H and M co-expressing TF1 (Figure 55 and Figure 56).

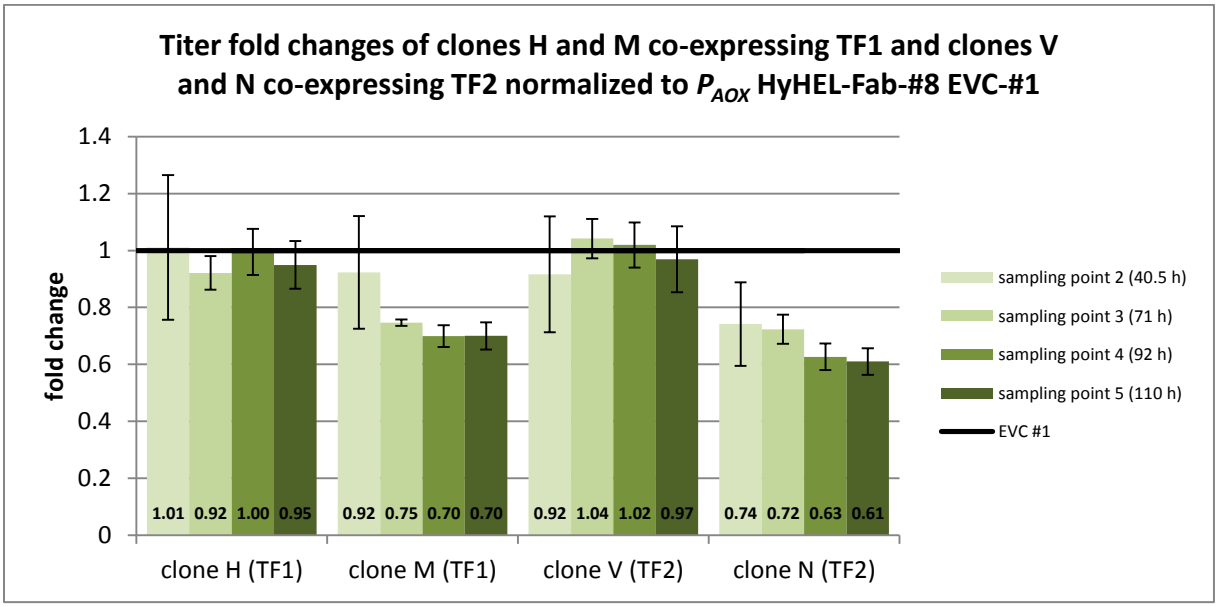

Figure 55: Titer fold changes of clones H and M co-expressing TF1 and clones V and N co-expressing TF2. Titers were normalized to the corresponding titer of the EVC-#1 at the sampling point. Data represented mean values and ±SD of 6 technical replicates derived from two separate ELISA measurements.

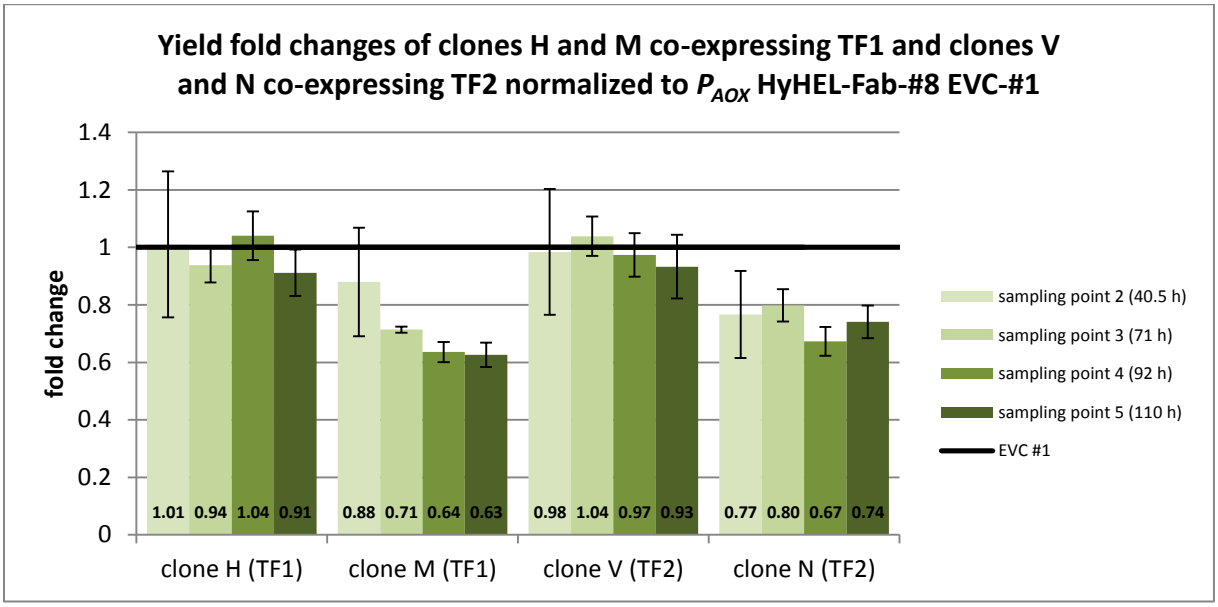

Figure 56: Yield fold changes of clones H and M co-expressing TF1 and clones V and N co-expressing TF2. Yields were normalized to the corresponding yield of the EVC-#1 at the sampling point. Data represented mean values and ±SD of 6 technical replicates derived from two separate ELISA measurements.

ELISA was repeated in our laboratory again with supernatant samples obtained from VTU in order to confirm the ELISA results. Unfortunately, it was not possible to reproduce the slightly positive result of clone N for titer and yield (Figure 55 and Figure 56). Despite slightly promising re-screening result for clones H and N regarding titers, no improvement of secretion capacity could be detected after bioreactor cultivation for any of the studied clones. The trend of HyHEL-Fab secretion of the respective clones showed that the EVC-#1 threshold was only exceeded at the sampling points 3 (71 h) and 4 (92 h) by clone V co-expressing TF2. Clone H co-expressing TF1 almost reached the level of the EVC #1, while clone M (TF1) and clone N (TF1) produced a level far below EVC #1 (Figure 57).

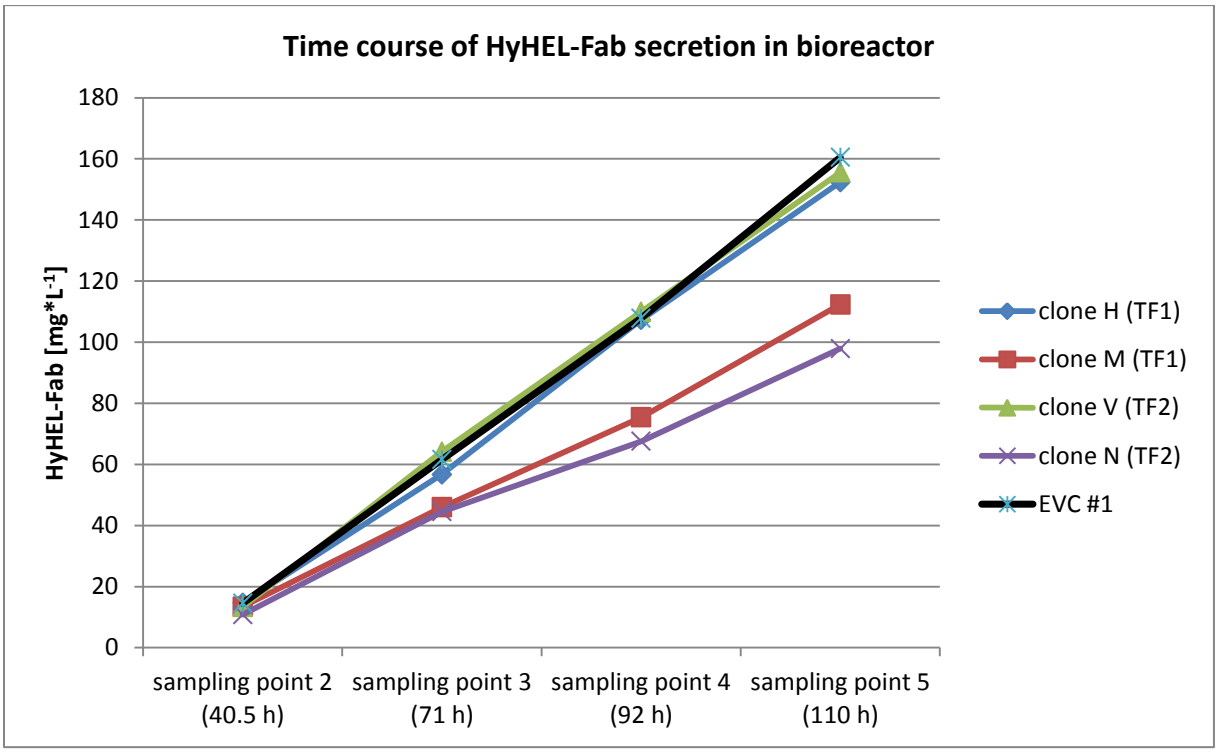

Figure 57: Secretion level over time for clones H (blue) and M (red) co-expressing TF1 and clones V (green) and N (violet) co-expressing TF2 and P_{AOX} HyHEL-Fab-#8 EVC-#1 (black) during the bioreactor cultivation at VTU. Data representd mean values and ±SD of 6 technical replicates derived from two separate ELISA measurements.

3.5. Attempts of Unravelling the Loss of Secretion Capacity of Clones H and M Co-Expressing TF1 and Clones V and N Co-Expressing TF2

A possible explanation of the bad bioreactor results is the progressive age of the clones. This could be a problem related to clone storage and altered phenotype. To elucidate this, a 24 DWP cultivation with clones from several storage conditions was performed. Clones H and V were studied. Clones were analysed as duplicates and taken from the original masterplate (stored for ~ 2 months), from a single streak out (stored for ~ 3 weeks), from a newly pinned masterplate (stored for ~ 2 weeks) and from a fresh glycerol stock single streak out. An old (stored for ~ 3 weeks) and freshly streaked out EVC-#1 strain was used as reference.

A trend of slightly increasing titer was observed for clone H from old to fresh clones. Supernatants of clones cultivated from the newly pinned masterplate and the freshly streaked glycerol stock showed the highest titer with 1.41-fold and 1.35-fold increase compared to the old EVC-#1. Nevertheless, the titer levels of the single-clone-screening (2.55-fold) and re-screening (2.25-fold) could not be reproduced and the high levels of the initial screening were not reached (Figure 58).

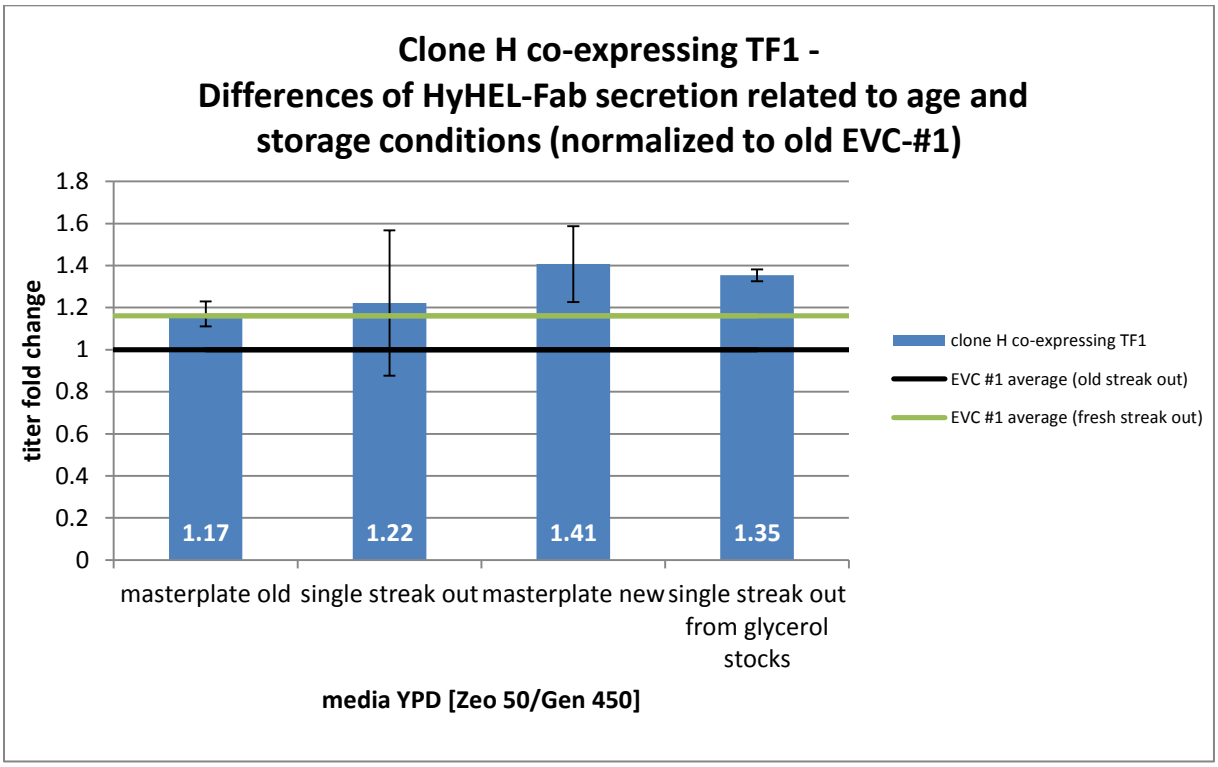

Figure 58: Altered secretion behaviour related to age and storage conditions of clone H co-expressing TF1. Data represent mean value and ±SD of biological duplicates.

Different results were obtained for the cultivations of clone V. There seemed to be a trend of decreasing titer from old to fresh clones. Supernatants of clone V, which were cultivated from the original masterplate showed the highest titer with a 1.60-fold increase. In contrast, the clone cultivated from the glycerol stock had the lowest titer with a 1.24-fold increase compared to the average of EVC#1. Additionally, a clear difference between the titers of old and fresh EVC-#1 was observed. Fresh EVC #1 had a 16 % improved titer compared to the old EVC-#1 (Figure 59). Unfortunately, the results of this attempt were not congruent. That is why a clear statement about the reasons of the obvious decrease of secretion capacity cannot be made. Additionally the results of the re-screening performed in parallel to the bioreactor cultivation suggested that the observed bad performance of the clones sent to VTU for bioreactor cultivation was no coincidence.

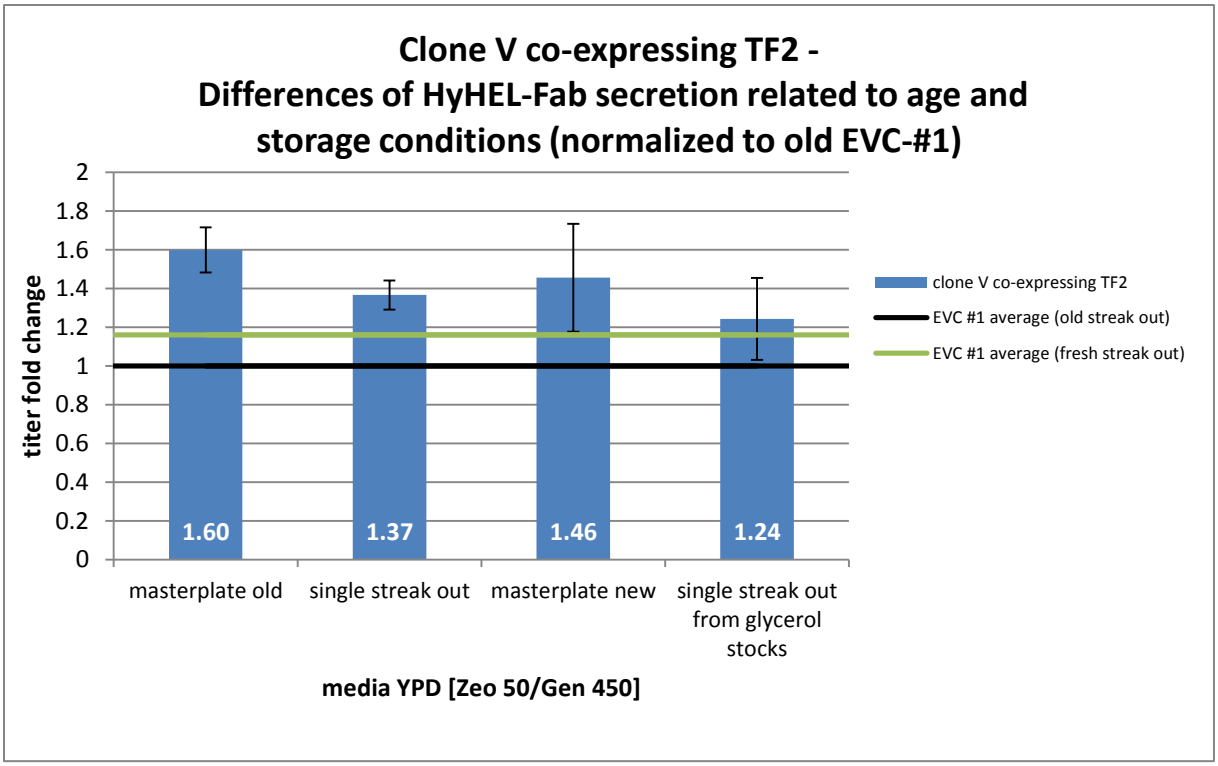

Figure 59: Altered secretion behaviour related to age and storage conditions of clone V co-expressing TF2. Data represent mean value and ±SD of biological duplicates.

3.6. Colony-PCR of Clone H and Clone M Co-Expressing TF1 and Clone V and Clone N Co-Expressing TF2

As a final attempt to detect possible alterations at the genomic level, a colony PCR was performed. For this reason gDNA of the clones H, M, N and V was isolated and used as template for the PCR reaction. GDNA of the P_{AOX} HyHEL-Fab-#8 parent strain was used as negative control. The plasmid pPUZZLE_KanR_P_{GAP}_PAS_chr4_0626 (TF1) was used as positive control for clones H and M co-expressing TF1. The plasmid pPUZZLE_KanR_P_{GAP}_PAS_chr4_0271 (TF2) was used as positive control for clones V and N co-expressing TF2. The first colony PCR approach included the amplification of the expression cassette ranging from P_{GAP} to *CYC1*tt, spanning a 2.6 kb fragment for TF1 and a 2.2 kb fragment for TF2 (Figure 60 and Figure 62). The second colony PCR approach was the amplification of a 2.6 kb fragment for TF1 and a 2.34 kb fragment for TF2, ranging from the middle of the respective ORF to the end of the KanR resistance cassette (Figure 61 and Figure 63). The fragments amplified for clone H corresponded to the fragment sizes of the positive control, which were 2.6 kb (Figure 60) for the first approach amplifying the expression cassette and again 2.6 kb (Figure 61) for the second approach amplifying a fragment ranging from the TF ORF to the KanR cassette. Interestingly, PCR results of clone M showed unspecific bands similar to the negative control performed with gDNA of the parent strain. A slight band was observed at the correct size of 2.6 kb for clone M, but also for the negative control. It is most likely that these fragments are caused by unspecific binding of the primers (Figure 60). The second colony PCR approach for clone M revealed two fragments, one at the correct size of 2.6 kb as for the positive control and not seen in the negative control, and a second

fragment with a size of ~ 3.5 kb, which corresponded to a fragment also obtained in the negative control. Notably, this was not observed for clone H and the positive control. In summary and taking the growth on selective media into account, it seems likely that also clone M has an integrated cassette. Clone M was categorised as a medium secretor compared to clone H, which might indicate a lower copy number and so fewer binding sites for the primers.

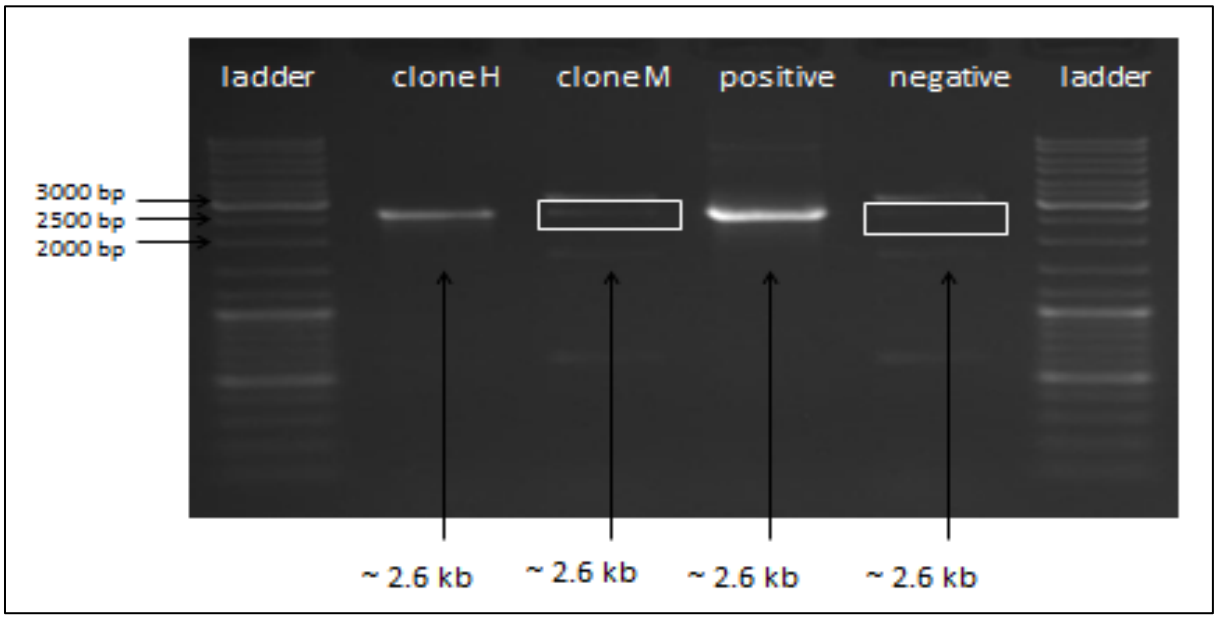

Figure 60: Agarose gel of colony PCR for clones H and M co-expressing TF1. Genomic DNA of clones H and M was used as template. Plasmid pPUZZLE_KanR_P_{GAP}_PAS_chr4_0626 (TF1) was used as template for the positive control. Genomic DNA of P_{AOX} HyHEL-Fab-#8 parent strain was used as template for the negative control. Used primers were pPuzzle_expcas_fw (5WP-66) and pPuzzle_expcas_rv (5WP-67). Ladder was GeneRuler DNA ladder mix (Figure 64).

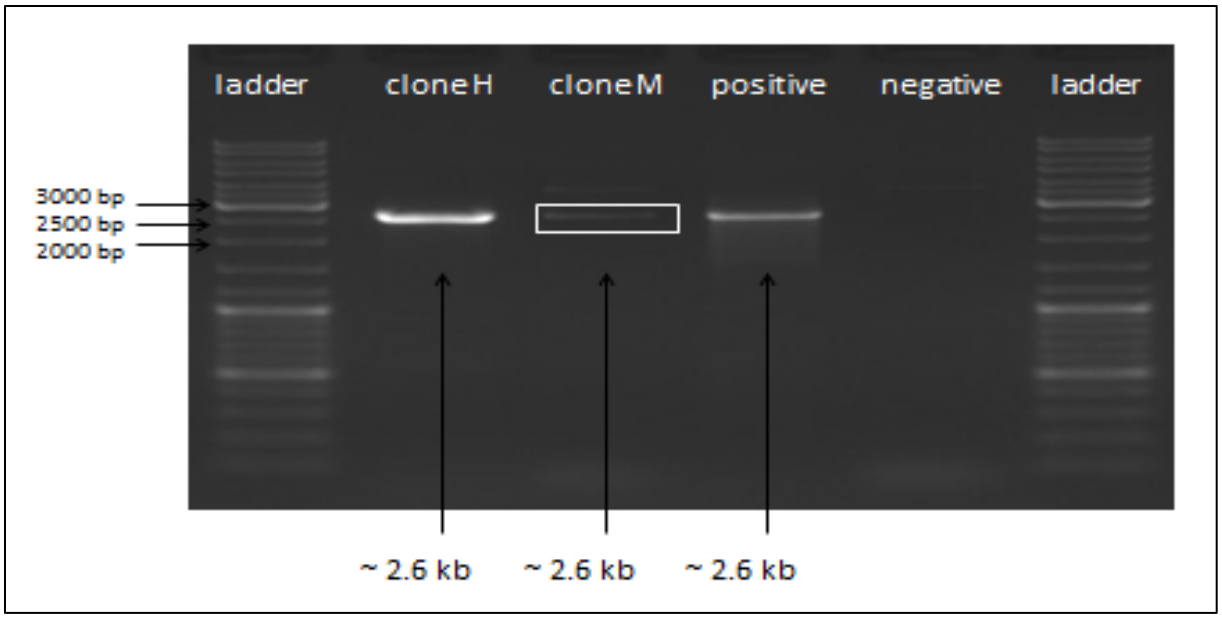

Figure 61: Agarose gel of colony PCR for clones H and M co-expressing TF1. Genomic DNA of clones H and M was used as template. Plasmid pPUZZLE_KanR_P_{GAP}_PAS_chr4_0626 (TF1) was used as template for the positive control. Genomic DNA of P_{AOX} HyHEL-Fab-#8 parent strain was used as template for the negative control. Used primers were TF1_seq 1_fw (5WP-7) and pPuzzle_expcas_kanrv (5WP-72). Ladder was GeneRuler DNA ladder mix (Figure 64).

The obtained fragments for clone N and clone V from colony PCR corresponded clearly to the positive control and indicated a successful integration of the pPUZZLE_KanR_P_{GAP}_PAS_chr4_0271 (TF2) plasmid into the genome (Figure 62 and Figure 63).

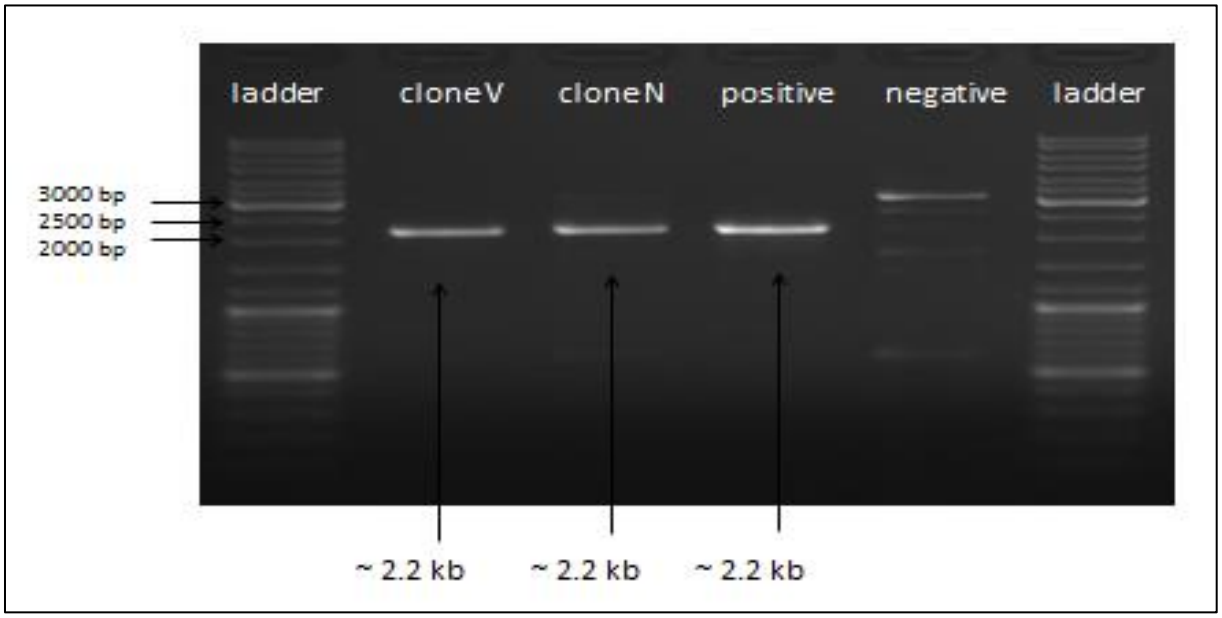

Figure 62: Agarose gel of colony PCR for clones V and N co-expressing TF2. Genomic DNA of clones V and N was used as template. Plasmid pPUZZLE_KanR_P_{GAP}_PAS_chr4_0271 (TF2) was used as template for the positive control. Genomic DNA of P_{AOX} HyHEL-Fab-#8 parent strain was used as template for the negative control. Used primers were pPuzzle_exp-cas_fw (5WP-66) and pPuzzle_expcas_rv (5WP-67). Ladder was GeneRuler DNA ladder mix (Figure 64).

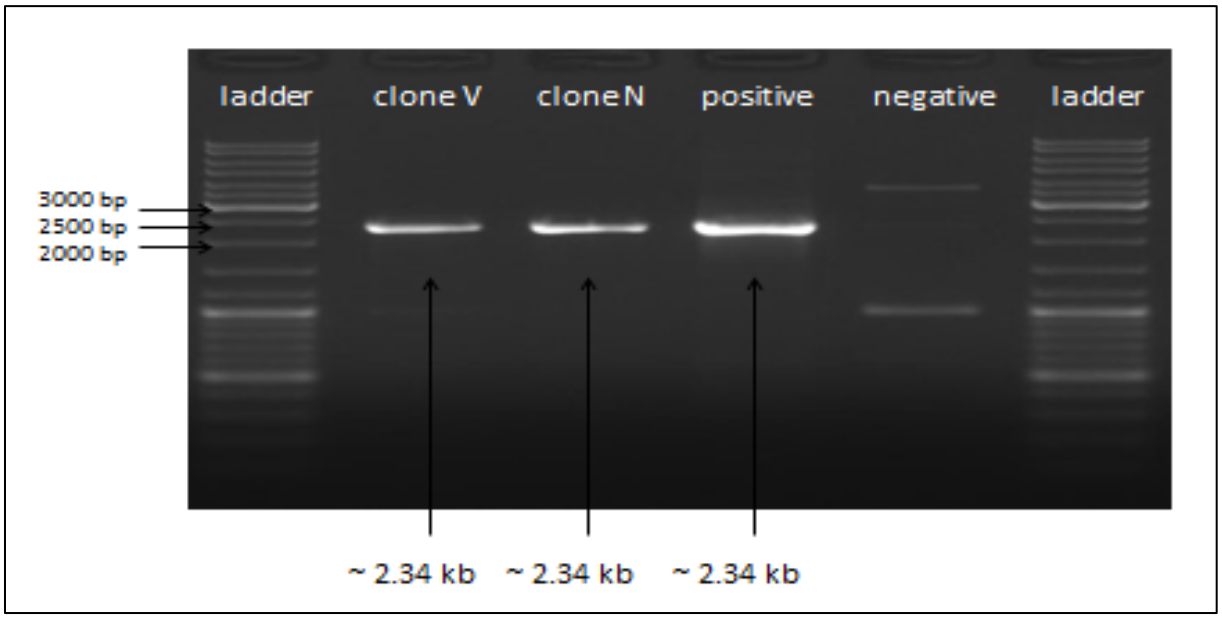

Figure 63: Agarose gel of colony PCR for clones V and N co-expressing TF2. Genomic DNA of clones V and N was used as template. Plasmid pPUZZLE_KanR_P_{GAP}_PAS_chr4_0271 (TF2) was used as template for the positive control. Genomic DNA of P_{AOX} HyHEL-Fab-#8 parent strain was used as template for the negative control. Used primers were TF2_seq 1_fw (5WP-13) and pPuzzle_expcas_kanrv (5WP-72). Ladder was GeneRuler DNA ladder mix (Figure 64).

4. Conclusion and Perspective

The transformation of the P_{AOX} HyHEL-Fab-#8 parent strain with increasing amounts (0.8, 2, 5 and 8 µg) of linearized plasmid or expression cassette of the pPUZZLE_KanR_P_{GAP}_TF plasmid was successfully performed. The results of the pool-screening indicated that different amounts DNA impacted the obtained yield/titer changes. The optimal amount of DNA for transformation differed for the TFs. The EVC showed a clear optimum at 2 µg of transformed DNA. Clones of this transformation were therefore used as benchmark clones for the subsequent single-clone screenings. To take a closer look at the relation between the amount of transformed DNA/presumable gene dosage to the observed secretion levels it might be useful to check the integrated copy number by real-time PCR at the genomic level[79]. The performance of pool-screenings in 24 DWP allowed a rapid investigation of the target TFs for their ability to improve the secretion capacity of the parent strain, however might have also led to the loss of some good clones especially when secretion depends on gene dosage. TF1 and TF2 were identified to enhance the secretion capacity of the parent strain for both titer and yield, and were therefore selected as secretion enhancing transcription factors for further investigation by single-clone-screenings. Also other TFs, such as TF3 or TF5, were able to raise the yield in the parent strain background, indicating potential there. Also co-expression of TF2ni showed promising results for titer and yield, but because of the similar results to its native counterpart TF2 it was decided to work with the native TF2 only, harbouring one intron in its coding sequence. The approach of transforming the parent strain with the expression cassette of the pPUZZLE_KanR_P_{GAP}_TF plasmid also resulted in co-expressing strains with improved secretion efficiency. Unfortunately, the observed titer levels stayed behind the titer level of the corresponding EVC. Bad growth raised the yield levels to considerable extents for TF1, TF2 for almost all amounts of transformed expression cassette and for TF5, TF6 and TF2ni for specific amounts of transformed expression cassette. Growth deficiencies of expression cassette-transformed clones led the decision to work on with linearized plasmids rather than PCR-amplified expression cassettes.

The positive effect of TF1 and TF2 could also be confirmed in a 24 DWP single-clone-screening procedure after a colony-size dependent effect was eliminated by a random selection of clones. The first screen of the twelve biggest single colonies revealed only a slight increase of titer compared to the previous pool-screening. But, yield was improved for 7 of 12 clones by more than 20 % over the EVC average. Clones randomly selected and newly transformed TF1 clones showed an overall increase of product concentration of 1.17-fold and 1.90-fold, respectively. The yield was increased 1.37-fold and 2.25 fold. Randomly selected and newly transformed TF2 clones showed an overall increase of the product concentration of 1.17-fold and 1.64-fold, while the yield was increased 1.36-fold and 1.92-fold, respectively. The positive impact of TF1 and TF2 on the secretion capacity of the parent strain was safeguarded by student's t-test.

The use of another promoter for TF co-expression might be interesting. For example Co-expression of native *P. pastoris* Hac1p under control of the P_{AOX} increased the secretion of trans-sialidase (TS) by 2.2-fold. However, clear predictions for the performance under a new promoter system remain difficult. The re-screening confirmed the performance of clone H (TF1) and clone N (TF2), though the obtained yields were significantly lower than the yields observed in the single-clone-screenings. Clone M (TF1) and clone V (TF2) hardly reached the EVC #1 benchmark in re-screening. Promising single clones co-expressing TF1 or TF2 were studied in bioreactor. The clones H and M (TF1) and V and N (TF2), which were tested in a re-screening experiment were studied in comparison to the VTU benchmark EVC P_{AOX} HyHEL-Fab-#8 EVC #1. The new EVC #1 should have been used earlier in the screening procedure to make the decision finding more accurate towards a highly secreting clone, although the difference to the previous EVCs remained modest. Further the copy number of EVC#1 has not yet been studied. A switch of to using 0.8 µg of DNA for *Pichia* transformation might be considered because of the very promising results for 0.8 µg in pool-screenings. On the other hand, the procedure of a pool-screening to this extent (40 – 48 clones cultivated together) should be questioned. Inefficiently secreting clones cultivated together with good clones would neutralize the positive effect of the latter. Single-clone-screenings as performed afterwards could replace the pool-screenings and would give information about statistical relevance too. Good clones could be missed in a pool screen, but could be identified using a single-clone-screening procedure. The number of clones selected for re-screening should be raised to identify good clones with higher probability and the attention should be given to high yield levels rather than high titer levels.

Nevertheless, the four single clones H, M, N and V were cultivated in bioreactor. In order to present results of the bioreactor cultivation at the upcoming corporate meeting, the selection of clones was made based on the single-clone-screening results. The re-screening was still in progress at this time. Unfortunately, the performance of the all clones was below the level of the EVC #1 benchmark. A possible effect of age and storage conditions of the clones might be the reason for their loss of secretion capacity. Also the media components differed for example for carbon source, which was glycerol in bioreactor and glucose in 24 well, and the pH conditions, which were 5.5 in 24 well instead of 5 in the bioreactor.

The positive impact of TF co-expression in order to elevate HyHEL-Fab secretion in *P. pastoris* could only be confirmed in 24 DWP scale. The use of other promoter systems might be interesting and could allow for the fine tuning necessary for high HyHEL-Fab titers. Also the knowledge of the relationship between gene dosage and secretion level could help to optimize the screening procedure towards the best performing clones.

A last point to consider is the selection of TF targets for co-expression in *Pichia*. Instead of an *in silico* analysis of promoter binding sites or micro-array analysis of expression levels of possible TFs, a functional screening of TFs could be a promising attempt. The co-expression of a TF-library in *Pichia* could give useful information of secretion enhancing TFs. A functional screening could provide a direct linkage between the co-expression of a specific TF to an

improved secretion level, while the results of a micro array analysis can hardly be connected to secretion. Expression studies combined with micro array analysis give information about the up and down-regulation of genes/factors when overexpressing the model-protein. But the conclusion that an up or-down-regulation of such genes/factors would lead to higher expression or secretion is rather limited. The greater effort in target TF selection when performing a functional screening could pay off in the subsequent screening and re-screening procedures.

References

1. Cereghino, J. L. & Cregg, J. M. Heterologous protein expression in the methylotrophic yeast *Pichia pastoris*. *FEMS Microbiol. Rev.* **24,** 45–66 (2000).

2. Cereghino, G. P. L., Cereghino, J. L., Ilgen, C. & Cregg, J. M. Production of recombinant proteins in fermenter cultures of the yeast *Pichia pastoris*. *Curr. Opin. Biotechnol.* **13,** 329–32 (2002).

3. Cereghino, G. L., Sunga, A., Cereghino, J. & Cregg, J. in *Genet. Eng. Princ. Methods SE - 9* (Setlow, J.) **23,** 157–69 (Springer US, 2001).

4. Veenhuis, M., Van Dijken, J. P. & Haderer, W. The Significance of Peroxisomes in the Metabolism of One-Carbon Compounds in Yeast. *Adv. Microb. Phyisiology* **24,** 1–81 (1983).

5. Egli, T., Van Dijken, J. P., Veenhuis, M., Harder, W. & Fiechter, A. Methanol Metabolism in Yeasts: Regulation of the Synthesis of Catabolic Enzymes. *Arch. Microbiol.* **124,** 115–21 (1980).

6. Hartner, F. S. & Glieder, A. Regulation of methanol utilisation pathway genes in yeasts. *Microb. Cell Fact.* **5,** 39 (2006).

7. Van der Klei, I. J., Yurimoto, H., Sakai, Y. & Veenhuis, M. The significance of peroxisomes in methanol metabolism in methylotrophic yeast. *Biochim. Biophys. Acta* **1763,** 1453–62 (2006).

8. Ahmad, M., Hirz, M., Pichler, H. & Schwab, H. Protein expression in *Pichia pastoris*: recent achievements and perspectives for heterologous protein production. *Appl. Microbiol. Biotechnol.* **98,** 5301–17 (2014).

9. Macauley-Patrick, S., Fazenda, M. L., McNeil, B. & Harvey, L. M. Heterologous protein production using the *Pichia pastoris* expression system. *Yeast* **22,** 249–70 (2005).

10. Waterham, H. R., Digan, M. E., Koutz, P. J., Lair, S. V & Cregg, J. M. Isolation of the *Pichia pastoris* glyceraldehyde-3-phosphate dehydrogenase gene and regulation and use of its promoter. *Gene* **186,** 37–44 (1997).

11. Ellis, S. B. *et al.* Isolation of alcohol oxidase and two other methanol regulatable genes from the yeast *Pichia pastoris*. *Mol. Cell. Biol.* **5,** 1111–21 (1985).

12. Tschopp, J. F., Brust, P. F., Cregg, J. M., Stillman, C. A. & Gingeras, T. R. Expression of the *lacZ* gene from two methanol-regulated promoters in *Pichia pastoris*. *Nucleic Acids Res.* **15 ,** 3859–76 (1987).

13. Vogl, T. & Glieder, A. Regulation of *Pichia pastoris* promoters and its consequences for protein production. *N. Biotechnol.* **30,** 385–404 (2013).

14. Inan, M. & Meagher, M. M. Non-repressing carbon sources for alcohol oxidase (*AOX1*) promoter of *Pichia pastoris*. *J. Biosci. Bioeng.* **92,** 585–89 (2001).

15. Qin, X. *et al. GAP* promoter library for fine-tuning of gene expression in *Pichia pastoris*. *Appl. Environ. Microbiol.* **77,** 3600–08 (2011).

16. Näätsaari, L. *et al.* Deletion of the *Pichia pastoris* KU70 homologue facilitates platform strain generation for gene expression and synthetic biology. *PLoS One* **7,** e39720 (2012).

17. Kit, E. *Pichia* Expression Kit, Invitrogen by life technologies.

18. Vassileva, A., Chugh, D. A., Swaminathan, S. & Khanna, N. Effect of copy number on the expression levels of hepatitis B surface antigen in the methylotrophic yeast *Pichia pastoris*. *Protein Expr. Purif.* **21,** 71–80 (2001).

19. Chu, G. Double Strand Break Repair. *J. Biol. Chem.* **272,** 24097–25000 (1997).

20. Daley, J. M., Palmbos, P. L., Wu, D. & Wilson, T. E. Nonhomologous end joining in yeast. *Annu. Rev. Genet.* **39,** 431–51 (2005).

21. Damasceno, L. M., Huang, C.-J. & Batt, C. a. Protein secretion in *Pichia pastoris* and advances in protein production. *Appl. Microbiol. Biotechnol.* **93,** 31–39 (2012).

22. Idiris, A., Tohda, H., Kumagai, H. & Takegawa, K. Engineering of protein secretion in yeast: strategies and impact on protein production. *Appl. Microbiol. Biotechnol.* **86,** 403–17 (2010).

23. Kurjan, J. & Herskowitz, I. Structure of a yeast pheromone gene (MF alpha): a putative alpha-factor precursor contains four tandem copies of mature alpha-factor. *Cell* **30,** 933–43 (1982).

24. Caplan, S., Green, R., Rocco, J. & Kurjan, J. Glycosylation and Structure of the Yeast *MFa1 α*-Factor Precursor Is Important for Efficient Transport through the Secretory Pathway. **173,** 627–35 (1991).

25. Waters, M. G., Evans, E. a & Blobel, G. Prepro-alpha-factor has a cleavable signal sequence. *J. Biol. Chem.* **263,** 6209–14 (1988).

26. Julius, D., Brake, A., Blair, L., Kunisawa, R. & Thorner, J. Isolation of the putative structural gene for the lysine-arginine-cleaving endopeptidase required for processing of yeast prepro-α-factor. *Cell* **37,** 1075–89 (1984).

27. Brake, A. J. *et al.* Alpha-factor-directed synthesis and secretion of mature foreign proteins in *Saccharomyces cerevisiae*. *Proc. Natl. Acad. Sci.* **81,** 4642–46 (1984).

28. Julius, D., Blair, L., Brake, A., Sprague, G. & Thorner, J. Yeast α factor is processed from a larger precursor polypeptide: The essential role of a membrane-bound dipeptidyl aminopeptidase. *Cell* **32,** 839–52 (1983).

29. Achstetter, T. Regulation of a-Factor Production in *Saccharomyces cerevisiae* : α-Factor Pheromone-Induced Expression of the *MFαl* and *STEJ3* Genes. *Molecular and Cellular Biology*. **9**, 4507-14 (1989).

30. Guerfal, M. *et al.* The *HAC1* gene from *Pichia pastoris*: characterization and effect of its overexpression on the production of secreted, surface displayed and membrane proteins. *Microb. Cell Fact.* **9,** 49 (2010).

31. Mattanovich, D., Gasser, B., Hohenblum, H. & Sauer, M. Stress in recombinant protein producing yeasts. *J. Biotechnol.* **113,** 121–35 (2004).

32. Ron, D. & Walter, P. Signal integration in the endoplasmic reticulum unfolded protein response. *Nat. Rev. Mol. Cell Biol.* **8,** 519–29 (2007).

33. Cox, J. S., Shamu, C. E. & Walter, P. Transcriptional induction of genes encoding endoplasmic reticulum resident proteins requires a transmembrane protein kinase. *Cell* **73,** 1197–1206 (1993).

34. Okamura, K., Kimata, Y., Higashio, H., Tsuru, A. & Kohno, K. Dissociation of Kar2p/BiP from an ER sensory molecule, Ire1p, triggers the unfolded protein response in yeast. *Biochem. Biophys. Res. Commun.* **279,** 445–50 (2000).

35. Gardner, B. M., Pincus, D., Gotthardt, K., Gallagher, C. M. & Walter, P. Endoplasmic reticulum stress sensing in the unfolded protein response. *Cold Spring Harb. Perspect. Biol.* **5,** a013169 (2013).

36. Chawla, A., Chakrabarsti, S., Ghosh, G. & Niwa, M. Attenuation of yeast UPR is essential for survival and is mediated by *IRE1* kinase. *J. Cell Biol.* **193,** 41–50 (2011).

37. Lu, G. *et al. PPM1l* encodes an inositol requiring-protein 1 (IRE1) specific phosphatase that regulates the functional outcome of the ER stress response. *Mol. Metab.* **2,** 405–16 (2013).

38. Ng, D. T., Spear, E. D. & Walter, P. The unfolded protein response regulates multiple aspects of secretory and membrane protein biogenesis and endoplasmic reticulum quality control. *J. Cell Biol.* **150,** 77–88 (2000).

39. Travers, K. J. *et al.* Functional and Genomic Analyses Reveal an Essential Coordination between the Unfolded Protein Response and ER-Associated Degradation. *Cell* **101,** 249–58 (2000).

40. Bollok, M., Resina, D., Valero, F. & Ferrer, P. Recent patents on the *Pichia pastoris* expression system: expanding the toolbox for recombinant protein production. *Recent Pat. Biotechnol.* **3,** 192–201 (2009).

41. De Schutter, K. *et al.* Genome sequence of the recombinant protein production host *Pichia pastoris*. *Nat. Biotechnol.* **27,** 561–66 (2009).

42. Küberl, A. *et al.* High-quality genome sequence of *Pichia pastoris* CBS7435. *J. Biotechnol.* **154,** 312–20 (2011).

43. Valkonen, M., Penttilä, M., Saloheimo, M. & Penttila, M. Effects of Inactivation and Constitutive Expression of the Unfolded- Protein Response Pathway on Protein Production in the Yeast *Saccharomyces cerevisiae*. *Appl. Environ. Microbiol.* **69**, 2065–72 (2003)

44. Gasser, B., Maurer, M., Gach, J., Kunert, R. & Mattanovich, D. Engineering of *Pichia pastoris* for Improved Production of Antibody Fragments. *Wiley InterScience*. (2006). doi:10.1002/bit

45. Gasser, B., Sauer, M., Maurer, M., Stadlmayr, G. & Mattanovich, D. Transcriptomics-based identification of novel factors enhancing heterologous protein secretion in yeasts. *Appl. Environ. Microbiol.* **73,** 6499–6507 (2007).

46. Gasser, B., Mattanovich, D., Sauer, M. & Stadlmayr, G. Yeast expression systems. (2008). at <http://www.google.lt/patents/WO2008128701A2?cl=en>

47. Graf, A. *et al.* Novel insights into the unfolded protein response using *Pichia pastoris* specific DNA microarrays. *BMC Genomics* **9,** 390 (2008).

48. Stadlmayr, G., Benakovitsch, K., Gasser, B., Mattanovich, D. & Sauer, M. Genome-scale analysis of library sorting (GALibSo): Isolation of secretion enhancing factors for recombinant protein production in *Pichia pastoris*. *Biotechnol. Bioeng.* **105,** 543–55 (2010).

49. Park, P. J. ChIP-seq: advantages and challenges of a maturing technology. *Nat. Rev. Genet.* **10,** 669–80 (2009).

50. Farnham, P. J. Insights from genomic profiling of transcription factors. *Nat. Rev. Genet.* **10,** 605–16 (2009).

51. Aparicio, O. *et al.* Chromatin immunoprecipitation for determining the association of proteins with specific genomic sequences in vivo. *Curr. Protoc. Mol. Biol.* **Chapter 21,** Unit 21.3 (2005).

52. Furey, T. S. ChIP-seq and beyond: new and improved methodologies to detect and characterize protein-DNA interactions. *Nat. Rev. Genet.* **13,** 840–52 (2012).

53. Landt, S. G. *et al.* ChIP-seq guidelines and practices of the ENCODE and modENCODE consortia. *Genome Res.* **22,** 1813–31 (2012).

54. Park, D., Lee, Y., Bhupindersingh, G. & Iyer, V. R. Widespread misinterpretable ChIP-seq bias in yeast. *PLoS One* **8,** e83506 (2013).

55. Magasanik, B. & Kaiser, C. A. Nitrogen regulation in *Saccharomyces cerevisiae*. *Gene* **290,** 1–18 (2002).

56. Scherens, B., Feller, A., Vierendeels, F., Messenguy, F. & Dubois, E. Identification of direct and indirect targets of the Gln3 and Gat1 activators by transcriptional profiling in response to nitrogen availability in the short and long term. *FEMS Yeast Res.* **6,** 777–91 (2006).

57. Coffman, J. A. *et al.* Gat1p , a GATA family protein whose production is sensitive to nitrogen catabolite repression , participates in transcriptional activation of nitrogen-catabolic genes in *Saccharomyces cerevisiae* . *Molecular and Cellular Biology*. 16, 847–58. (1996).

58. Beck, T. & Hall, M. N. The TOR signalling pathway controls nuclear localization of nutrient-regulated transcription factors. *Nature* **402,** 689–92 (1999).

59. Bertram, P. G. *et al.* Tripartite regulation of Gln3p by TOR, Ure2p, and phosphatases. *J. Biol. Chem.* **275,** 35727–33 (2000).

60. Lu, Y., Su, C. & Liu, H. A GATA transcription factor recruits Hda1 in response to reduced Tor1 signaling to establish a hyphal chromatin state in Candida albicans. *PLoS Pathog.* **8,** e1002663 (2012).

61. Du, H. *et al.* Roles of Candida albicans Gat2, a GATA-type zinc finger transcription factor, in biofilm formation, filamentous growth and virulence. *PLoS One* **7,** e29707 (2012).

62. Turcotte, B., Liang, X. B., Robert, F. & Soontorngun, N. Transcriptional regulation of nonfermentable carbon utilization in budding yeast. *FEMS Yeast Res.* **10,** 2–13 (2010).

63. Hedges, D. & Proft, M. *CAT8* , a new zinc cluster-encoding gene necessary for derepression of gluconeogenic enzymes in the yeast *Saccharomyces cerevisiae*. *Molecular and Cellular Biology*. **15,** 1915–22 (1995).

64. Balzi, E. & Goffeau, A. Yeast multidrug resistance: The PDR network. *J. Bioenerg. Biomembr.* **27,** 71–76 (1995).

65. Lucau-Danila, A., Delaveau, T., Lelandais, G., Devaux, F. & Jacq, C. Competitive promoter occupancy by two yeast paralogous transcription factors controlling the multidrug resistance phenomenon. *J. Biol. Chem.* **278,** 52641–50 (2003).

66. Cui, Z., Shiraki, T., Hirata, D. & Miyakawa, T. Yeast gene *YRR1*, which is required for resistance to 4-nitroquinoline N-oxide, mediates transcriptional activation of the multidrug resistance transporter gene SNQ2. *Mol. Microbiol.* **29,** 1307–15 (1998).

67. Marchler-Bauer, A. *et al.* CDD: conserved domains and protein three-dimensional structure. *Nucleic Acids Res.* **41,** D348–52 (2013).

68. Vik, Å. & Rine, J. Upc2p and Ecm22p , Dual Regulators of Sterol Biosynthesis in *Saccharomyces cerevisiae*. *Molecular and Cellular Biology*. **21**, 6395–6405 (2001).

69. Davies, B. S. J., Wang, H. S. & Rine, J. Dual Activators of the Sterol Biosynthetic Pathway of *Saccharomyces cerevisiae* : Similar Activation / Regulatory Domains but Different Response Mechanisms. *Molecular and Cellular Biology*. **25**, 7375–85 (2005).

70. Hoffman, C. S. & Winston, F. A ten-minute DNA preparation from yeast efficiently releases autonomous plasmids for transformaion of *Escherichia coli*. *Gene* **57,** 267–72 (1987).

71. Gibson, D. G. *et al.* Enzymatic assembly of DNA molecules up to several hundred kilobases. *Nat. Methods* **6,** 343–45 (2009).

72. Lin-Cereghino, J. *et al.* Condensed protocol for competent cell preparation and transformation of the methylotrophic yeast *Pichia pastoris*. *Biotechniques* **38,** 44, 46, 48 (2005).

73. Cooper, T. G. Nitrogen GATA factors participate in transcriptional regulation of vacuolar protease genes in *Saccharomyces cerevisiae*. *Jounal of Bacteriology*. **179,** 5609–13 (1997).

74. Pfeffer, M. *et al.* Intracellular interactome of secreted antibody Fab fragment in *Pichia pastoris* reveals its routes of secretion and degradation. *Appl. Microbiol. Biotechnol.* **93,** 2503–12 (2012).

75. Vanz, A. L. *et al.* Physiological response of *Pichia pastoris* GS115 to methanol-induced high level production of the Hepatitis B surface antigen: catabolic adaptation, stress responses, and autophagic processes. *Microb. Cell Fact.* **11,** 103 (2012).

76. Young, E. T., Dombek, K. M., Tachibana, C. & Ideker, T. Multiple pathways are co-regulated by the protein kinase Snf1 and the transcription factors Adr1 and Cat8. *J. Biol. Chem.* **278,** 26146–58 (2003).

77. Tachibana, C. *et al.* Combined Global Localization Analysis and Transcriptome Data Identify Genes That Are Directly Coregulated by Adr1 and Cat8. *Molecular and Cellular Biology*. **25,** 2138–46 (2005).

78. Schiestl, R. H., Dominska, M. & Petes, T. D. Transformation of *Saccharomyces cerevisiae* with nonhomologous DNA : illegitimate integration of transforming DNA into yeast chromosomes and in vivo ligation of Transforming DNA to Mitochondrial DNA Sequences. *Molecular and Cellular Biology.* **13,** 2697-2705 (1993).

79. Abad, S. *et al.* Real-time PCR-based determination of gene copy numbers in *Pichia pastoris*. *Biotechnol. J.* **5,** 413–20 (2010).

Tables

Abbreviations

Table 31: Abbreviations used within this thesis

abbreviation	full name
aa	amino acid
AB	antibody
ACIB	Austrian Centre of Industrial Biotechnology
AOX	alcohol oxidase
bl	blank
(bp)	base pairs
cas	cassette
ChIP	chromatin immunoprecipitation
CSRE	carbon source-responsive element
dd	distilled deionized
DHAS	dihydroxyacetone synthase
DNA	Deoxyribonucleic acid
DSB	double stand break
DTT	dithiothreitol
DWP	deep well plate
EDTA	ethylenediaminetetraacetic acid
ELISA	enzyme linked immunosorbent assay
ENCODE	ENCyclopedia Of DNA Elements
ER	endoplasmic reticulum
ERAD	ER-Associated Degradation
EVC	EVC
Fab	fragment antigen binding
FACS	Fluorescence activated cell sorting
FD	fast digest
FDU	fast digest unit
fw	forward
GAP	glyceraldehyd-3-phosphate (dehydrogenase)
Gen	Geniticin
Glu	glutamine
HBsAG	Hepatitis B surface antigen
hEGF	human epidermic growth factor
HF	high fidelity
HR	homologous recombination
IgG	Immununglobulin G
IRE1	inositol-requiring protein-1
KanR	kanamycin resistance
LacZ	β-lactamase
LB	lysogeny broth
LsdB	exo-levanase
M	molar
MAQ	Mapping and Assembly with Qualities
MDR	multiple drug resistance

Mut	methanol utilization pathway
Mut^{S}	methanol utilization slow
MXR1	methanol expression regulator 1
NA	no annotation
NADH	nicotinamide adenine dinucleotide
NCR	nitrogen catabolite repression
NHEJ	non-homologous end joining
ni	no intron
OD	optical density
ONC	overnight culture
ORF	open reading frames
ORI	origin of replication
PCR	polymerase chain reaction
PDR	pleiotropic drug resistance
PEG	polyethylene glycol
P_{GAP}	*GAP*-promoter
PHO1	acid phosphatase
PP	polypropylene
PRM1	positive regulator of methanol
PS	polystyrene
rpm	revelations per minute
RT	room temperature
RT-PCR	real time PCR
rv	reverse
SCP	single cell protein
SD	standard deviation
Sh ble	*Streptoalloteichus hindustanus* bleomycin gene
SOC	Super Optimal broth with Catabolite repression
SRE	sterol regulatory element
SREBP	sterol regulatory element binding protein
sv	short version
TF	transcription factor
TFBS	TF-binding sites
Trl1	tRNA ligase
TS	trans-sialidase
TT	transcription termination region
UPR	Unfolded Protein Response
UTR	untranslated regions
UV	ultra violet
WP	working project
YPD	yeast extract peptone dextrose
Yrm1p	(yeast reveromycin resistance modulator
Zeo	Zeocin
α-MF	α-factor prepro peptide

5. Appendix

5.1. DNA Ladder

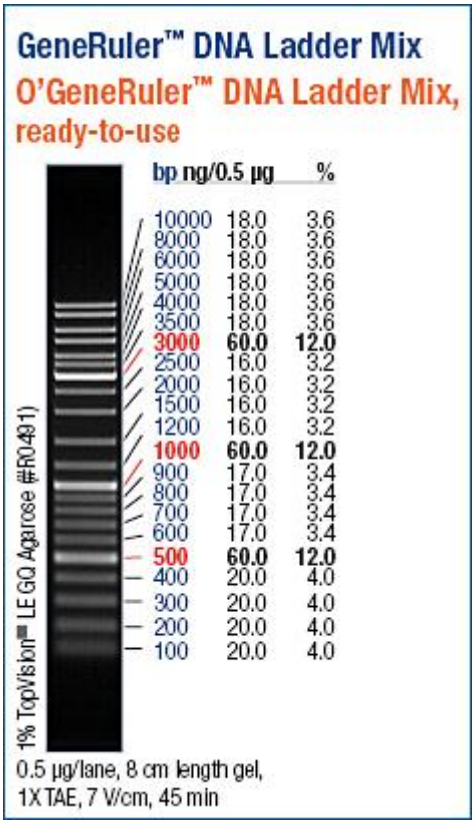

Figure 64: GeneRuler™ DNA Ladder Mix used for all agarose gel approaches. 6 µL were used per slot.

5.2. ORF-Sequences of TFs with Corresponding Amino Acid Sequences

5.2.1. PAS_chr4_0626 (*GAT1*/TF1)

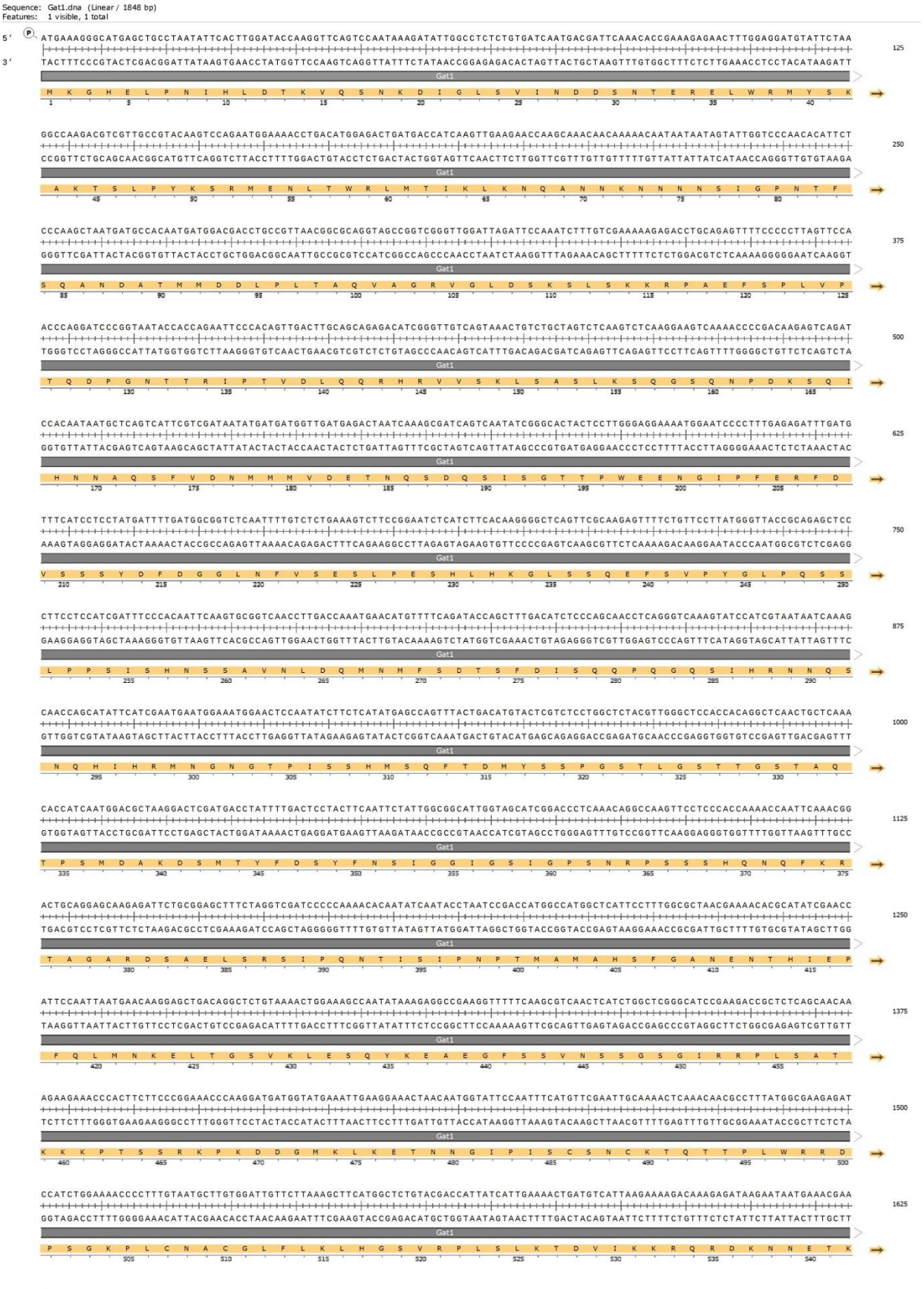

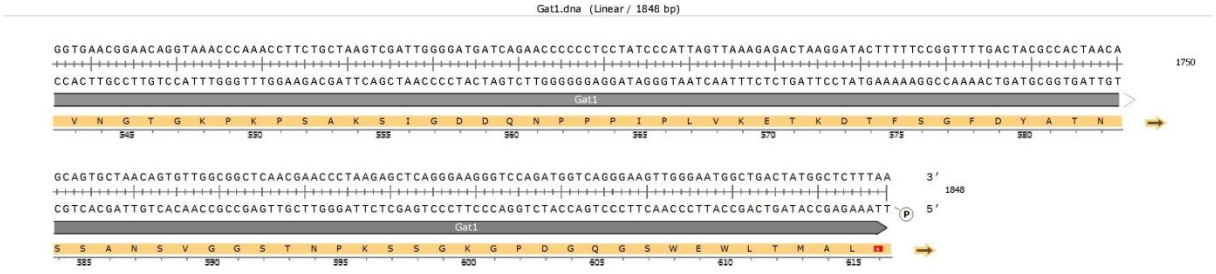

Figure 65: ORF and aa sequence of PAS_chr4_0626 (GAT1/TF1)

5.2.2. PAS_chr4_0271 (*GAT2*/TF2)

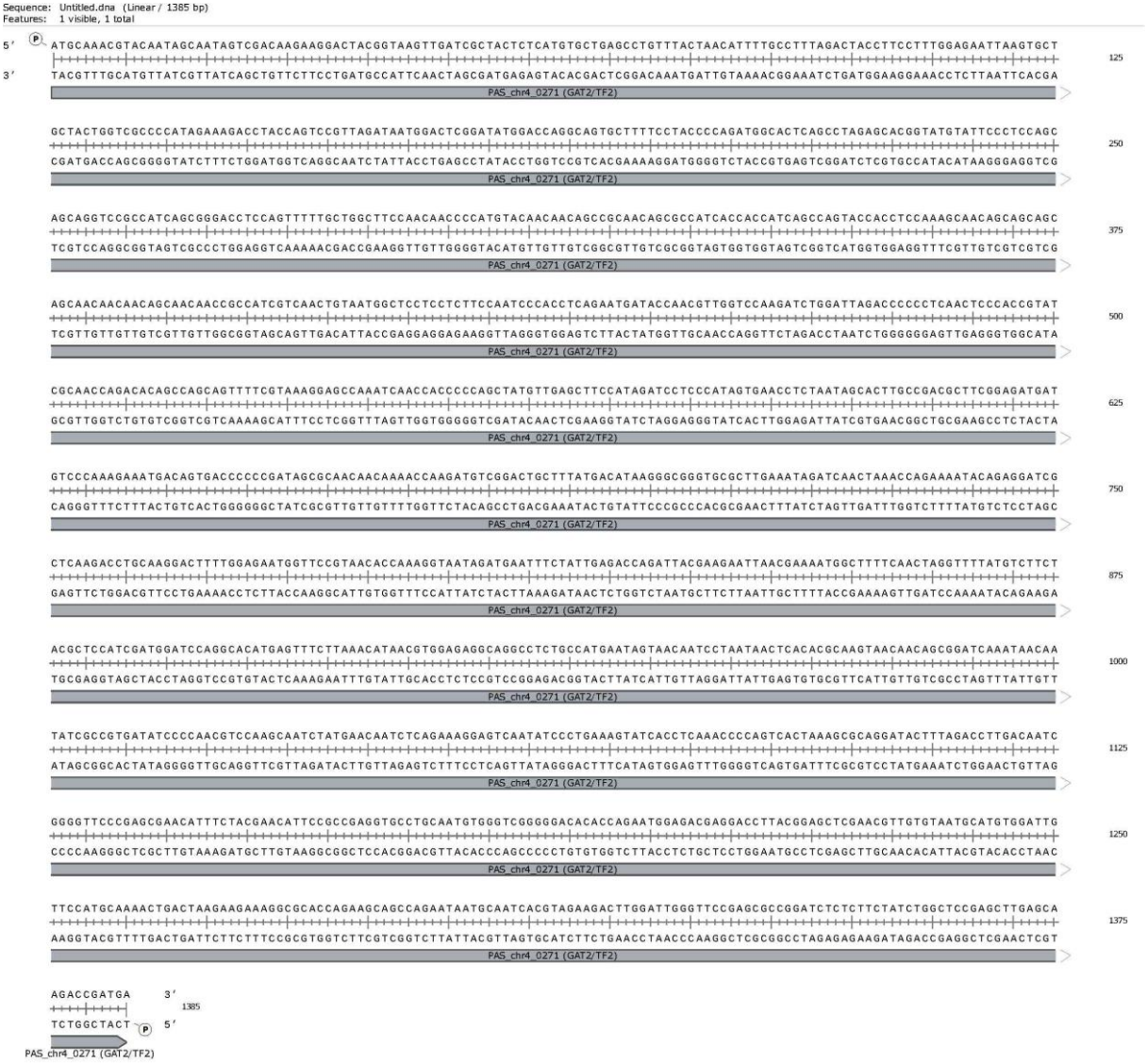

Figure 66: ORF (with intron) of PAS_chr4_0271 (GAT2/TF2)

5.2.3. PAS_chr4_0540 (*CAT8* or *SIT4*/TF3)

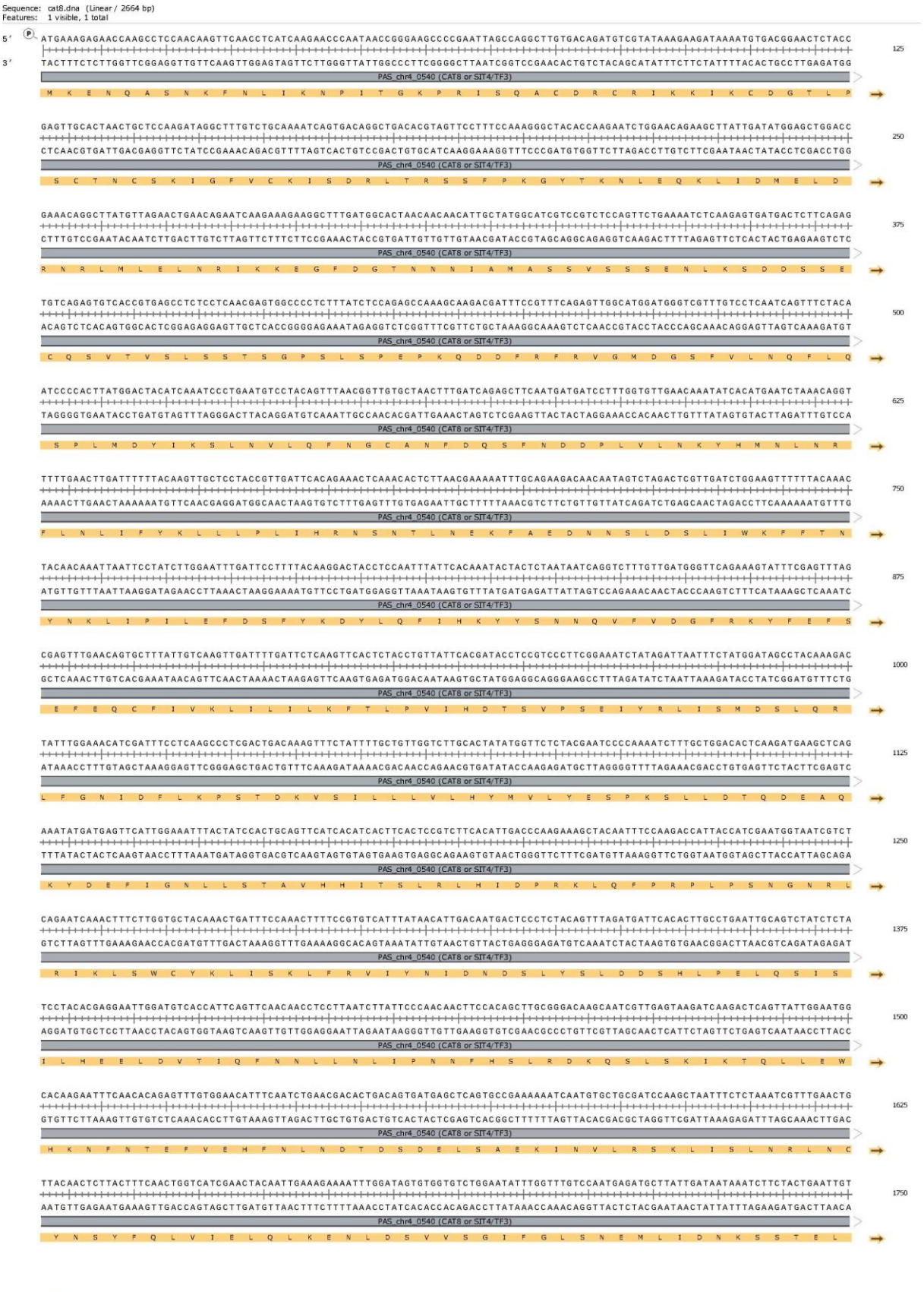

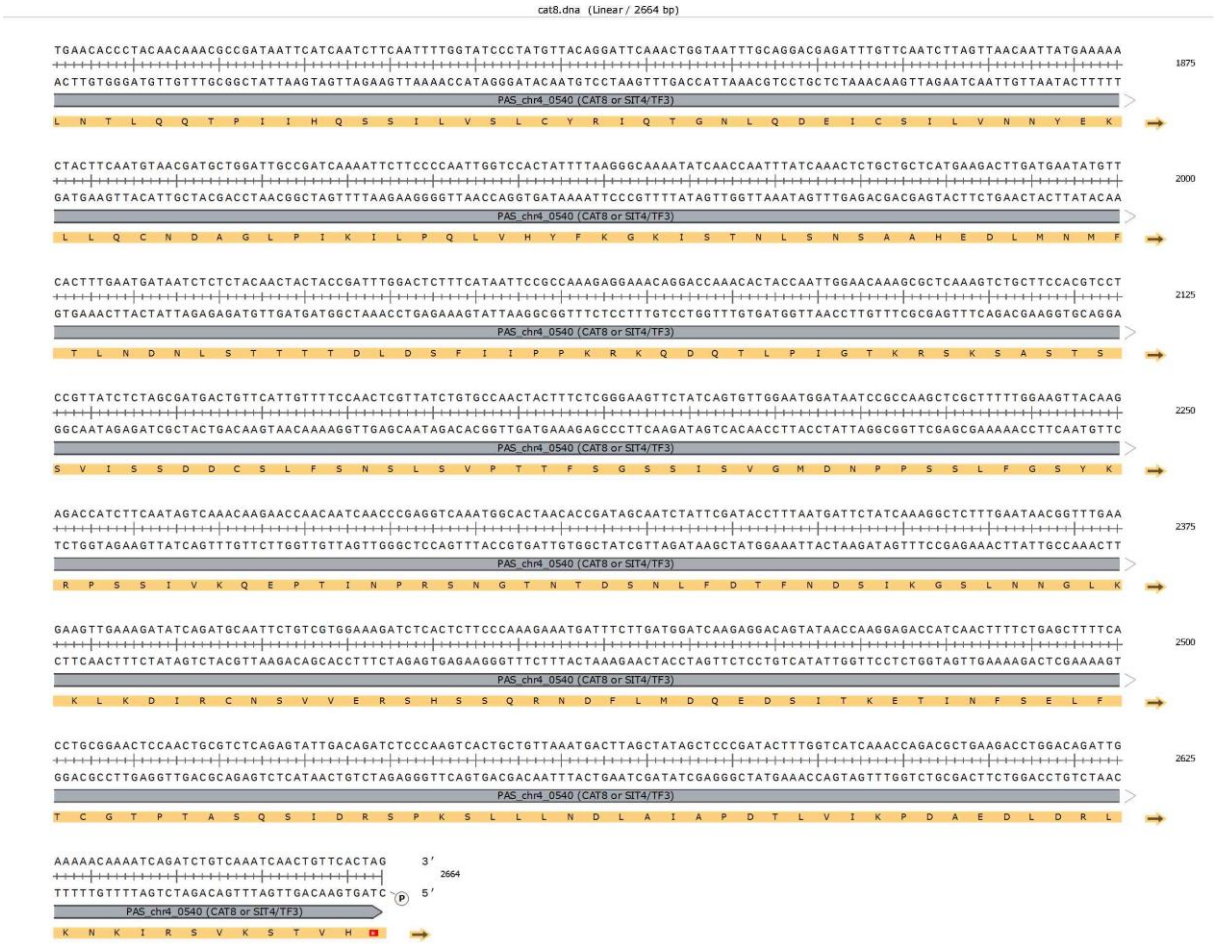

Figure 67: ORF and aa sequence of PAS_chr4_0540 (*CAT8* or *SIT4*/TF3)

5.2.4. PAS_chr4_0324 (*YRM1*/TF4)

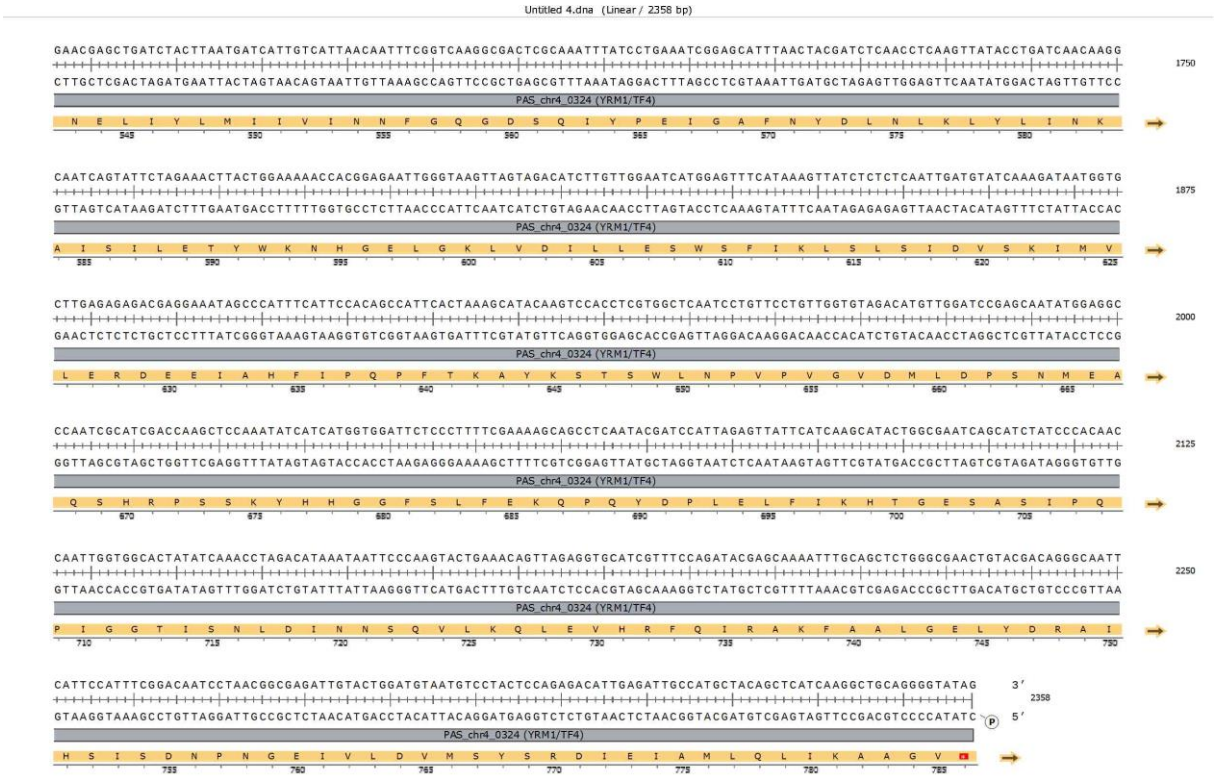

Figure 68: ORF and aa sequence of PAS_chr4_0324 (*YRM1*/TF4)

5.2.5. PAS_chr4_0425 (no annotation (NA)/TF5)

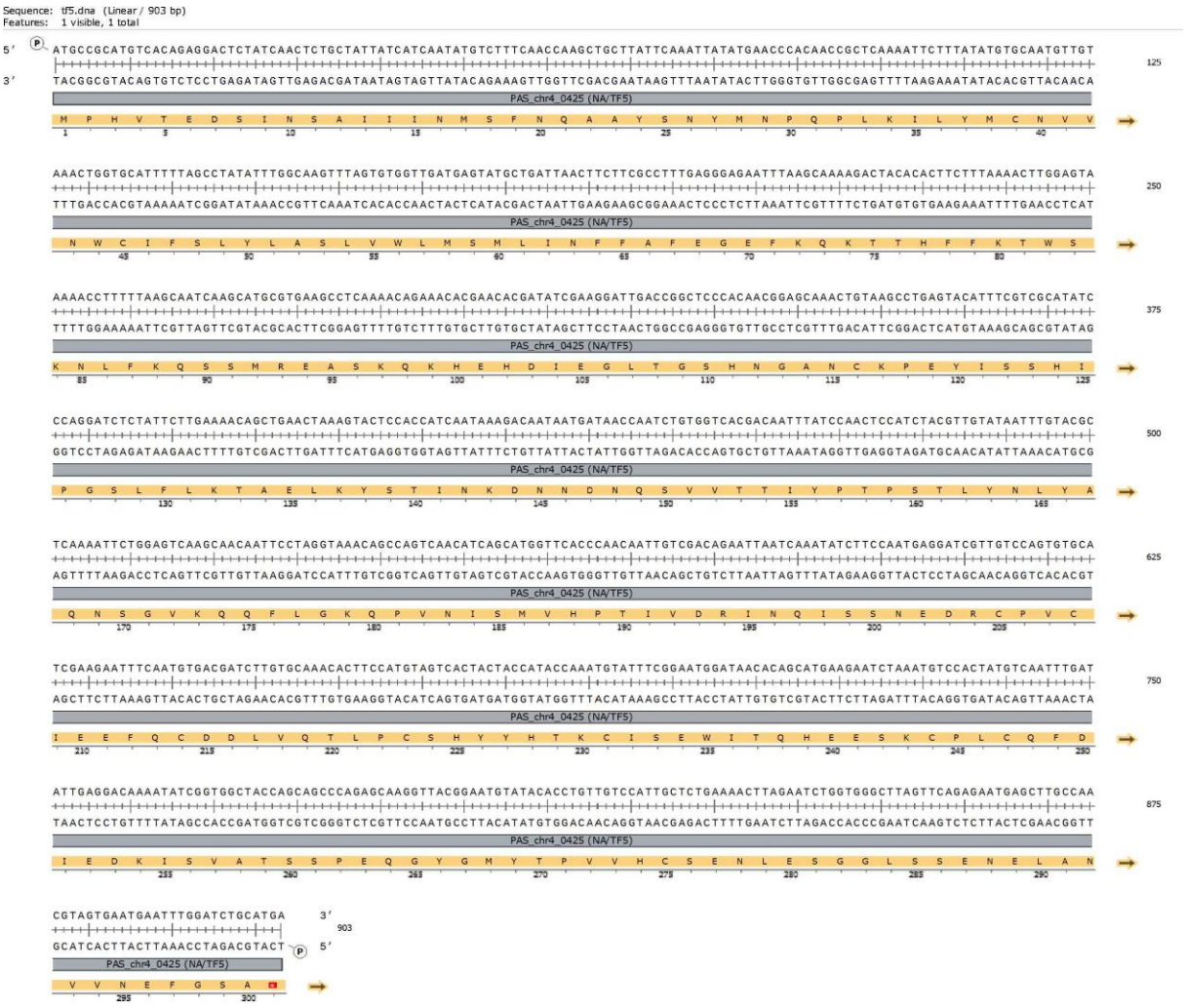

Figure 69: ORF and aa sequence of PAS_chr4_0425 (NA/TF5)

5.2.6. PAS_chr2-1_0114 (*UPC2*/TF6)

Figure 70: ORF and aa sequence of PAS_chr2-1_0114 (*UPC2*/TF6)

5.2.7. PAS_chr4_0271 (*GAT2*/TF2 no intron)

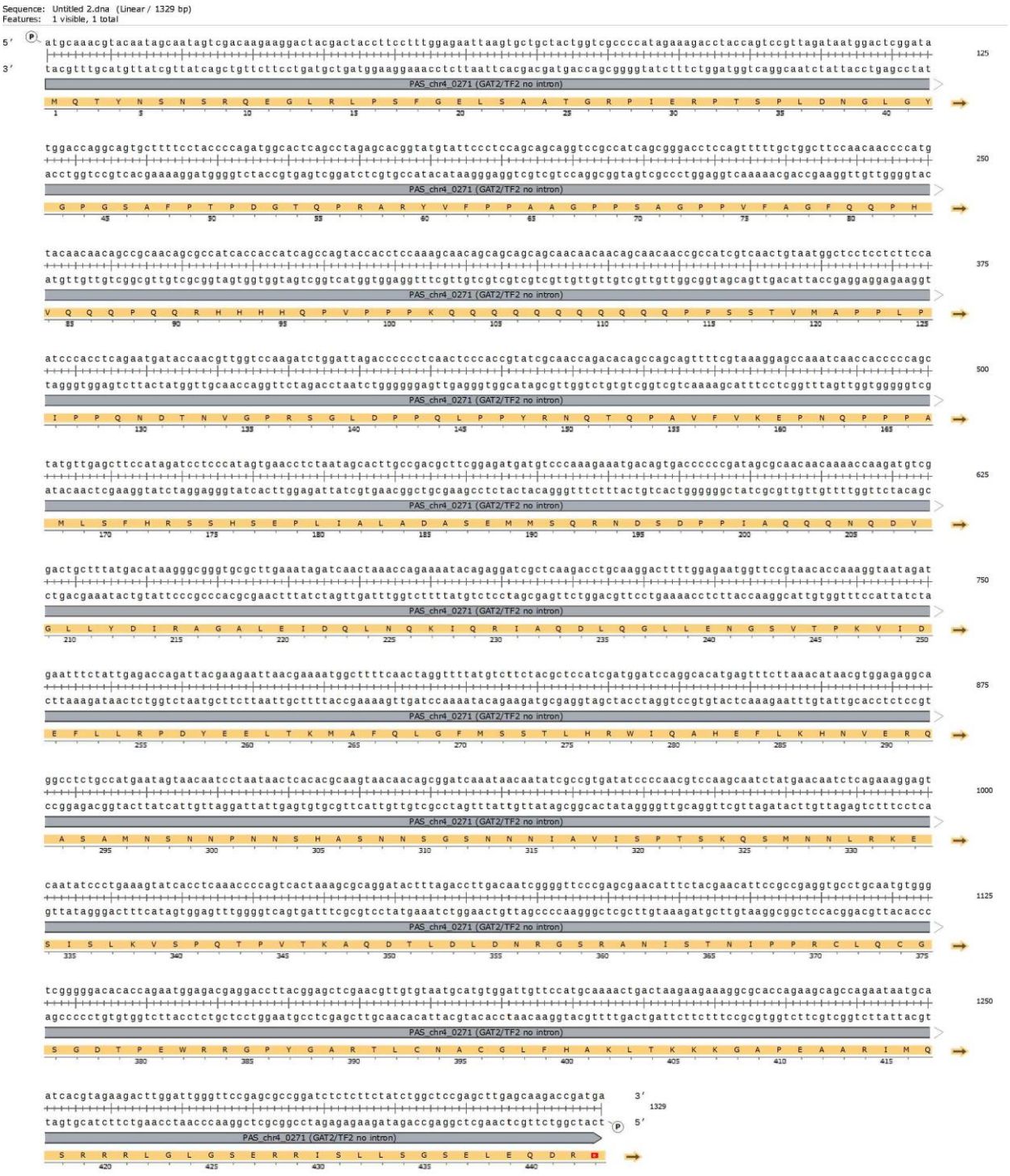

Figure 71: ORF and aa sequence of PAS_chr4_0271 (GAT2/TF2 no intron)

5.2.8. PAS_chr4_0425 (NA/TF5sv)

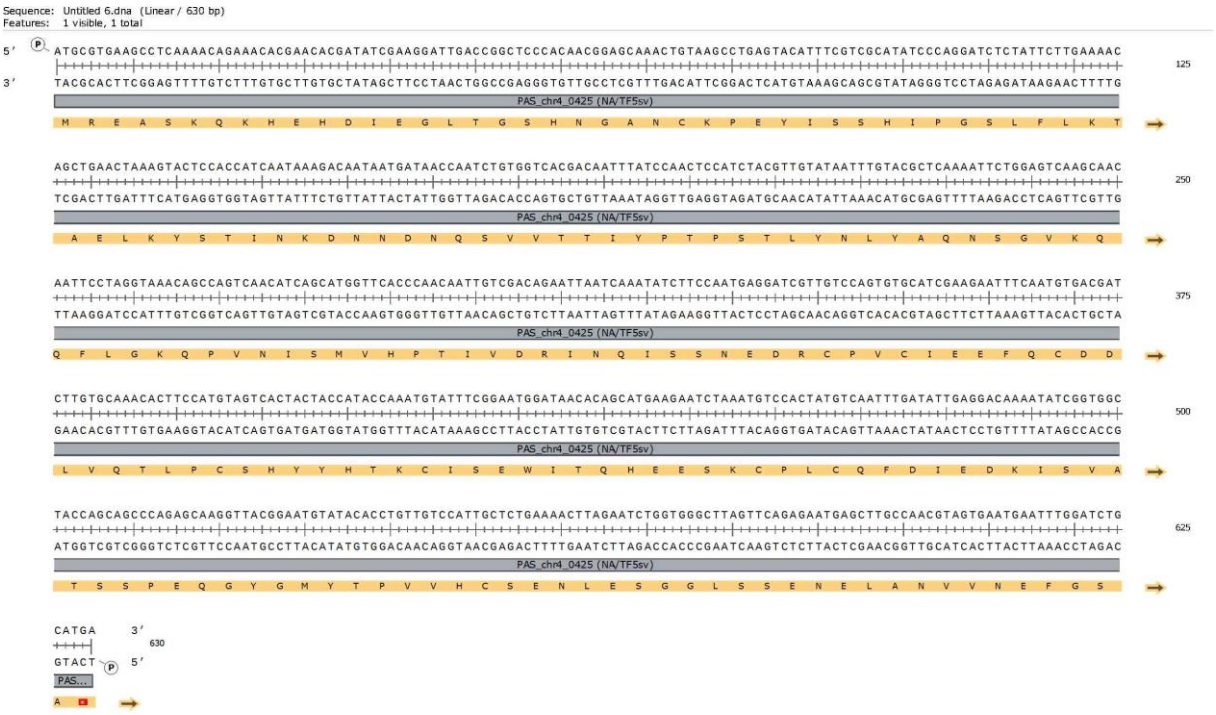

Figure 72: ORF and aa sequence of PAS_chr4_0425 (NA/TF5sv)